Final Report
Volume II

A NEW SHORT-TERM TRAFFIC PREDICTION AND INCIDENT DETECTION SYSTEM ON I-4

By

Haitham Al-Deek, Ph.D., P.E.
Associate Professor and Director of Transportation Systems Institute (TSI)
Email: haldeek@pegasus.cc.ucf.edu

Sherif Ishak, Ph.D.
Assistant Research Engineer and Manager of ITS lab
Email: sishak@mail.ucf.edu

And

Morgan Wang, Ph.D.
Associate Professor of Statistics
Email: cwang@mail.ucf.edu

Prepared for
The Florida Department of Transportation
University of Central Florida Account #: 16-21-701
Contract No.: BB-904

Department of Civil and Environmental Engineering
University of Central Florida
P.O. Box 162450
Orlando, FL 32816-2450
Phone: (407) 823-2988
Fax: (407) 823-3315

April 2001

TECHNICAL REPORT DOCUMENTATION PAGE

1. Report No.	2. Government Accession No.	3. Recipient's Catalog No.

4. Title and Subtitle

A New Short-Term Traffic Prediction and Incident Detection System on I-4 (Volume II)

5. Report Date

April 2001

6. Performing Organization Code

7. Author (s)

H. Al-Deek, S. Ishak, and M. Wang

8. Performing Organization Report No.

9. Performing Organization Name and Address

Dept. of Civil & Environmental Engineering
University of Central Florida
4000 Central Florida Boulevard
Orlando, FL 32816-2450

10. Work Unit No. (TRAIS)

11. Contract or Grant No.

BB-904

12. Sponsoring Agency Name and Address

Florida Department of Transportation
Research Center
605 Suwannee Street
Tallahassee, FL 32399-0450

13. Type of Report and Period Covered

Final Report

14. Sponsoring Agency Code

15. Supplementary Notes

Prepared in cooperation with Florida Department of Transportation

16. Abstract

Non-recurrent freeway congestion has increased substantially to cause an adverse impact on traffic conditions in terms of excessive delays, queue backups, reduced safety, and increased air pollution. Therefore, the need for accurate, fast detection of incidents to facilitate quick response and immediate dispatch of emergency services is still pressing. The automated detection of incidents on the freeways is essentially one of the primary components of a metropolitan infrastructure, which encompasses Advanced Traveler Information Systems (ATIS) and Advanced Traffic Management Systems (ATMS). Most of the previously developed incident detection algorithms have had a limited success in their overall performance in terms of detection rate (DR) and false alarm rate (FAR). Unlike traditional incident detection algorithms that compare individual occupancy, speed or volume values at successive loop detector stations, pattern recognition models have the ability to learn how to recognize traffic patterns with certain characteristics. This report presents the results of training and testing the Fuzzy ART network for the application of automatic freeway incident detection. The performance envelopes of the DR-FAR relationship were the basis for assessing the performance of the algorithm. The performance was evaluated under a variety of scenarios to address the impact of some factors on the overall algorithm performance. Those factors included the vigilance parameter, the temporal pattern size, and the type of traffic parameter. Comparative evaluation between the Fuzzy ART algorithm and California algorithms version 7 and 8 was presented. The results of this research study have demonstrated the potential of applying the artificial neural networks for automated detection of incidents on freeways using the existing loop detector data. The performance of the Fuzzy ART algorithm showed constant increase in detection rate up to nearly 88% at relatively low values of FAR. An interesting finding is that when compared with occupancy patterns, speed patterns constantly produce better results. This is likely to indicate that incidents can be detected with speed patterns better than occupancy patterns. The results of the Fuzzy ART network suggest that the combination of occupancy and speed in the representation of traffic pattern lead to a better performance.

17. Key Words	18. Distribution Statement
Incident Detection, Freeway Incident Detection, Artificial Neural Networks, Fuzzy ART	No restriction - this report is available to the public through the National Technical Information Service, Springfield, VA 22161

19. Security classif. (of this report)	20. Security Class. (of this page)	21. No. of Pages	22. Price
Unclassified	Unclassified	131	

ACKNOWLEDGEMENT

This report was prepared as part of Project Contract No.: BB904, "A New Short-Term Traffic Prediction and Incident Detection System on I-4". The research was conducted by the Transportation Systems Institute (TSI) of the University of Central Florida.

The authors would like to acknowledge the support of FDOT's Central Office in Tallahassee, Florida. In particular, the authors would like to thank Mr. Lap Hoang, Deputy State Traffic Engineer, for his help and support. Special thanks are also due to Mr. Greg Floyd and the traffic operators at the Freeway Management Center for their support and cooperation in maintaining real time access to the loop detector data on I-4.

DISCLAIMER

The opinions, findings, and conclusions in this publication are those of the authors' and not necessarily those of the Florida Department of Transportation of the US Department of Transportation. This report does not constitute a standard, specification, or regulation. This report is prepared in cooperation with the State of Florida Department of Transportation.

EXECUTIVE SUMMARY

Non-recurrent freeway congestion has increased substantially to cause an adverse impact on traffic conditions in terms of excessive delays, queue backups, reduced safety, and increased air pollution. Through the last three decades, numerous attempts have been made to reduce the effect of non-recurrent congestion by developing a reliable and efficient automatic incident detection system. Most of the developed incident detection algorithms have not yet shown the anticipated level of success required for on-line implementation. Therefore, the need for accurate, fast detection of incidents to facilitate quick response and immediate dispatch of emergency services is still pressing. The automated detection of incidents on the freeways is essentially one of the primary components of a metropolitan infrastructure, which encompasses Advanced Traveler Information Systems (ATIS) and Advanced Traffic Management Systems (ATMS).

Most of the previously developed incident detection algorithms have had a limited success in their overall performance in terms of detection rate (DR) and false alarm rate (FAR). The existing algorithms have limited ways of filtering the loop detector data and distinguishing incident conditions from incident-like conditions (recurrent congestion patterns). In addition, they do require intensive calibration efforts to select the most appropriate threshold values. Even after calibration the detection rate and the false alarm rate do not provide satisfactory results from the traffic operators' point of view. High false alarm rates swamp the traffic operators and render the incident detection system unreliable.

Unlike traditional incident detection algorithms that compare individual occupancy, speed or volume values at successive loop detector stations, pattern recognition models have the ability to learn how to recognize traffic patterns with certain characteristics. Recently Fuzzy ART (Adaptive Resonance Theory) has been introduced. Fuzzy ART is a clustering algorithm that has the ability to map traffic patterns to a set of categories. Incident traffic patterns can be mapped to similar clusters according to their common

characteristics. It has advantages over backpropagation networks in that they provide fast stable learning that is suitable for on-line implementation. Fuzzy ART is a synthesis of Fuzzy Logic and ART networks.

This report presents the results of training and testing the Fuzzy ART network for the application of automatic freeway incident detection. The performance envelopes of the DR-FAR relationship were the basis for assessing the performance of the algorithm. For performance improvement, a persistence period and a persistence factor were introduced to reduce the false alarm rate. The effect of the persistence factor was not significant for values in the range between 1 and 4. The performance was evaluated under a variety of scenarios to address the impact of some factors on the overall algorithm performance. Those factors included the vigilance parameter, the temporal pattern size, and the type of traffic parameter. The results showed that the performance could be significantly improved with increasing the value of the vigilance parameter (ρ=0.95) and the temporal pattern size. Also, results based on speed patterns outperformed those based on occupancy patterns. However, the combination of occupancy and speed has resulted in the highest performance. Comparative evaluation between the Fuzzy ART algorithm and California algorithms version 7 and 8 was presented.

TABLE OF CONTENTS

LIST OF FIGURES

LIST OF TABLES

1 INTRODUCTION

The objectives of this research project are twofold: First, to improve the short-term traffic prediction model and conduct sensitivity analysis to investigate the effect of various factors on the prediction accuracy; and second, to develop a neural network model (Fuzzy ART) for the automated detection of incidents on I-4. The tasks accomplished in each part are listed below:

Volume I: Short-term traffic prediction on I-4

1. Use Different decay factors such as half normal and exponential function to smooth detector data and improve on the performance of the existing off-line model.
2. Use additional traffic variable, e.g., occupancy, in addition to speed, to see if the accuracy of the existing prediction model will be improved.
3. Test the off-line prediction model using more incident-free days (recurring congestion) to examine the reliability of the prediction model and, most importantly, to avoid overestimation of traffic speed
4. Implement the on-line real time traffic prediction model
5. Evaluate the performance of the on-line prediction model

Volume II: Incident detection on I-4

1. Filter all the loop detector data and the incident database collected on the central corridor of I-4 in 1993 and 1994. The filtering mechanism should be suitable for on-line implementation.

2. Collect a new set of incident and loop detector data on I-4 via the dial-up connection between UCF and FMC. The new data will also be subject to filtering.
3. Develop software to process the data and train the proposed ANN models. The programming effort will be conducted in MS Visual Basic 6.0. The development process involves debugging and testing the software.
4. Split the data set into two subsets: one for training and the other for testing.
5. Train the proposed ANN models using the training data subset.
6. Evaluate the performance of the trained models using incident detection performance measures.
7. Test the proposed models off-line using the testing data subset.
8. Conduct the on-line testing of the new trained models by incorporating a new module into the existing on-line module.

2 INCIDENT DETECTION ON I-4

2.1 INTRODUCTION

Non-recurrent freeway congestion has increased substantially to cause an adverse impact on traffic conditions in terms of excessive delays, queue backups, reduced safety, and increased air pollution. Through the last three decades, numerous attempts have been made to reduce the effect of non-recurrent congestion by developing a reliable and efficient automatic incident detection system. Most of the developed incident detection algorithms have not yet shown the anticipated level of success required for on-line implementation. Therefore, the need for accurate, fast detection of incidents to facilitate quick response and immediate dispatch of emergency services is still pressing. The automated detection of incidents on the freeways is essentially one of the primary components of a metropolitan infrastructure, which encompasses Advanced Traveler Information Systems (ATIS) and Advanced Traffic Management Systems (ATMS).

Most of the previously developed incident detection algorithms have had a limited success in their overall performance in terms of detection rate (DR) and false alarm rate (FAR). The existing algorithms have limited ways of filtering the loop detector data and distinguishing incident conditions from incident-like conditions (recurrent congestion patterns). In addition, they do require intensive calibration efforts to select the most appropriate threshold values. Even after calibration the detection rate and the false alarm rate do not provide satisfactory results from the traffic operators' point of view. High

false alarm rates swamp the traffic operators and render the incident detection system unreliable.

Unlike traditional incident detection algorithms that compare individual occupancy, speed or volume values at successive loop detector stations, pattern recognition models have the ability to learn how to recognize traffic patterns with certain characteristics. Recently Fuzzy ART (Adaptive Resonance Theory) has been introduced. Fuzzy ART is a clustering algorithm that has the ability to map traffic patterns to a set of categories. Incident traffic patterns can be mapped to similar clusters according to their common characteristics. It has advantages over backpropagation networks in that they provide fast stable learning that is suitable for on-line implementation. Fuzzy ART is a synthesis of Fuzzy Logic and ART networks.

2.2 DATA COLLECTION

The process of data collection for incident detection analysis is divided into two phases. The first phase handles the collection of the loop detector data along the study corridor. The loop detector data is comprised of 30-second speed, lane occupancy, and traffic volume at each loop detector station. The second phase involves the compilation of incident data with information on their location and time. Each phase is described in greater detail in the following subsections.

2.2.1 Loop Detector Data

This section provides a detailed description of the methodology used to collect and filter the loop detector data. The occupancy, speed, and volume were collected every 30 seconds with loop detectors spaced at 0.5 miles along the central corridor of I-4 in 1993 and 1994. The point measurements of the three parameters are used to portray the traffic conditions on the freeway. Due to occasional loop detector failures or malfunctioning the data stream has to be examined and filtered to remove those abnormalities. Also, the loop detector data is smoothed out using the moving time average to reduce the amount of random traffic fluctuations. Both filtering and smoothing are suitable for on-line implementation.

The purpose of this stage is to ensure that the necessary data fixes are made before the data is processed by the incident detection algorithms. The data collection process was completed in two simultaneous phases. The first phase involved collecting loop detector data of occupancy, volume, and speed every 30 seconds. The second phase involved compiling as many incidents on the study section of I-4 as possible from all possible sources during the same time period the loop detector data was collected. The second phase is explained in a separate section later in this report. The integrated loop and incident databases are used to satisfy the input requirements of the proposed artificial neural networks.

Due to the temporary loop detector failures on site it is likely to find occasional discontinuities in the data stream, which could be reduced by applying a simplified data filtering technique. This is to ensure that the traffic patterns generated from the loop detector data represent, as much as possible, the real traffic conditions on the study section. In addition, the loop detector data will be smoothed out using the moving average technique.

2.2.1.1 Study Site

The freeway section selected for this study was the central corridor of I-4 in both directions within the jurisdiction of Orange County, Florida. The I-4 central corridor is the most congested section during peak periods since it connects the urban areas to the downtown area of the city of Orlando and extends to reach the tourists' attraction areas. Therefore, the corridor is heavily traveled by both commuters and tourists. The study section is nearly 11.2 miles long and extends from Maitland Blvd. to John Young Pkwy in both directions. Figure 1 shows a map of the study section of I-4.

The central corridor is covered with loop detectors spaced out at almost 0.5 miles in both directions. Each lane has dual loop detectors that allow for speed measurements. The collection of all loop detectors at one particular location in both directions is referred to as a loop detector station. Each station is wired to a 170-type controller that collects all the traffic data from the loop detectors and transmits them to the Freeway Management Center (FMC). The study section has a total of 25 stations, out of which only 24 are productive. Stations are numbered from 530 to 554 in the extended I-4 surveillance system. One middle station (539) serves as a master hub and does not collect any traffic

data. The configuration of a typical loop detector station is shown in Figure 2. Location of loop detector stations by milepost is shown in Table 1.

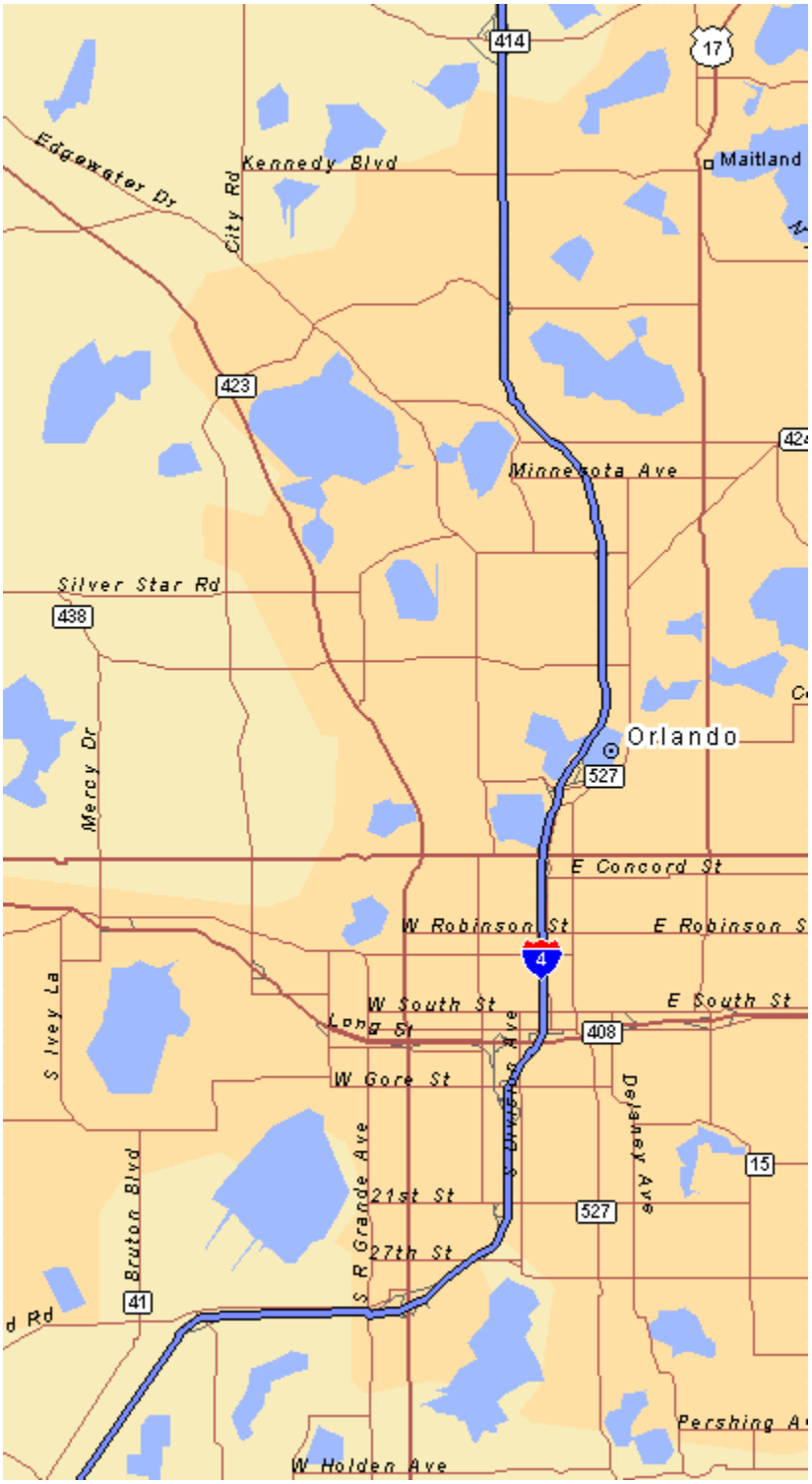

Figure 1: Map of I-4 showing the study section

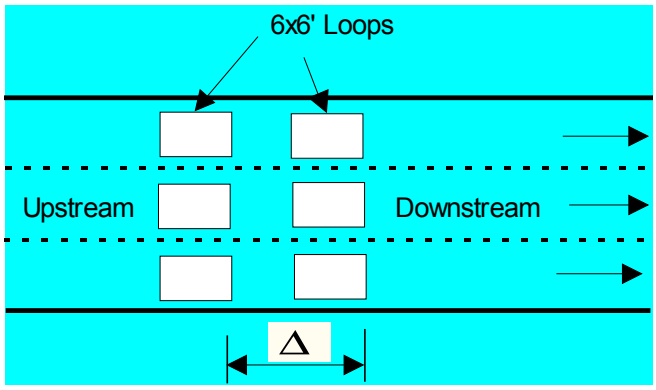

Figure 2: Configuration of a loop detector station

Table 1: Location of loop detector stations on the central corridor of I-4

Detector Station*	Eastbound Milepost	Eastbound Station	Westbound Milepost	Westbound Station
530	*79.14*	*1+00*	*79.14*	*1+00*
531	*79.63*	*27+00*	*79.63*	*27+00*
532	*80.16*	*55+00*	*80.16*	*55+00*
533	*80.63*	*80+00*	*80.44*	*70+00*
534	*81.06*	*102+50*	*81.04*	*101+50*
535	*81.51*	*126+00*	*81.51*	*126+00*
536	*82.03*	*153+25*	*82.03*	*153+25*
537	*82.53*	*179+50*	*82.53*	*179+50*
538	*82.90*	*178+75*	*82.90*	*178+75*
540	*83.43*	*266+75*	*83.43*	*266+75*
541	*83.92*	*252+75*	*83.92*	*252+75*
542	*84.47*	*281+50*	*84.47*	*281+50*
543	*84.93*	*306+00*	*84.93*	*306+00*
544	*85.42*	*332+00*	*85.42*	*332+00*
545	*85.92*	*358+50*	*85.92*	*358+50*
546	*86.48*	*388+00*	*86.48*	*388+50*
547	*86.90*	*410+00*	*86.90*	*410+00*
548	*87.34*	*433+00*	*87.34*	*433+00*
549	*87.84*	*459+15*	*87.84*	*459+50*
550	*88.25*	*481+00*	*88.25*	*481+00*
551	*88.70*	*504+50*	*88.70*	*504+50*
552	*89.24*	*533+00*	*89.24*	*533+00*
553	*89.59*	*551+50*	*89.59*	*551+50*
554	*90.16*	*581+60*	*90.16*	*581+60*

* Station 539 serves as a master hub and does not report any data

Each station reports measurements of three traffic parameters: volume, occupancy, and speed. The dual loops at each lane permit speed measurements by dividing the distance between the two loops over the time difference between the actuation of the upstream and downstream loops. The current system supports data resolution of 30 seconds. In other words, speed and occupancy data are averaged at 30-second intervals. Volume data are the 30-second vehicle counts accumulated at the end of each period. The three traffic parameters constitute the input to the proposed artificial neural network models.

2.2.1.2 Loop Detector Data Collection

The loop detector database contained a total of 376 days worth of 30-second occupancy, volume, and speed data. The data was collected in 1993 and 1994 in real time by a VAX 3300 computer with VMS operating system. At the end of each day the data was collected and dumped to a permanent file. The continuous data stream from the loop detector stations was the basis for generating the traffic patterns used in this study.

Due to the occasional loop detector failures and malfunctioning, the 30-second data stream may contain erroneous or missing data that causes discontinuity in the data stream. This discontinuity prohibits the generation of traffic patterns that represent the actual traffic conditions on the study section. Therefore, a simplified data filtering method is developed to fix the occurrences of such abnormalities. The filtering process is carried out at a preprocessing stage that involves substituting erroneous or missing loop data with data from adjacent operational loops, whenever possible.

2.2.1.3 Methodology of the Data Manipulation Process

This section explains the methodology for constructing the training and testing data sets required for the proposed artificial neural network model. The methodology, as shown in Figure 3, starts off with the extraction of loop detector data for the time periods when the incidents were reported. This process was completed using LOVATS© (Loop Output Verification and Testing Software), which was developed at the Transportation Systems Institute at the University of Central Florida in 1995 (see Al-Deek et al., 1995a, 1995b, and 1996). The extraction process was necessary to convert the loop detector data files from its original binary format to ASCII format. The next step was to split the loop detector data files by each of the three traffic parameters: volume, occupancy, and speed. Data for each parameter will be filtered and smoothed out to account for temporary loop failures and to reduce short-term traffic fluctuations. The filtering and smoothing processes are explained in the next section.

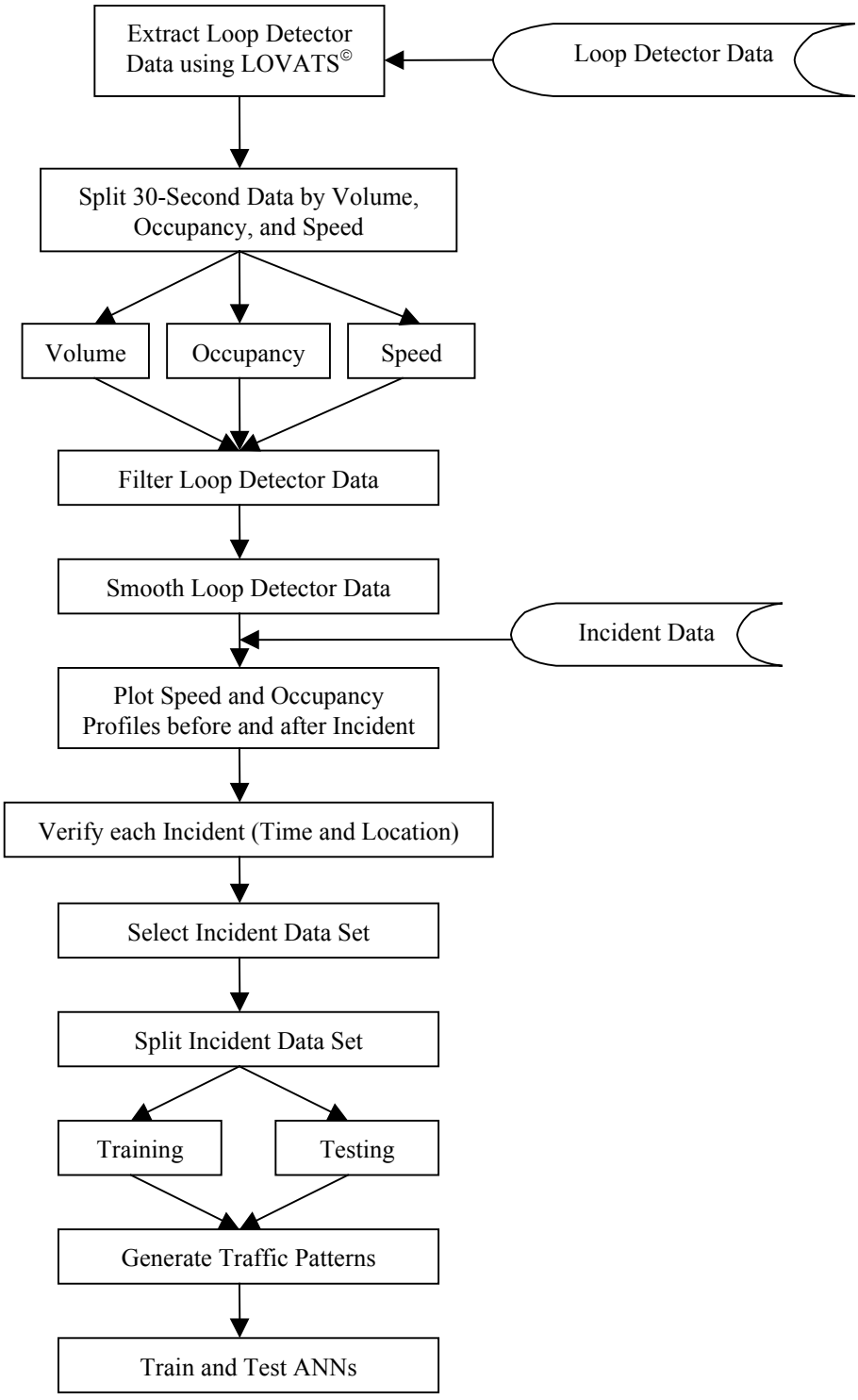

Figure 3: Methodology of the data manipulation process

2.2.1.4 Filtering and Smoothing Loop Detector Data

Due to occasional malfunctioning and failures in loop detectors it is likely to encounter missing or invalid measurements in the 30-second data stream. Thorough examination of the loop detector data has revealed the occurrences of zero, -xx, and -9xx values in the data stream. Depending on the type of loop detector failure these abnormal values may last from one 30-second period to several minutes or hours. Petty K. et al. (1995) showed a correction procedure that was developed in the Freeway Service Patrol (FSP) project and built in support software developed under UNIX platform. The correction procedure was based on the assumption that the calculated delay on the freeway section should be the same if the defective loop were not there in the first place. This procedure was devised to serve the purpose of the study.

In this study a simplified filtering scheme is proposed to fix the loop data before generating the training and testing traffic patterns. The filtering procedure is based on copying data from upstream or downstream loop detectors and averaging data from adjacent loop detectors. The filtering procedure is coded in MS Visual Basic and described in the following subsections.

2.2.1.4.1 Filtering Occupancy and Volume Data

The filtering process involves two steps. The first step replaces the incorrect loop detector measurement with the one observed at the upstream or downstream loop at the same lane. This step is sufficient when only one of the dual loops is down. At this step the missing or erroneous loop data is replaced with the data from the other operational

loop detector at the same lane. If both dual loops are down, filtering resumes by applying step 2. At step 2 the missing or misreported lane data is estimated from the average of the other two adjacent lanes, if they are both operational. If one of the two adjacent lanes is down, the data from the other lane is used. When the two adjacent lanes are down, the entire station is considered non-operational and cannot be used for representation of traffic patterns.

Based on observation of the loop detector data, all –xx occurrences in the data stream are valid measurements when the negative sign is simply dropped. Therefore, all detector data was screened first to remove the negative sign from all –xx encounters. This is followed by filtering 0 and –9xx observations as follows:

Let $X^t_{i,j,k}$ denote the occupancy or volume measured at time period *t*, station *i*, lane *j*, and loop *k,* as shown in Figure 4.

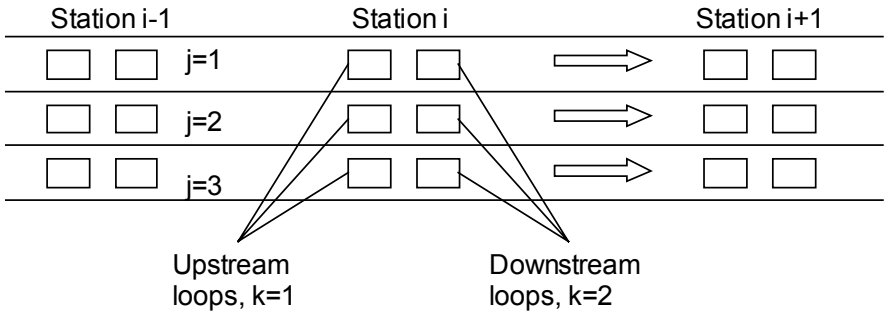

Figure 4: Schematic diagram of loop detector stations

Step 1: If $X^t_{i,j,k}$ = 0 or –9xx then,

$$X^t_{i,j,k} = \sum_{u=1}^{u=2} X^t_{i,j,u}.F_u \quad \forall u, u \neq k,\ j \in 1 \rightarrow 3,\ i \in 1 \rightarrow 25 \qquad [1]$$

Where,

$$F_u = \begin{cases} 0 & if\ \ X^t_{i,j,u} = 0\ \ or\ \ -9xx \\ 1 & Elsewhere \end{cases}$$

Step 2: If $X^t_{i,j,k}$ = 0 or –9xx then,

$$X^t_{i,j,k} = \frac{\sum_{v=1}^{v=3} X^t_{i,v,k}.F_v}{\sum_{v=1}^{v=3} F_v} \quad \forall v, v \neq j,\ k \in 1 \rightarrow 2,\ i \in 1 \rightarrow 25 \qquad [2]$$

$$F_v = \begin{cases} 0 & if\ X^t_{i,v,k} = 0\ or\ -9xx \\ 1 & Elsewhere \end{cases}$$

2.2.1.4.2 <u>*Filtering Speed Data*</u>

Filtering speed data is similar to occupancy and volume data except that speed measurements are generated from dual loops, and therefore, each lane reports only one speed value every 30 seconds. Hence, the filtering process is completed using step 2 only, where the missing lane speed data is estimated from the average of the other two adjacent lanes, if they are both operational. Similarly, if one of the two adjacent lanes is not operational, the data from the operational lane is used. When the two adjacent lanes are down, then the entire station is considered non-operational and cannot be used for representation of traffic patterns. The filtering steps are explained as follows:

Let $X^t_{i,j}$ denote the speed measured at time period *t*, station *i*, and lane *j*.

Step 1: If $X^t_{i,j}$ = 0 or –9xx then,

$$X^t_{i,j} = \frac{\sum_{v=1}^{v=3} X^t_{i,v}.F_v}{\sum_{v=1}^{v=3} F_v} \quad \forall v,\ v \neq j,\ \ i \in 1 \rightarrow 25 \qquad [3]$$

Where,

$$F_v = \begin{cases} 0 & if\ X^t_{i,v} = 0\ or\ -9xx \\ 1 & Elsewhere \end{cases}$$

2.2.1.5 Smoothing Loop Detector Data

To reduce noise and short-term traffic fluctuations the loop detector data is smoothed out using the moving average technique. The smoothing time window is carefully selected as two minutes. Although wider smoothing time windows are more likely to further reduce the random noise in the traffic pattern, the effect of smoothing can be detrimental to the mean time to detect an incident. For instance, if an incident happens at time t, its effect on the moving averaged patterns will be smoothed out with the prior non-incident conditions until time $t+\Delta t$, where Δt denotes the smoothing time window.

Let $Y_{i,j}^{t}$ denote the smoothed value of occupancy, volume, or speed at time period t, lane j, and station i. The smoothing time period is two minutes, which is equivalent to 4 consecutive 30-second periods.

$$Y_{i,j}^{t} = \frac{\sum_{u=0}^{u=3} X_{i,j}^{t-u} . F_u}{\sum_{u=0}^{u=3} F_u} \qquad j \in 1 \to 3, i \in 1 \to 25 \qquad [4]$$

Where,

$$F_u = \begin{cases} 0 & if\ X_{i,u}^{t-u} = 0\ or\ -9xx \\ 1 & Elsewhere \end{cases}$$

2.2.1.6 A New Set of Loop Detector Data

This task involves collecting a new set of loop detector data and incident data on I-4 via the software developed by the transportation research team at UCF within the context of

the project titled "On-line testing of incident detection algorithms", sponsored by the FDOT. When running on-line, the program continuously downloads 30-second data of speed, volume and occupancy via the dial-up connection between UCF and FMC. The program has been running incessantly since September 1997 for 24 hours a day, 7 days a week. The loop detector data was compiled every day in a separate text file. The compiled text files were stored on CDs and then converted to database access format (mdb) to provide fast and easy access though the new on-line software.

2.2.1.7 Data Conversion Process

The data conversion process was completed as a part of the online incident detection and traffic prediction module developed in this project. The initial design of the program interface is shown in Figure 5. The figure shows the main menus of the program. The main features currently available are:

1. Conversion of the data text files to MS Access database format (mdb).
2. Querying the mdb database files to extract the information requested by the user.

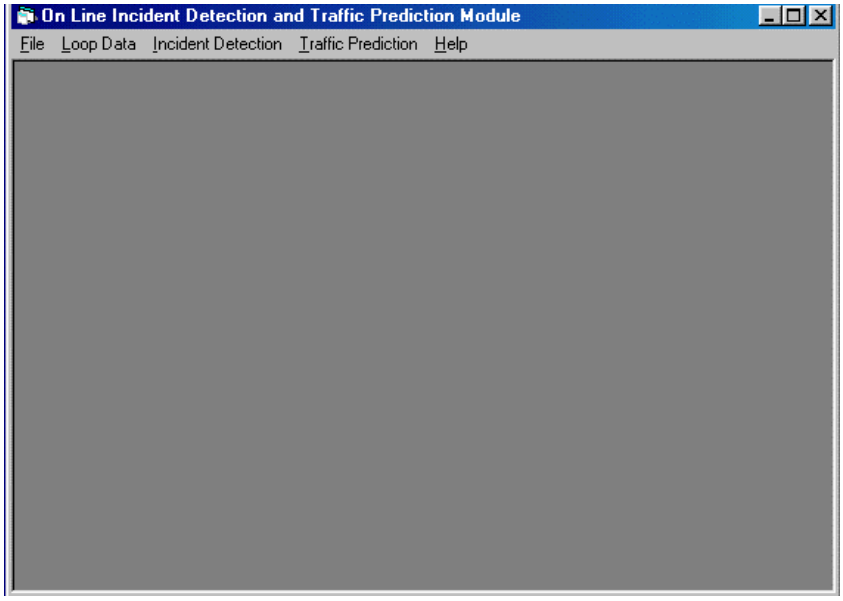

Figure 5: Snapshot of the main menu

2.2.1.7.1 *Conversion of text files to database files*

The purpose of this feature is to convert the text files compiled by the on-line incident detection program to more efficiently accessible database files. As mentioned previously, the 30-second data is collected from I-4 and compiled on a daily basis in ASCII files. Although the text files can be opened with any text editor under windows (e.g. Wordpad), it is very time consuming to attempt to access any particular information within the file. To make use of the efficient and fast database engines, the text files were converted to database files. Access to particular records in the database can be easily and quickly achieved through querying the database tables using SQL (Structured Query Language) statements. The database files are grouped by month and stored on CDs to provide portability. In other words, each database file contains all the loop detector data collected within a particular month. Figure 6 shows a snapshot of the data conversion process while converting data for the month of June '98.

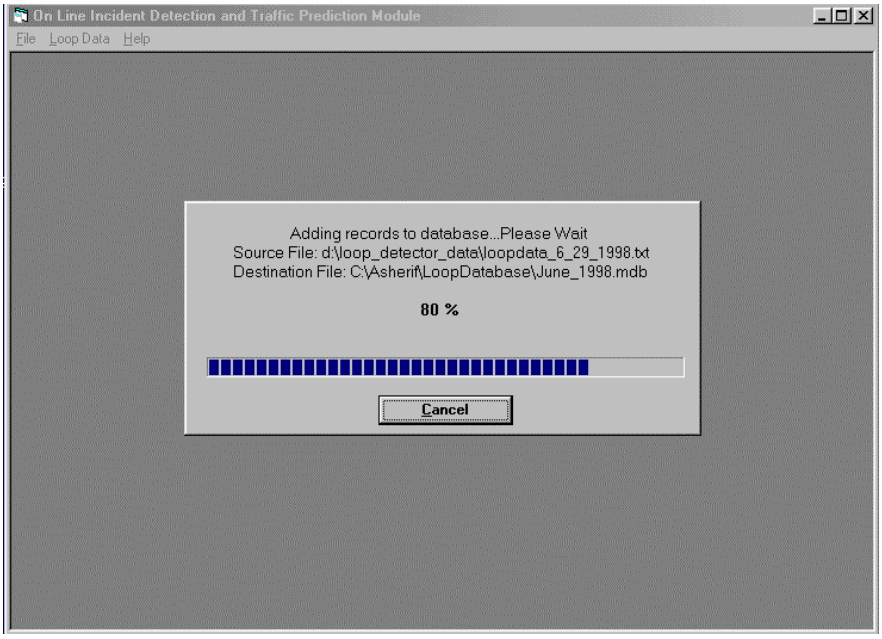

Figure 6: Snapshot of the data conversion process

2.2.1.7.2 *Querying the database files*

Upon conversion of loop data from text to database format, the user can now query the database to check the traffic information at any location along the I-4 corridor and for any specific time period. In order to query the loop detector database, the user must open one of the database files under 'File' menu. Then, the 'Loop Data' menu will be activated to allow the user to select 'Query'. As the user selects 'Query' the program will establish a connection with the database file for a few seconds until the 'Querying Loop Database' window appears as shown in Figure 7. The figure shows the available days in the selected database file that the user has just opened. The user can select one or more of the available days using the selection buttons. When done, the user can move forward by clicking on 'Next'.

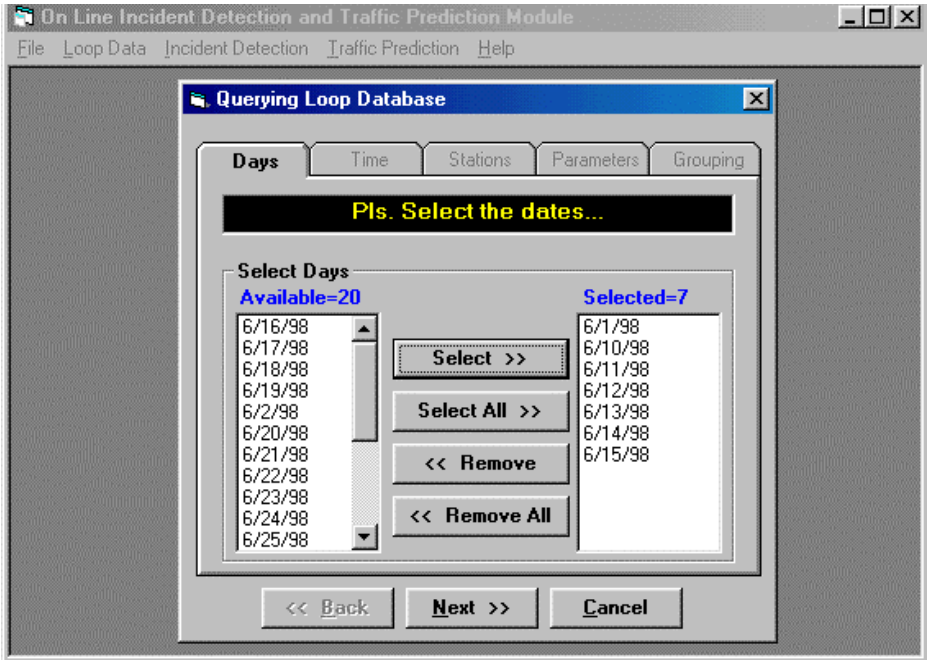

Figure 7: Snapshot of the 'Querying Loop Database' dialog window showing selection of days

The next tab allows the user to select the time period to query the database within as shown in Figure 8. In the figure, the user is assumed to have selected the time period from 6:00:00 AM to 10:00:00 AM. After the selection of the time period, the user can move forward by clicking 'Next'.

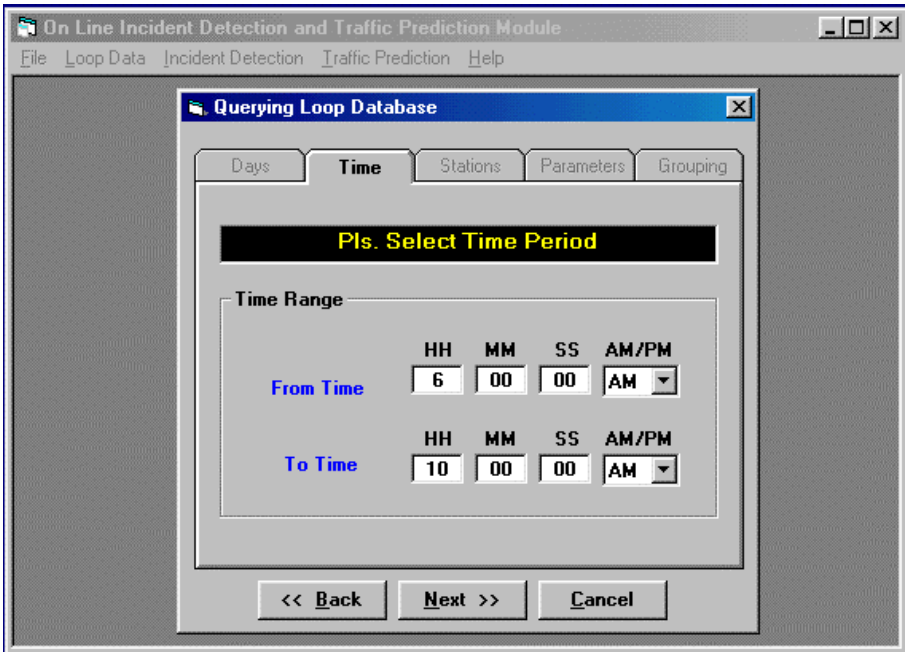

Figure 8: Snapshot of the 'Querying Loop Database' dialog window showing selection of time period

The next tab, shown in Figure 9, allows the user to select one of more of the loop detector stations along the I-4 corridor. The user must also select at least one direction and one lane. If more than one lane has been selected, the user will also have the option to check the 'average' checkbox, which calculates the average of the selected lanes. In this example, the user has selected to view the loop data for each of the three lanes in the eastbound direction, as well as the average of all three lanes. Clicking on 'Next' will take the user to the following tab.

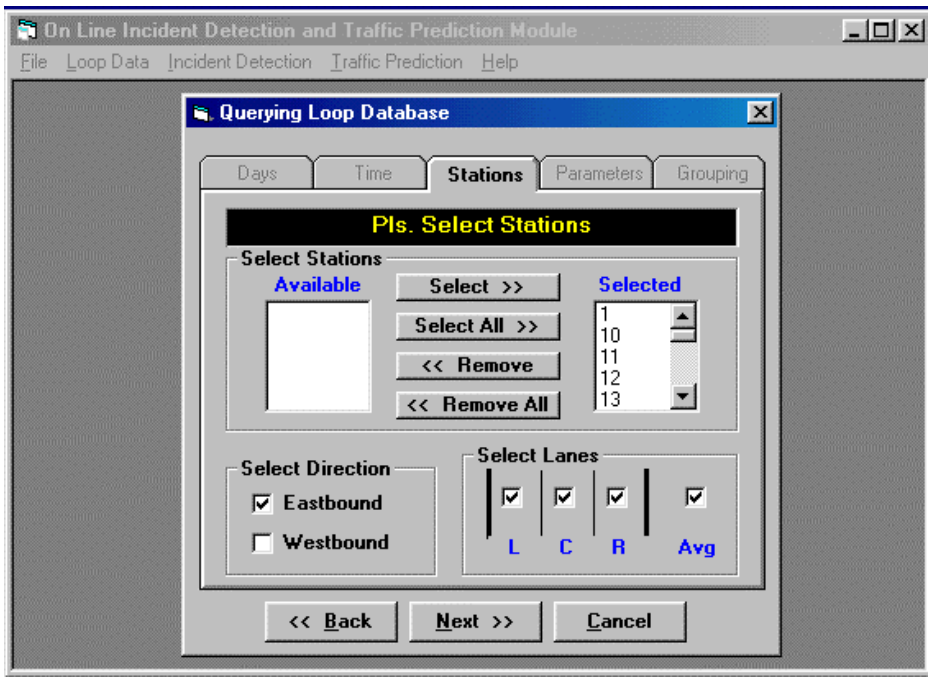

Figure 9: Snapshot of the 'Querying Loop Database' dialog window showing selection of stations, direction, and lanes

The next tab, shown in Figure 10, gives the user the option to choose one or more of the available traffic parameters namely, speed, volume, and occupancy. All three have been checked in this example. Again, clicking on 'Next' will take the user to the last tab of the query input parameters. The last tab is shown in Figure 11 and allows the user to either list the loop detector data every 30 seconds (the default) by checking the 'No Grouping' checkbox or group the query results by date, time, or both. Grouping the data by date only will result in the average of the selected traffic parameters over the entire selected time period for each selected station and for each selected day. Grouping the data by time only requires the user to choose the time interval over which the data will be averaged. This results in the averages of the selected traffic parameters over each time interval (say 5 minutes) and over all the selected days for each selected station. In this

example, we selected to group the data by time using 5 min time intervals. The user can also group the data by day and time. In this case, the results will be shown for each selected day independently.

Throughout the query input process, the user can go back and forth between the query tabs using the 'Back' and 'Next' button. When done, the user can start the querying process by clicking on 'Finish'. The querying process may take a few seconds until the results are displayed as shown in Figure 12. The query results are shown in a database grid format.

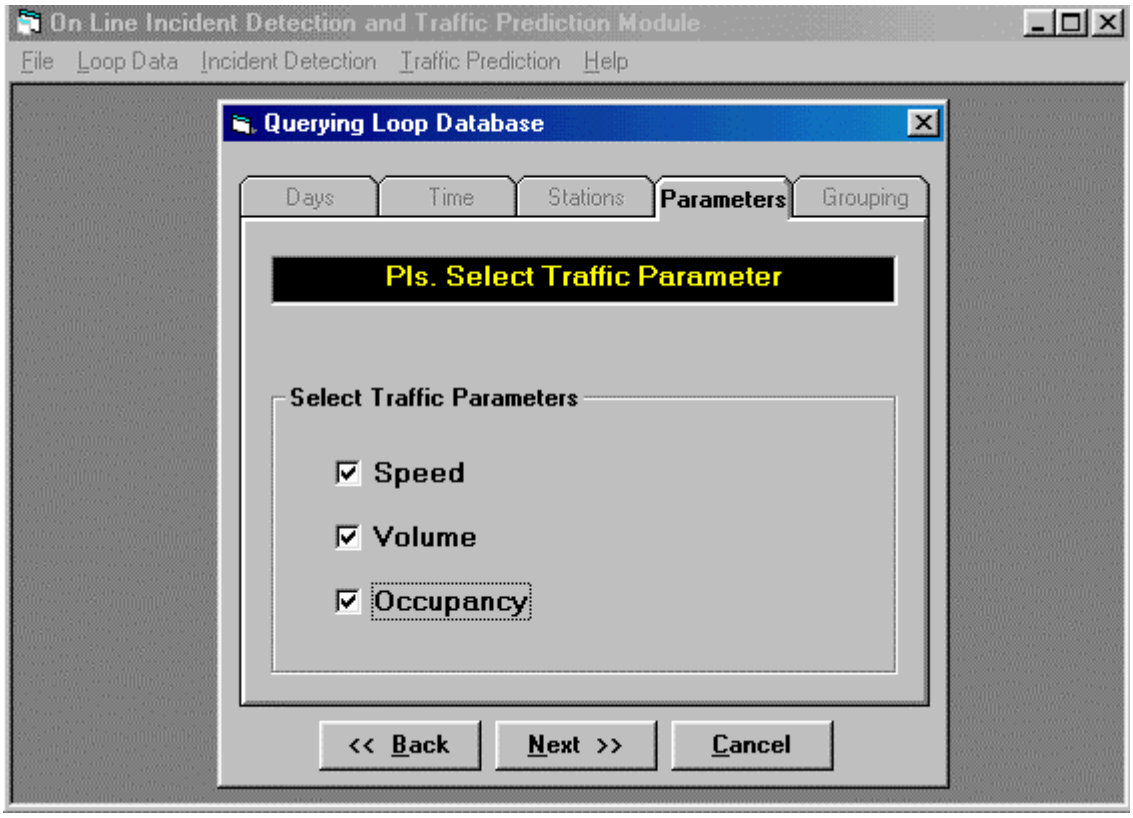

Figure 10: Snapshot of the 'Querying Loop Database' dialog window showing selection of traffic parameters

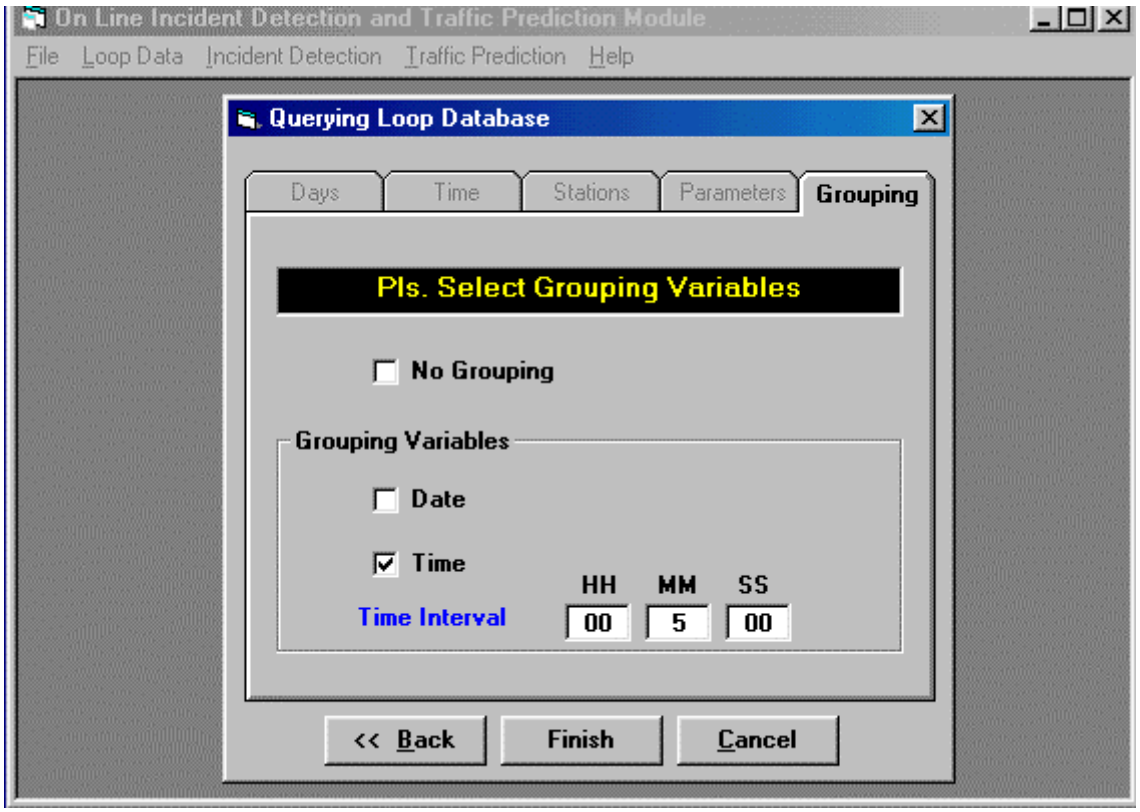

Figure 11: Snapshot of the 'Querying Loop Database' dialog window showing selection of grouping variables

Query Results

FromTime	ToTime	Station	E_L_SPD	E_C_SPD	E_R_SPD	E_L_VOL	E_C_VOL	E_R_VOL	E_L_OCC	E_C_OCC	E_R_
6:00:11 AM	6:04:49 AM	11	56	59.4	67.2	45	64	58	1.8	2.6	
6:00:11 AM	6:04:42 AM	13	64.4	57	54.6	72	77	55	3	3.1	
6:00:11 AM	6:04:44 AM	14	64.1	57.8	54.7	66	68	50	4.4	5.9	
6:00:11 AM	6:04:44 AM	15	59.4	64.6	58.8	72	61	47	3.3	2.7	
6:00:11 AM	6:04:49 AM	16	64.2	58.2	55.9	35	35	20	2.8	2.9	
6:00:11 AM	6:04:49 AM	17	64.2	65.5	55.4	46	50	40	4.8	2.7	
6:00:11 AM	6:04:49 AM	18	55.6	54.8	59.4	14	15	10	1.5	1.6	
6:00:11 AM	6:04:42 AM	20	50.4	62.2	56	3	3	4	1.2	1.6	
6:00:11 AM	6:04:41 AM	26	70.2	54.1	61.1	27	39	17	3.5	13.1	
6:00:11 AM	6:04:49 AM	28	62.2	57.3	55.7	87	87	57	3.6	3.6	
6:00:11 AM	6:04:49 AM	29	68.7	65.5	59.7	85	81	49	4	3.7	
6:00:11 AM	6:04:49 AM	30	53.7	52.7	64.5	77	67	32	7.9	8.7	
6:00:11 AM	6:04:49 AM	31	55.9	60.6	65.2	52	57	62	8.5	9.4	
6:00:11 AM	6:04:49 AM	32	65.1	59.8	60.7	93	90	78	6.2	7.6	
6:00:11 AM	6:04:49 AM	33	64.1	58.7	57.4	87	89	52	6.4	8.2	
6:00:11 AM	6:04:49 AM	34	55.6	54.5	49.7	111	93	56	9.3	7.9	
6:00:11 AM	6:04:49 AM	35	60.5	56.2	61.1	93	76	103	7.1	6.1	
6:00:11 AM	6:04:44 AM	36	66.7	64.1	60.1	31	72	58	2.7	6	
6:00:11 AM	6:04:44 AM	37	54.8	57.9	62	94	78	68	4.2	9	
6:00:11 AM	6:04:44 AM	38	55.8	58.9	61.8	96	85	72	9.7	9	
6:00:11 AM	6:04:44 AM	40	62.8	57.7	61.3	102	86	69	6.7	6.8	
6:00:11 AM	6:04:49 AM	41	52.6	56.1	57.9	51	98	83	3.4	6.3	
6:00:11 AM	6:04:49 AM	42	65.3	57.9	54.8	104	52	86	8.5	2	
6:00:11 AM	6:04:49 AM	45	58	49.1	50.8	131	111	79	10.1	11.2	
6:00:11 AM	6:04:49 AM	46	59.2	55.2	51.3	136	114	83	10.3	10.3	
6:00:11 AM	6:04:49 AM	47	56.1	59.7	53.2	114	133	67	6.8	7.2	
6:00:11 AM	6:04:49 AM	48	59.1	54.8	59	114	94	60	8.7	8.9	
6:00:11 AM	6:04:49 AM	51	74.6	56.6	60.1	89	78	64	7.6	3.9	
6:00:11 AM	6:04:41 AM	54	68.1	60.9	59.4	71	57	42	7.5	6.5	
6:00:11 AM	6:04:49 AM	55	60.3	48.7	60	92	51	75	6.7	7	
6:00:11 AM	6:04:49 AM	56	54.9	58	62.9	48	74	79	4.4	8.1	
6:00:11 AM	6:04:49 AM	57	54.6	58	62.3	31	59	70	1.7	3.5	

1723 Records

Figure 12: Snapshot of the query results

2.2.2 Incident Data

2.2.2.1 The 1993 and 1994 Incident Data Set

Similar to the treatment of loop detector data, the collected incidents were screened first to eliminate any duplication in incident records. In this report we also present the common characteristics of incidents on the study section of I-4. The characteristics of training and testing incident data sets are also compared to those of the entire incident database. It should be noted here that the proposed artificial neural network models are developed only for lane blocking incidents due to their perceived impact on the freeway capacity and the subsequently excessive delays to the motorists.

2.2.2.1.1 Incident Data Collection

Incident data was collected from logs compiled by the Freeway Management Center (FMC), Florida Highway Patrol (FHP), Orlando Police Department (OPD), and Maitland Police Department (MPD). The incident information provided by the FMC was collected by the traffic operator and based on surveillance observations using CCTV cameras.

The first data collection period started January 19th, 1993 through August 27th, 1994. The total number of incidents compiled from all sources was 1217. The distribution of incidents that occurred within the central corridor of I-4 with respect to each data source is shown in Figure 13. The majority of the incidents (83%) were compiled from the Orlando Police Department (OPD) reports and citations. The number of incidents collected by the traffic operator at FMC accounted for 10% of the entire database. A

small proportion of incidents were also collected from the FHP citations (6%) and Maitland Police Department (MPD) (1%).

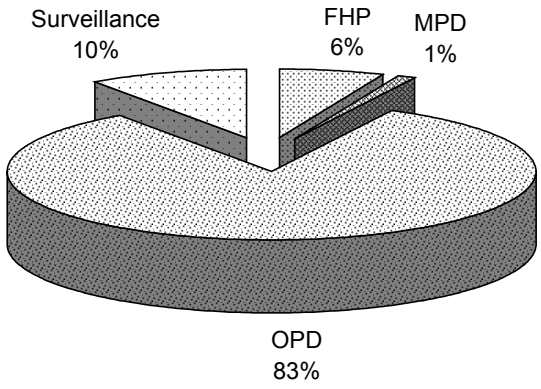

Figure 13: Distribution of incidents by data source

All incidents were classified as either lane blocking or non lane-blocking. Lane-blocking incidents include those that resulted in closing at least one lane of I-4. The proportions of lane blocking and non lane-blocking incidents for each direction of I-4 are shown in Figure 14. The figure shows that the proportion of non lane-blocking incidents slightly exceeds that of lane blocking incidents for each and both directions of I-4. Lane blocking incidents accounted for 45% of all incidents. Bearing in mind that lane-blocking incidents cause significant reduction in the freeway capacity, the high percentage of this incident type would substantially increase the amount of non-recurring congestion on I-4. The directional distribution of lane blocking incidents shows that the proportion of incidents in the eastbound direction is slightly higher than the westbound direction. No difference between the two directions was exhibited for non lane-blocking incidents. The overall proportion of both types does not show a significant difference between both directions.

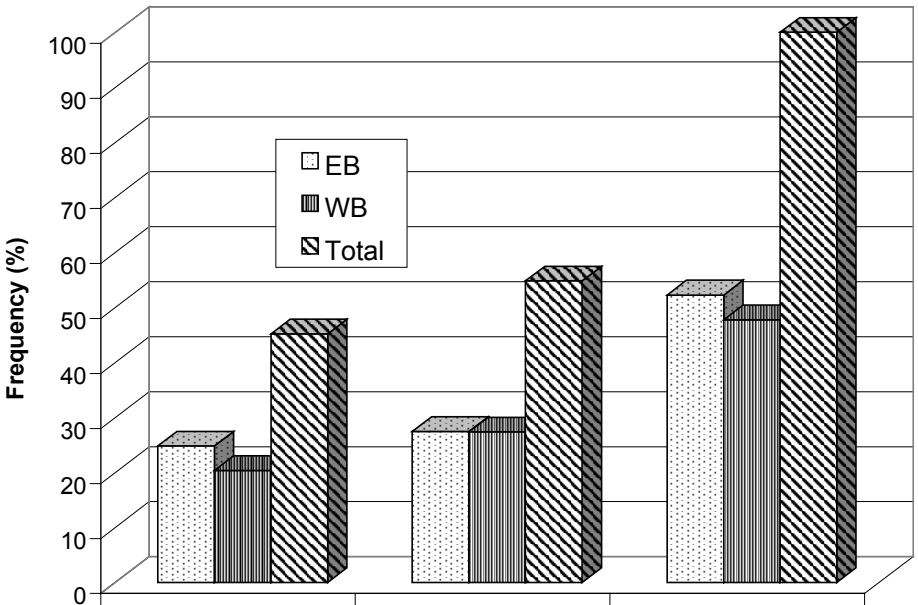

	LB	NLB	Total
EB	25	27	52
WB	20	27	48
Total	45	55	100

Figure 14: Distribution of incidents by incident type and direction of traffic

Because of the adverse impact of lane-blocking incidents on traffic conditions this research project attempts to improve the performance of lane blocking incident detection algorithms. Non lane-blocking incidents do not usually cause perceivable impact on the traffic conditions, and therefore, are much harder to detect automatically. Before selecting the incident data set, some of the relevant characteristics of lane blocking incidents are demonstrated next.

2.2.2.1.2 *Filtering the Incident Data Set*

This section provides a detailed description of the methodology used to collect and filter the incident data set. The characteristics of the incidents are exhibited in terms of the effect of incident type, location, time, and direction of travel on the distribution of incidents on I-4. All incidents were filtered using the associated speed and occupancy

profiles to validate their time and location. The total incident data set that was used in training and testing the Fuzzy ART model was narrowed down to 130 lane-blocking incidents. This set was further split into two subsets with the ratio of 2:1 for training and testing, respectively. Again, the characteristics of the selected incident data set were examined to ensure that they are representative of the entire data set.

Due to possible errors or inaccuracies in the data sources each lane-blocking incident was verified independently. The verification process involved plotting the speed and occupancy profiles at the time of the incident and observing the effect of the incident on the upstream and downstream stations. Verification required seeking enough evidence that the upstream and downstream stations have perceived the effect of the incident. In other words, an incident is verified if there was a drop in occupancy at the downstream station, associated with an increase in occupancy at the upstream station, or an increase in speed at the downstream station, associated with a drop in speed at the upstream station. The screening criterion was based only on visual observations of the effect of the incident on the occupancy and speed profiles. The screening process has two objectives. The first objective is to disqualify all incidents that were classified as lane blocking but did not show any perceived effect on the traffic conditions at the time and location reported by the incident data source. The second objective is to visually verify the time and location of each incident. In most cases, the reported incident time was a few minutes after the actual incident time. Determination of the actual incident time was based on observing sudden significant change in occupancy and speed between upstream and downstream stations.

For illustration we present an example of one of the lane blocking incidents in Figure 15. The figure shows the occupancy patterns before and after the reported incident time. This incident was reported between station 15 and station 14 on the westbound direction of I-4, where station numbering decreases in the direction of travel. The figure shows that occupancy at the upstream station (15) increases from 12% to 25% after the incident occurred. Meanwhile, the occupancy at the downstream station (14) slightly dropped to nearly 7%. It should be noted that while the incident was reported at time period 48 from the beginning of the profile, the figure indicates that the change in occupancy patterns started earlier at time period 36. This indicates that the reported incident time was nearly 6 minutes past the actual incident time. This bias was observed in most of the examined incident profiles, and therefore, screening each individual incident profile was deemed necessary. Likewise, speed patterns, as shown in Figure 16, exhibit a sudden drop in speed at the upstream station (15) after the incident occurred, while maintaining high speed at the downstream station (14). Both occupancy and speed profiles were used to verify each individual incident case in the incident database.

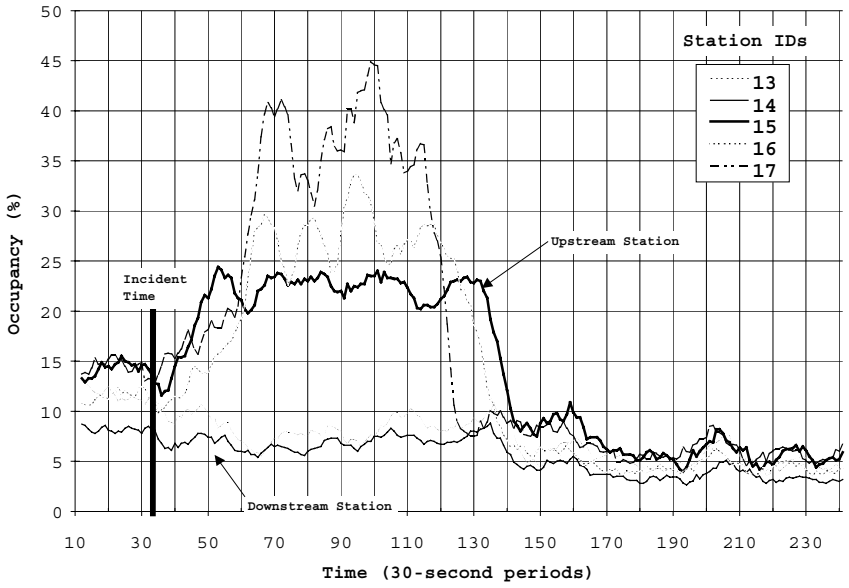

Figure 15: Occupancy patterns in the vicinity of the incident location

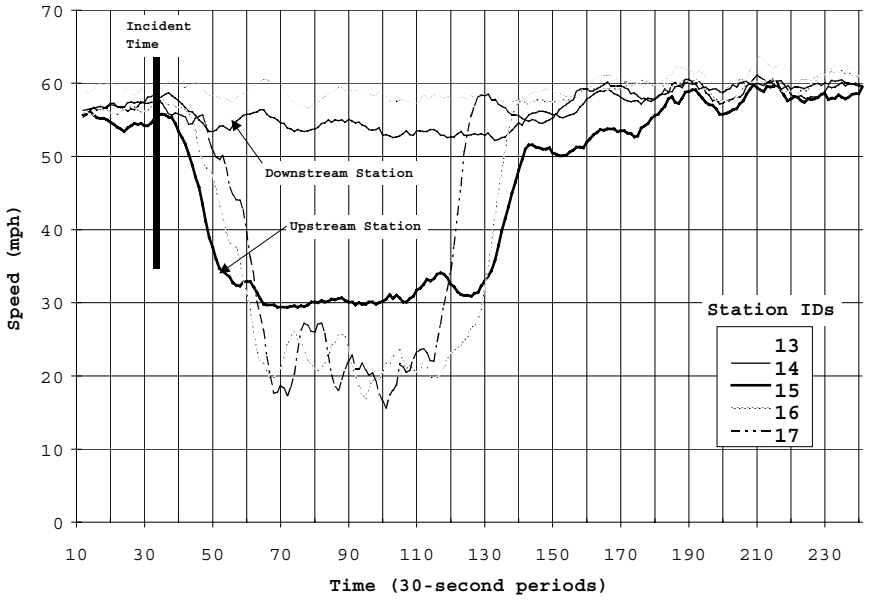

Figure 16: Speed patterns in the vicinity of the incident location

Not only was the verification process necessary to check the incident information gathered from the data sources but also to verify the quality of the loop detector data at the time and location of the incident. In a few circumstances occupancy and speed patterns were not available at the incident time and location because of a complete failure in the upstream and downstream loop detectors. In such situations the effect of the incident on traffic patterns was not available and the corresponding incident had to be discarded from the study. At the end of the verification process the incident database was narrowed down to a total of 130 lane-blocking incidents. The resulting data set was randomly split up into subsets, one for training and the other for testing. The ratio between the size of the training and testing data sets was arbitrarily selected as 2:1. In the next section we highlight some of the characteristics of the selected incident data set.

2.2.2.1.3 Lane-Blocking Incident Characteristics

One of the other important incident characteristics is the distribution of incidents by time of day for each direction. Figure 17 clearly shows the high frequency of incidents in the afternoon peak period (from 3:00 to 6:00 PM). The eastbound lane-blocking incident frequency is higher than the westbound frequency in the afternoon peak period. Observation of the directional peaking characteristics on I-4 has revealed that the peaking conditions prevail in the eastbound direction in the evening and the westbound direction in the morning. This is illustrated in Figure 18 that shows the proportion of incidents during peak and off-peak periods for each direction. The overall proportion of incidents observed during morning (6:00 AM to 9:00 AM) and evening (3:00 PM to 6:00 PM) peak periods constituted 58% of all incidents. The high occurrence of lane blocking incidents

is expected during peak periods due to the high traffic demand and the subsequent recurring congested conditions. The adverse impact of an incident on the traffic conditions, coupled with the existing recurring congestion, then becomes worsened. Fast and reliable detection and clearance of such incidents will alleviate the unduly delays and congestion at such times.

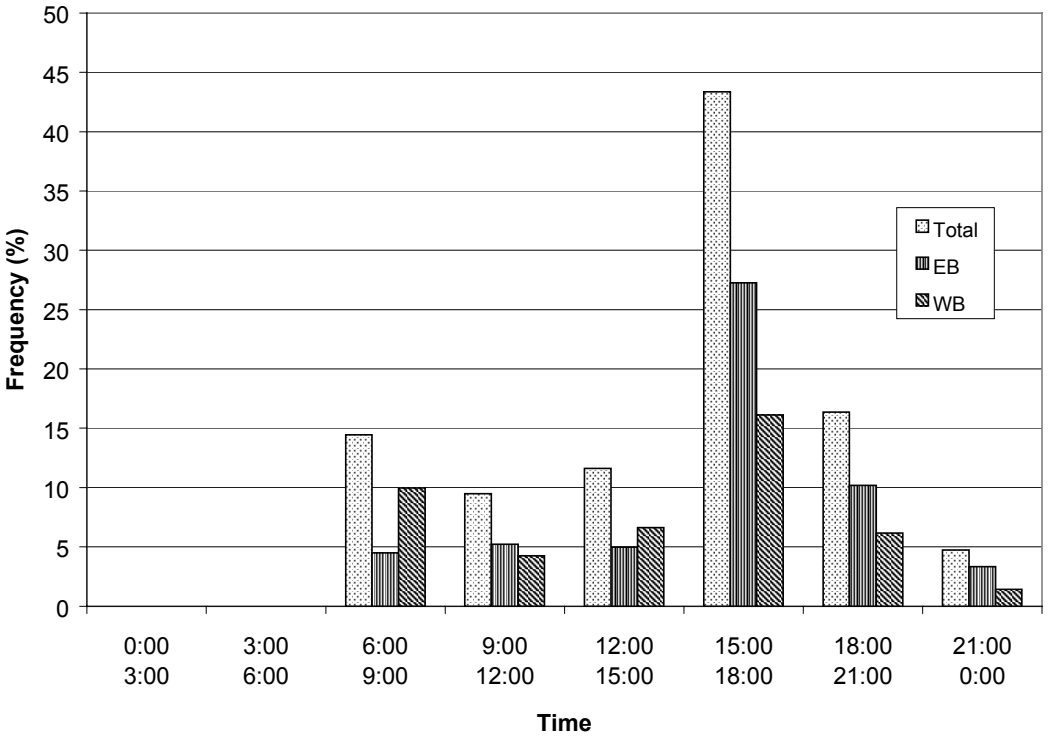

Figure 17: Temporal distribution of lane blocking incidents by direction of traffic

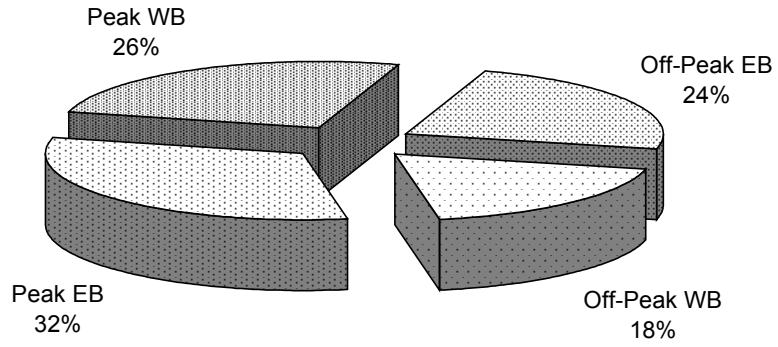

Figure 18: Peaking characteristics of lane blocking incidents

Similarly, the spatial distribution of lane blocking incidents for each direction is shown in Figure 19. The figure shows the proportion of incidents at each loop detector station to reveal high frequency areas of I-4. High frequency is observed at certain locations such as the vicinity of Rio Grande and Winter Park interchanges. Locations in the vicinity of the downtown of Orlando are also characterized with high incident frequency, most likely due to the high maneuvering activities at merging and diverging points near on- and off-ramps.

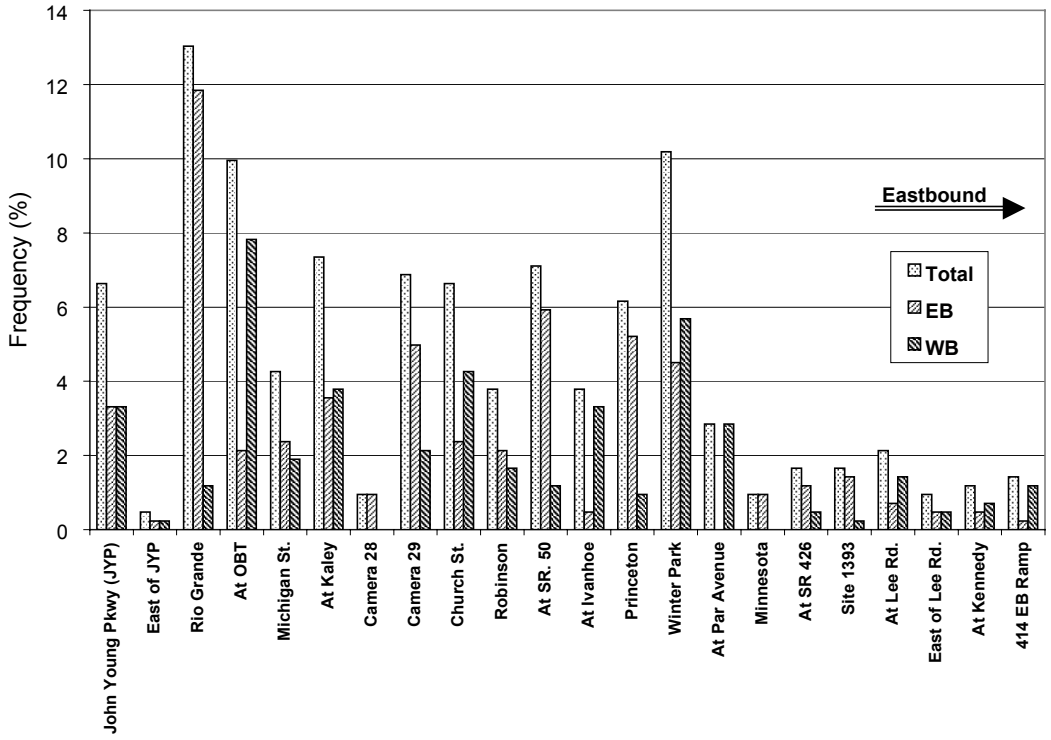

Figure 19: Spatial distribution of lane blocking incidents by direction of traffic

2.2.2.1.4 *Characteristics of the Selected Incident Set*

The distribution of the lane-blocking incidents for the verified incident data set by the data source is shown in Figure 20. The proportion of verified incidents that were collected by FHP and MPD is similar to that of the entire data set. However, the proportion of surveillance incidents increased from 10% of all lane-blocking incidents in the original data set (450 incidents) to 25% of the lane-blocking incidents in the verified data set. This was accompanied by a decrease in the proportion of incidents collected by OPD from 83% to 67%. Such observation leads to the conclusion that surveillance data quality was the most accurate and reliable among all other sources. On the contrary, the largest proportion of incidents removed from the original database was compiled by OPD, leading to the conclusion that OPD was the least accurate source.

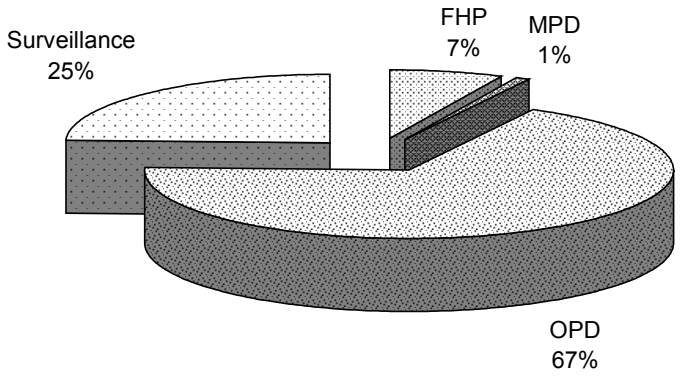

Figure 20: Distribution of the verified lane blocking incidents by data source

In this section we present the temporal distribution of the verified incident data set, as well as the two subsets used for training and testing. The distribution of the verified incident data set, shown in Figure 21, appears to be similar to that of the original incident database, except for the morning peak that shows a higher proportion of incidents. The proportion during the evening peak period remains to be dominant. This suggests that the selected incident data set is a representative sample of the original data set.

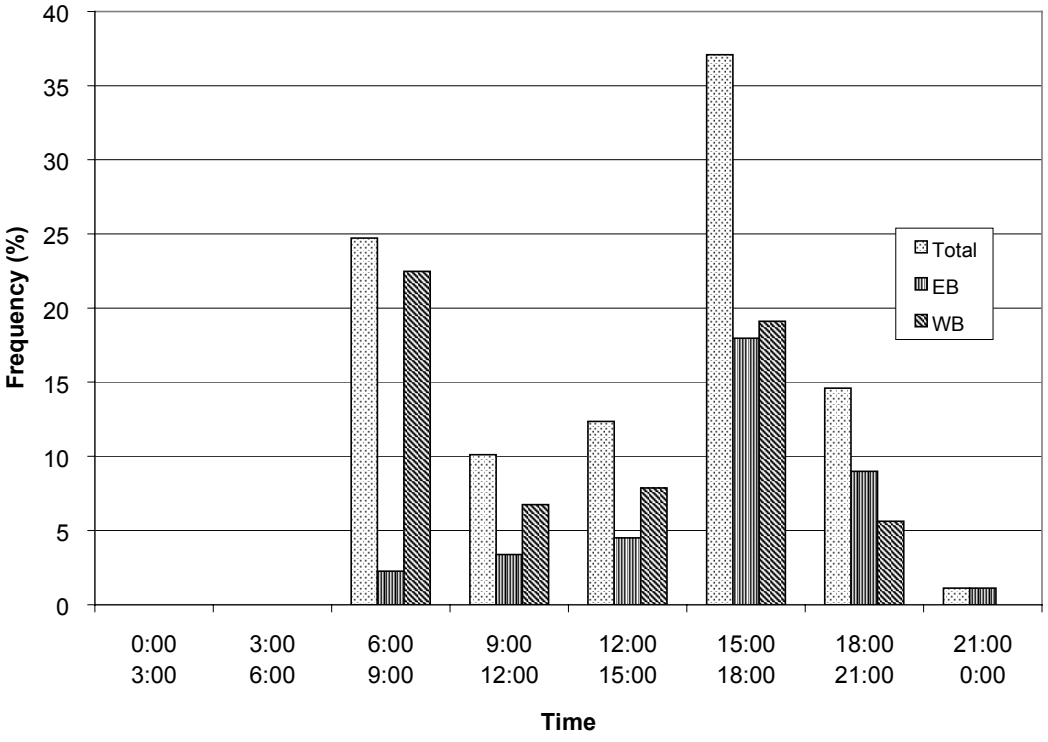

Figure 21: Temporal distribution of the verified lane blocking incidents

2.2.2.2 The New Incident Data Set

A new set of incidents was collected from Orlando Police Department, Maitland Police Department, Florida Highway Patrol, and Highway Helpers. The new incident set was collected for the period from September '97 to September '98 and was processed to extract the necessary information from the accident reports. The total number of incidents collected on I-4 for this period was 4946. A sample of the incident set is shown in Figure 22.

DATE	ID	SOURCE	LOCATION	Direction	TYPE	TM RPT	DISPAT	ARRIVAL	COMPLT	DISPOSITION	US STATION
9/15/97	9700337844	OPD	ROBINSON	WBO	ACC W/BLOCK	17:50	18:39	18:39	18:39		40
9/15/97	9700337387	OPD	PRINCETON	WBO	ACC	10:34	10:42	10:55	12:13	CR	44
9/15/97	9700337224	OPD	ANDERSON	EBO	ACC	7:45	7:49	8:17	8:17	T	37
9/15/97	9700337846	OPD	COLONIAL	WBO	ACC W/BLOCK	17:51	17:58	18:06	18:34	T	41
9/15/97	9700337855	OPD	JOHN YOUNG	EBO	ACC W/BLOCK	18:03	18:03	18:13	19:32	B	29
9/15/97	9700337235	OPD	KIRKMAN	EBO	ACC	7:57	7:59	8:15	8:31	J	23
9/15/97	97285866407	FHP	I4 EBO AT MM 89	EBO	ACC	16:54					52
9/15/97	97285868007	FHP	I4 WBO & SR600	WBO	OBSTRUCTION	18:45					52
9/15/97	97285866107	FHP	I4 EBO & FAIRBANKS	EBO	ACC W/BLOCK	16:38					46
9/15/97	97285857507	FHP	I4 EBO W OF KIRKMAN	EBO	ACC	8:30					23
9/15/97	97285865507	FHP	I4 EBO & LEE RD	EBO	ACC	16:26					48
9/15/97	97285867607	FHP	I4 & PAR		ACC	18:09					45
9/17/97	9700340324	OPD	IVANHOE	EBO	ACC	16:01	16:02	16:15	17:51	T	41
9/17/97	9700339841	OPD	JOHN YOUNG	EBO	ACC W/INJ	7:56	7:56	8:06	13:57	B	29
9/17/97	9700339881	OPD	JOHN YOUNG	EBO	ACC W/BLOCK	8:38	8:46	9:25	9:25	CR	29
9/17/97	9700340331	OPD	COLONIAL	EBO	ACC W/INJ	16:04	16:15	16:15	16:15		40
9/17/97	9700339876	OPD	JOHN YOUNG	EBO	ACC	8:33	8:33	8:33	9:34	T	29
9/17/97	9700339863	OPD	KIRKMAN	WBO	ACC	8:16	8:17	8:17	8:17		24
9/17/97	9700340462	OPD	IVANHOE	EBO	ACC W/BLOCK	18:03	18:21	18:37	19:54	T	41
9/17/97	9700340087	OPD	CENTRAL	EBO	HIT & RUN	12:40	12:40	12:40	14:45	B	38
9/17/97	97285887707	FHP	I4 WBO W OF SAND LAKE	WBO	DAV	7:03					21
9/17/97	97285894707	FHP	I4 EBO AT ENT TO SR 535	EBO	OBSTRUCTION	15:00					9
9/17/97	97285898907	FHP	I4 EBO & IVANHOE	EBO	ACC	18:10					41
9/18/97	9700341777	OPD	1/2 MI. WEST OF S. ORANGE BLOSSOM	EBO	ACC W/BLOCK	16:56	16:56	17:07	18:57	T	31
9/18/97	9700341667	OPD	100 FT. EAST OF IVANHOE	EBO	ACC W/BLOCK	15:29	15:35	15:51	16:29	T	41
9/18/97	9700341425	OPD	KALEY	WBO	DAV	12:06	12:06	12:06	12:48	JB	37
9/18/97	97341809	OPD	500 FT. WEST OF SR408 (E-W EXPRWY)	EBO	HIT&RUN	17:28	17:36	17:45			37
9/18/97	97341678	OPD	1/4 MI. WEST OF E. KALEY	EBO	HIT&RUN	15:30	15:38	15:57			35
9/18/97	9700341778	OPD	ORANGE BLOSSOM	EBO	ACC W/BLOCK	16:56	16:56	16:56	16:56		31
9/18/97	9700341808	OPD	SOUTH	EBO	ACC	17:27	17:30	17:30	17:30		38
9/18/97	9700341810	OPD	PRINCETON	WBO	ACC W/BLOCK	17:29	17:30	17:47	17:47	JB	44
9/18/97	9700341849	OPD	300 FT. WEST OF PAR	WBO	ACC	17:30	17:42	17:52	19:35	T	46
9/18/97	9700341818	OPD	3/4 MI. WEST OF IVANHOE	EBO	ACC W/BLOCK	17:32	17:36	18:11	19:31	T	41
9/18/97	9700341847	OPD	PRINCETON	WBO	ACC	17:51	17:57	17:57	17:57		44
9/18/97	9700341835	OPD	GORE	WBO	ACC W/BLOCK	17:41	18:19	18:23	18:40	C	35
9/18/97	9700341807	OPD	SOUTH (STREET)	WBO	ACC	17:27	17:59	17:59	17:59		38
9/18/97	97285903707	FHP	I4 & SR 536		ABAND. VEH.	8:08					8
9/18/97	97285907307	FHP	I4 WBO & SR 50	WBO	ACC	15:16					41
9/18/97	97285903507	FHP	I4 WBO & SR 536	WBO	ABAND. VEH.	8:03					8
9/18/97	97285904807	FHP	I4 WBO OFF RAMP TO SR 535	WBO	ACC	10:26					11
9/18/97	97285902707	FHP	I4 EBO & EXIT 29	EBO	ACC	6:44					19
9/18/97	9700341809	OPD	ANDERSON	EBO	ACC W/BLOCK	17:28	17:36	17:45	19:27	B	37
9/18/97	9700341680	OPD	COLONIAL	EBO	ACC	15:37	15:37	15:37	15:53	C	40
9/18/97	97285906807	FHP	I4 WBO EXIT RAMP TO LEE RD	WBO	ACC	15:02					49
9/18/97	97285909407	FHP	I4 EBO E OF SR 535	EBO	DAV	16:47					10
9/19/97	9700343100	OPD	KIRKMAN	WBO	ACC W/INJ	15:19	15:25	15:25	15:25		24
9/19/97	97343391	OPD	1/2 MI. WEST OF OBT	EBO	HIT&RUN	18:00	18:05	18:19			32
9/19/97	97281351817	FHP	I4 WBO W OF SR 434 IN MEDIAN	WBO	DAV	15:08					60
9/19/97	9700343195	OPD	PRINCETON	EBO	ACC	16:30	16:30	16:35	16:35	JB	43
9/19/97	97343393	OPD	6200 INTERNATIONAL DR.	EBO	ACC	18:30	19:20	19:30			21
9/19/97	9700343132	OPD	JOHN YOUNG	EBO	ACC	15:45	15:45	15:45	16:05	C	29
9/19/97	9700343125	OPD	1/2 MI. WEST OF SR500	EBO	ACC	15:38	15:43	15:56	16:58	B	29
9/19/97	9700343193	OPD	PRINCETON	WBO	ACC W/INJ	16:29	16:30	16:39	16:39	JB	44
9/19/97	9700343165	OPD	ORANGE BLOSSOM	EBO	ACC W/BLOCK	16:11	16:14	16:16	16:16	JB	32
9/19/97	97285919507	FHP	I4 & SR 528		ABAND. VEH.	10:10					17
9/19/97	97285919607	FHP	I4 & SR 528 IN MEDIAN		ABAND. VEH.	10:29					17
9/19/97	97285918107	FHP	I4 & CENTRAL FL PKWY		ABAND. VEH.	8:14					15
9/19/97	97285919407	FHP	I4 & CENTRAL FL PKWY		ABAND. VEH.	10:04					15
9/19/97	97285920407	FHP	I4 & SR 91		FIRE	11:18					25
9/19/97	97285919207	FHP	I4 WBO & SR 536	WBO	ABAND. VEH.	9:45					8
9/19/97	97285921707	FHP	I4 EBO & SR 408	EBO	OBSTRUCTION	13:26					37
9/19/97	97285929907	FHP	I4 & KALEY		HIT & RUN	18:01					36
9/19/97	97285917907	FHP	I4 WBO W OF 482	WBO	DAV	8:04					20
9/19/97	97285927107	FHP	I4 WBO & PRINCETON	WBO	ACC	16:51					44
9/22/97	9700347058	OPD	EW EBO	EBO	ACC W/BLOCK	18:02	18:22	18:32	18:32	JB	37
9/22/97	9700346974	OPD	KALEY	EBO	DAV	16:30	16:34	16:46	16:51	JB	36
9/22/97	97347088	OPD	SR408 EXIT RAMP		ACC	18:15	18:22	18:22			37
9/22/97	9700347004	OPD	50 FT. SOUTH OF ANDERSON EXIT	WBO	ACC	17:01	17:30	17:38	18:56	B	39
9/22/97	97285971107	FHP	I4 & SR 535		ABAND. VEH.	10:00					10

Figure 22: A sample of the incident data set collected in 1997/1998 on I-4

The figure shows the information collected on each incident as follows:

DATE: The date of the incident

ID: A unique incident identification number

SOURCE: The source of the incident report: FHP, OPD, or MPD

LOCATION: A description of the incident location in terms of the nearest interchange.

DIRECTION: The direction in which the incident happened (EB or WB)

TYPE: The incidents were classified according to the reports into one of the following types:

Accident
Abandoned vehicle
Disabled Vehicle
Hit and Run
Obstruction
Others: such as fire, etc.

TM RPT: The time the incident was reported

DISPAT: The time the emergency vehicles were dispatched.

ARRIVAL: The time the assistance arrived at the incident scene

COMPLT: The time the incident was removed from the freeway

DISPOSITION: The following explains the abbreviations adopted in this field

For MPD data

SF short accident form
LF long "
IR incident report
NR no report
GOA gone on arrival
TOT turned over to another agency
UNF unfounded
TOW towed
AR arrest

For OPD data

CR accident report
J turned over to another agency (no report)

JB turned over to another agency (report filed)

BB incident cancelled and no report filed

DUP duplicate call for the same incident

US STATION: The nearest upstream station number.

The new incident data set was examined to reveal the common characteristics of the incidents on I-4 collected from OPD, MPD and FHP. Figure 23 shows the distribution of all incidents collected on the study section of I-4 by the source of information. The majority of incidents were collected from the incident reports obtained from OPD, totaling 65% of all incidents, followed by 34% from FHP and 1% from MPD. The spatial distribution of all incidents by source is also depicted in Figure 24.

Another important characteristic of the incident data set is the distribution of incidents by type. Figure 25 shows that the majority of incidents on I-4 are classified as accidents, regardless of the type, and they constitute a total of 62% of the entire set. This is followed by abandoned vehicle (15%), disabled vehicle (12%), hit and run (8%), obstruction (3%), and others (less than 1%). Also, the spatial distribution of all incidents and accidents is shown in Figure 26. The figure indicates that the section of I-4 between station 37 and station 42 has the highest concentration of incidents and accidents. This area falls within the downtown of the city of Orlando and has the highest density of on- and off-ramps.

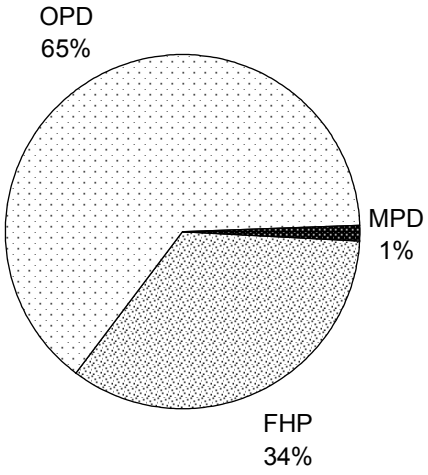

Figure 23: Distribution of incidents on I-4 by source

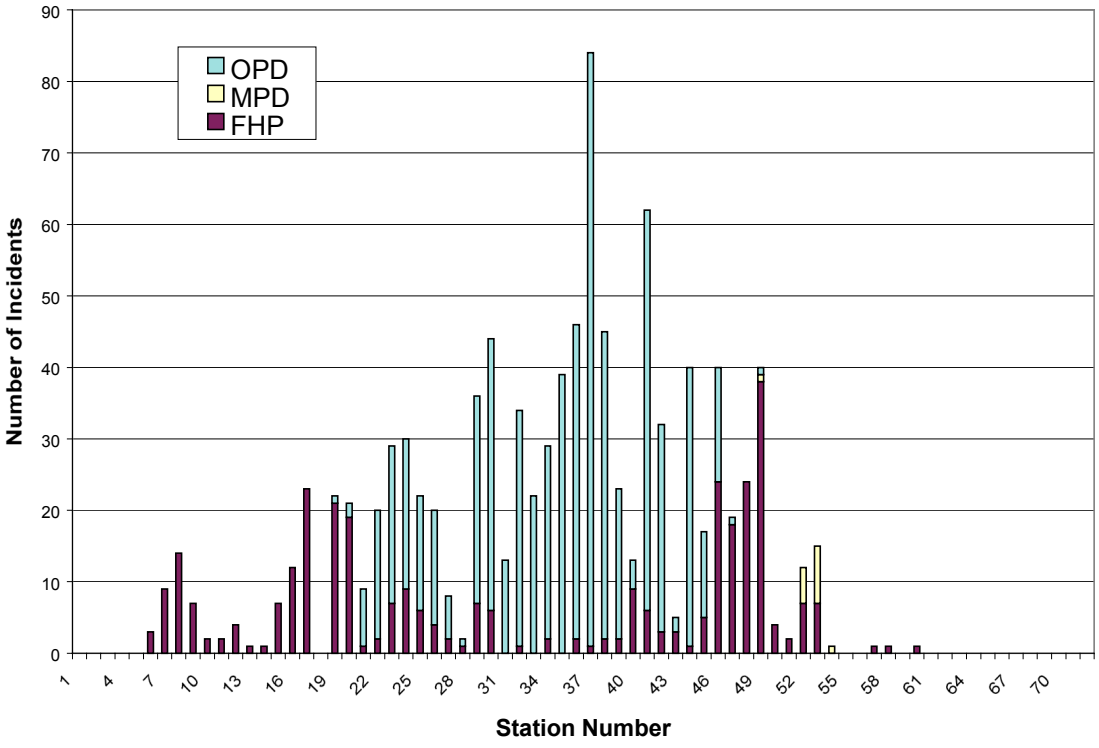

Figure 24: Spatial distribution of incidents on I-4 by source

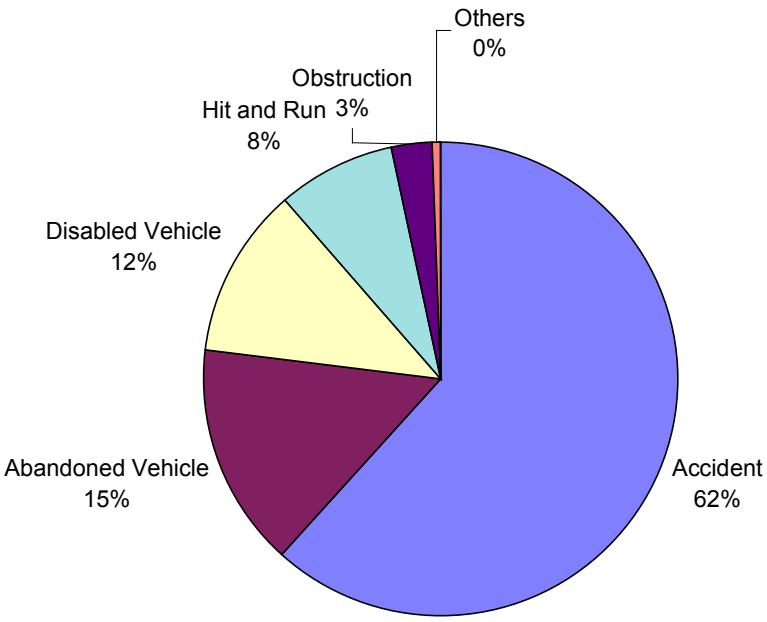

Figure 25: Distribution of incidents on I-4 by type

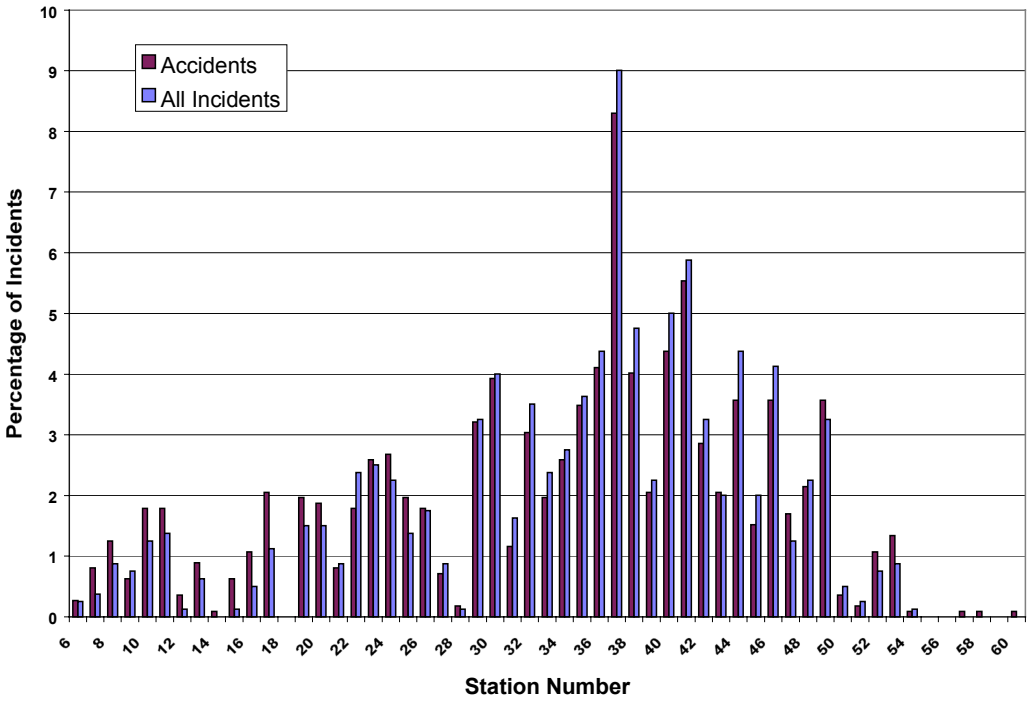

Figure 26: Spatial distribution of all incidents and accidents on I-4

2.3 INCIDENT DETECTION MODULE

This task involves the development of an incident detection system on I-4 that is based on Artificial Neural Networks (ANN). The new algorithm was developed using the Fuzzy ART network. The major improvements in the new module were in the underlying mechanism in data retrieval and storage. The data retrieval mechanism is now more robust and flexible than it used to be. It has better error handling routines to account for unexpected runtime errors due to poor communications. Also, the real time data is now directed to a database rather than a text-based (ASCII) file. This allows the users to access the data and conduct queries on the database more efficiently. The incident detection module used in the analysis is described in detail in this section.

2.3.1 Software Conversion

Throughout the development process, this module underwent a conversion from MS Visual Basic 5.0 to MS Visual Basic 6.0 in order to incorporate the new enhancements in data access and management introduced in the new version of VB 6.0. The improved data access features improved the overall performance of the software through faster and more efficient data access objects. Another major improvement in the software is its ability to manipulate the old loop detector data that was collected back in 1993 and 1994. The data was also converted to a database MS Access format, known as "mdb" format, which was compatible with the software. This feature allows for viewing, querying, and filtering the old loop database.

2.3.2 Real Time Loop Detector Data

The developed module allows for retrieval of real time loop detector data from the Freeway Management Center (FMC) over the phone line. A dial-up connection can be easily established between the ITS lab at UCF and the computer system located at FMC, allowing for direct communication with the existing surveillance system. The communication is established between a PC (client running Windows 98) at the ITS lab and another PC (server running also Windows 98 and a dial-up server) at FMC. The server PC is networked at FMC with the communication server (D5MISCOM with NT platform), where the loop detector data is collected every 30 seconds. The main role of the dial-up server is to link the client PC at the ITS lab to the D5MISCOM server.

The real time feature of downloading loop detector data was significantly improved over the last version produced in a previous research project titled "Online Testing of Incident Detection Algorithms". The feature is explained in detail in the following subsections. The steps explained here assume that a dial-up connection has been already established between the computer running this application and the dial-up server at FMC. First the user should invoke the real time data collection function from the main menu by selecting "Setup" from the "On-Line" menu as shown in Figure 27.

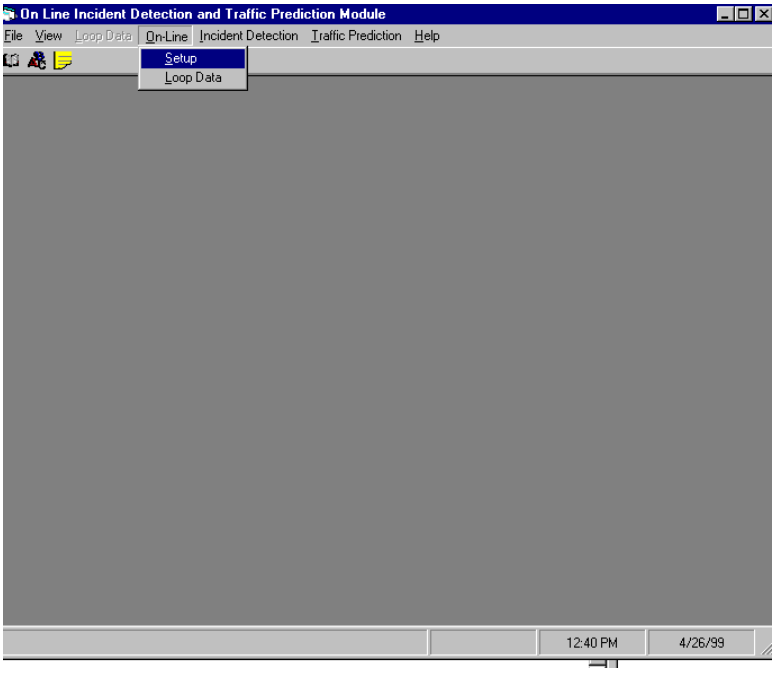

Figure 27: Main Menu of the Online Incident Detection and Traffic Prediction System

2.3.2.1 'Setup' option

The setup option must be configured before the user can launch the real time data retrieval process. The properties that must be set are shown in Figure 28. The dialog window prompts the user for the following information:

- Computer Name: This refers to the name of the remote computer where the loop detector data is initially compiled. At this time, this refers to the "D5MISCOM" server previously mentioned.
- Directory: This points to the remote directory where the device drivers are located. The default directory name is 'detectordd'.

On the local system, the user must also select a log file, where the real time data will be routed and stored cumulatively. This file must be a MS Access database file (mdb format). Currently, loop detector data collected in the same year is stored in one file,

where each day is compiled in one table. Each table is given a name that starts with the letter "d" followed by the date in the format "mmddyy", where mm, dd, and yy refer to the month, day, and year, respectively. For instance, data collected on March 21, 2000 is stored in the table "d032100". The user must click on the button "Save As" to point to the location and name of the selected database file. When done, the user can click "OK" and proceed to the next section.

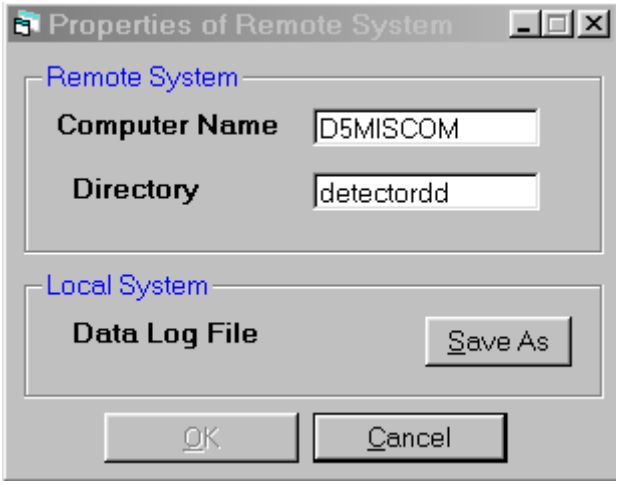

Figure 28: Setting remote and local connection properties

2.3.2.2 'Loop Data' option

After setting up the connection properties, the user can launch the real time loop data function by selecting 'Loop Data' from the 'On-line' menu as shown previously in Figure 27. This action will launch a new window as shown in Figure 29. The grid shown in the figure will appear blank, except for the station 'IDS' and the description of station locations, until the user clicks on the Start button. The connection will be established and the process of data retrieval will begin. After 30 seconds, the first data packet will arrive and parsed into the data grid as shown in Figure 29.

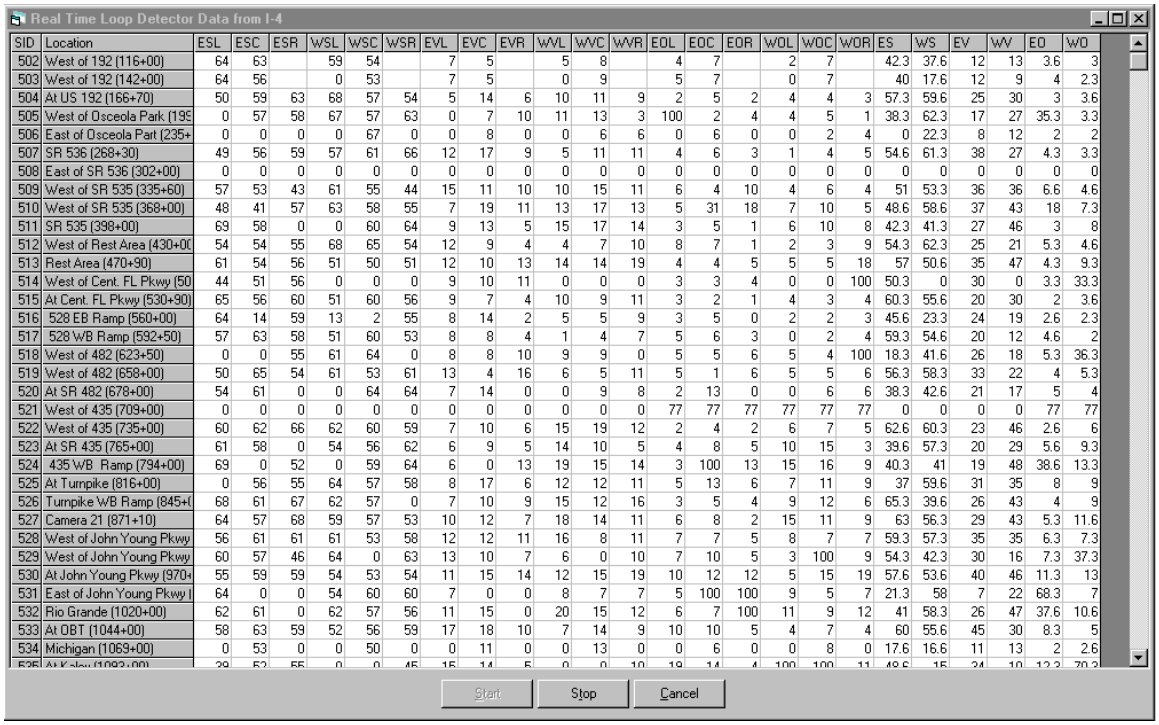

SID	Location	ESL	ESC	ESR	WSL	WSC	WSR	EVL	EVC	EVR	WVL	WVC	WVR	EOL	EOC	EOR	WOL	WOC	WOR	ES	WS	EV	WV	EO	WO
502	West of 192 (116+00)	64	63		59	54		7	5		5	8		4	7		2	7		42.3	37.6	12	13	3.6	3
503	West of 192 (142+00)	64	56		0	53		7	5		0	9		5	7		0	7		40	17.6	12	9	4	2.3
504	At US 192 (166+70)	50	59	63	68	57	54	5	14	6	10	11	9	2	5	2	4	4	3	57.3	59.6	25	30	3	3.6
505	West of Osceola Park (19	0	57	58	67	57	63	0	7	10	11	13	3	100	2	4	4	5	1	38.3	62.3	17	27	35.3	3.3
506	East of Osceola Part (235+	0	0	0	0	67	0	0	8	0	0	6	6	0	6	0	0	2	4	0	22.3	8	12	2	2
507	SR 536 (268+30)	49	56	59	57	61	66	12	17	9	5	11	11	4	6	3	1	4	5	54.6	61.3	38	27	4.3	3.3
508	East of SR 536 (302+00)	0	0	0	0	0	0	0	0	0	0	0	0	0	0	0	0	0	0	0	0	0	0	0	0
509	West of SR 535 (335+60)	57	53	43	61	55	44	15	11	10	10	15	11	6	4	10	4	6	4	51	53.3	36	36	6.6	4.6
510	West of SR 535 (368+00)	48	41	57	63	58	55	7	19	11	13	17	13	5	31	18	7	10	5	48.6	58.6	37	43	18	7.3
511	SR 535 (398+00)	69	58	0	0	60	64	9	13	5	15	17	14	3	5	1	6	10	8	42.3	41.3	27	46	3	8
512	West of Rest Area (430+0(	54	54	55	68	65	54	12	9	4	4	7	10	8	7	1	2	3	9	54.3	62.3	25	21	5.3	4.6
513	Rest Area (470+90)	61	54	56	51	50	51	12	10	13	14	14	19	4	4	5	5	5	18	57	50.6	35	47	4.3	9.3
514	West of Cent. FL Pkwy (50	44	51	56	0	0	0	9	10	11	0	0	0	3	3	4	0	0	100	50.3	0	30	0	3.3	33.3
515	At Cent. FL Pkwy (530+90)	65	56	60	51	60	56	9	7	4	10	9	11	3	2	1	4	3	4	60.3	55.6	20	30	2	3.6
516	528 EB Ramp (560+00)	64	14	59	13	2	55	8	14	2	5	5	9	3	5	0	2	2	3	45.6	23.3	24	19	2.6	2.3
517	528 WB Ramp (592+50)	57	63	58	51	60	53	8	8	4	1	4	7	5	6	3	0	2	4	59.3	54.6	20	12	4.6	2
518	West of 482 (623+50)	0	0	55	61	64	0	8	8	10	9	9	0	5	5	6	5	4	100	18.3	41.6	26	18	5.3	36.3
519	West of 482 (658+00)	50	65	54	61	53	61	13	4	16	6	5	11	5	1	6	5	5	6	56.3	58.3	33	22	4	5.3
520	At SR 482 (678+00)	54	61	0	0	64	64	7	14	0	0	9	8	2	13	0	0	6	6	38.3	42.6	21	17	5	4
521	West of 435 (709+00)	0	0	0	0	0	0	0	0	0	0	0	0	77	77	77	77	77	77	0	0	0	0	77	77
522	West of 435 (735+00)	60	62	66	62	60	59	7	10	6	15	19	12	2	4	2	6	7	5	62.6	60.3	23	46	2.6	6
523	At SR 435 (765+00)	61	58	0	54	56	62	6	9	5	14	10	5	4	8	5	10	15	3	39.6	57.3	20	29	5.6	9.3
524	435 WB Ramp (794+00)	69	0	52	0	59	64	6	0	13	19	15	14	3	100	13	15	16	9	40.3	41	19	48	38.6	13.3
525	At Turnpike (816+00)	0	56	55	64	57	58	8	17	6	12	12	11	5	13	6	7	11	9	37	59.6	31	35	8	9
526	Turnpike WB Ramp (845+(	68	61	67	62	57	0	7	10	9	15	12	16	3	5	4	9	12	6	65.3	39.6	26	43	4	9
527	Camera 21 (871+10)	64	57	68	59	57	53	10	12	7	18	14	11	6	8	2	15	11	9	63	56.3	29	43	5.3	11.6
528	West of John Young Pkwy	56	61	61	61	53	58	12	12	11	16	8	11	7	7	5	8	7	7	59.3	57.3	35	35	6.3	7.3
529	West of John Young Pkwy	60	57	46	64	0	63	13	10	7	6	0	10	7	10	5	3	100	9	54.3	42.3	30	16	7.3	37.3
530	At John Young Pkwy (970+	55	59	59	54	53	54	11	15	14	12	15	19	10	12	12	5	15	19	57.6	53.6	40	46	11.3	13
531	East of John Young Pkwy (	64	0	0	54	60	60	7	0	0	8	7	7	5	100	100	9	5	7	21.3	58	7	22	68.3	7
532	Rio Grande (1020+00)	62	61	0	62	57	56	11	15	0	20	15	12	6	7	100	11	9	12	41	58.3	26	47	37.6	10.6
533	At OBT (1044+00)	58	63	59	52	56	59	17	18	10	7	14	9	10	10	5	4	7	4	60	55.6	45	30	8.3	5
534	Michigan (1069+00)	0	53	0	0	50	0	0	11	0	0	13	0	0	6	0	0	8	0	17.6	16.6	11	13	2	2.6
535	At Kaley (1083+00)	39	52	55	0	0	45	15	14	5	0	0	10	19	14	4	100	100	11	48.6	15	24	10	12.3	70.2

Figure 29: Snapshot of the real time loop detector data window

The columns of the data grid are labeled from left to right as follows:

- Station ID (SID) which ranges from 502 to 571.
- Location of each station
- Eastbound Speed from left lane (ESL)
- Eastbound Speed from center lane (ESC)
- Eastbound Speed from right lane (ESR)
- Westbound Speed from left lane (WSL)
- Westbound Speed from center lane (WSC)
- Westbound Speed from right lane (WSR)
- Eastbound Volume from left lane (EVL)
- Eastbound Volume from center lane (EVC)
- Eastbound Volume from right lane (EVR)
- Westbound Volume from left lane (WVL)
- Westbound Volume from center lane (WVC)
- Westbound Volume from right lane (WVR)
- Eastbound Occupancy from left lane (EOL)
- Eastbound Occupancy from center lane (EOC)
- Eastbound Occupancy from right lane (EOR)
- Westbound Occupancy from left lane (WOL)
- Westbound Occupancy from center lane (WOC)
- Westbound Occupancy from right lane (WOR)

- Eastbound Average Speed (ES)
- Westbound Average Speed (WS)
- Eastbound Cumulative Volume (EV)
- Westbound Cumulative Volume (WV)
- Eastbound Average Occupancy (EO)
- Westbound Average Occupancy (WO)

The data will be updated every 30 seconds until the user chooses to stop the process by clicking on the 'Stop' button. Before a new data packet arrives, the existing one is appended to the database log file as described before. It should be noted from Figure 29 that blank cells indicate areas on I-4 where the number of lanes changes from three to two or vise versa. Locations with entirely blank rows indicate non-operational stations.

2.4 STUDY AREA

The loop detector stations along the 11.2-mile central corridor of I-4 provide point measurements of occupancy, speed, and volume every 30 seconds. The location of the central corridor of I-4 in Orlando is shown in Figure 30. The point measurements portray the up-to-date traffic conditions on the freeway. The occurrence of a lane-blocking incident causes a bottleneck at the incident location, where the capacity is reduced by a percentage proportional to the type and severity of the incident. If the capacity reduction is perceived by traffic, then the effect of the incident will propagate to reach the upstream and downstream loop detector stations. As such, the effect of the incident is perceived enough to cause traffic disruptions and changes in the associated traffic patterns. If the incident traffic patterns are captured and distinguished from other similar patterns, then the detection rate will increase and the false alarm rate will decrease.

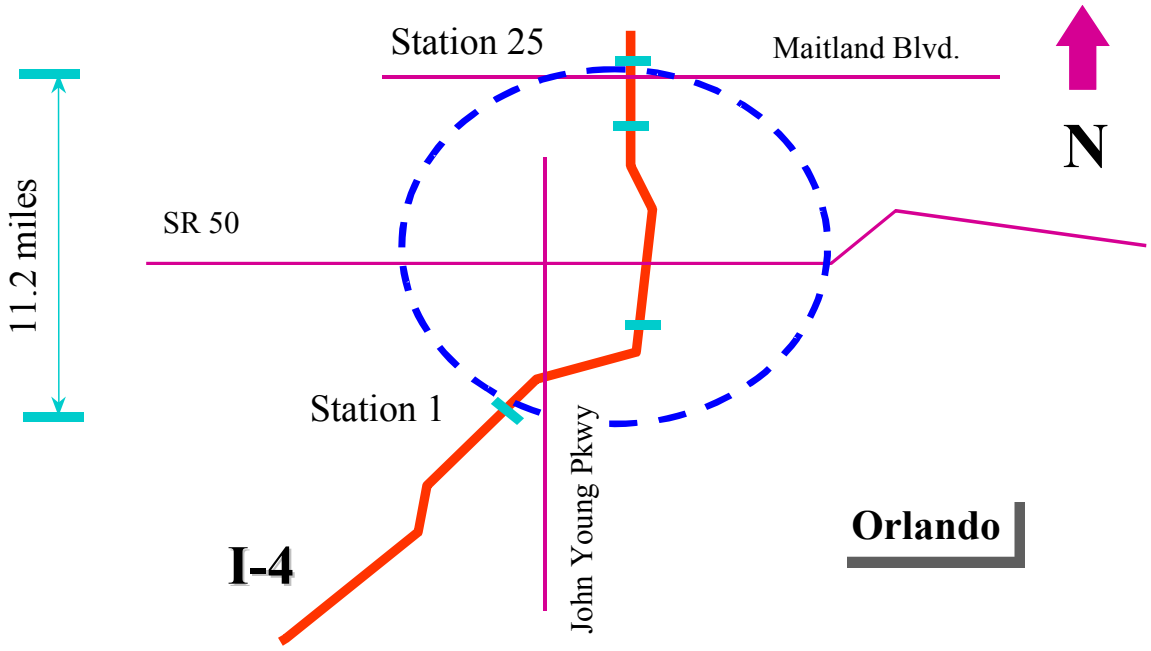

Figure 30: Study section showing the central corridor of I-4 in Orlando

2.5 THE FUZZY ART NETWORK

The Fuzzy ART (Adaptive Resonance Theory) network is based on unsupervised learning, which does not require the knowledge of the output to each input pattern. It is a clustering algorithm that maps a set of input patterns to a set of categories based on similarity of characteristics. The Fuzzy ART network is composed of a preprocessor layer, an input layer, and a class representation layer. The Fuzzy ART network takes the traffic patterns as inputs, which are represented in two dimensions: space and time. During training the network assigns a category to each input pattern such that similar patterns are assigned to the same category. The topology of the Fuzzy ART model is presented in the next section.

2.5.1 Topology of the Fuzzy ART Network

Fuzzy ART was developed by Carpenter et al. in 1991. It is a clustering algorithm that maps a set of input patterns to a set of categories. It is basically a synthesis of ART and Fuzzy logic. This algorithm has advantages over backpropagation networks as it provides fast stable learning in response to analog or binary input patterns. By incorporating the basic features of the ART networks, Fuzzy ART overcomes the stability/plasticity dilemma. Also, it is an incremental approach that has the potential for on-line implementation. Moreover, the learning process is less time-consuming than it is with backpropagation models.

The Fuzzy ART neural network consists of two layers: the input layer (F_1) and the class representation layer (F_2). A simplified layout of the network is shown in Figure 31. Before the input patterns are presented to F_1, they are normalized using complement coding at a preprocessor layer F_0. In particular, if a = (a_1, a_2,..., a_M), $a_i \in [0,1]$ and M denoting the input pattern size, represents an input pattern to Fuzzy ART, then the preprocessor layer computes the complement coding a^c of the vector a as follows:

$$a^c = 1 - a = (1-a_1, 1-a_2, ..., 1-a_M) \quad [5]$$

And the new input pattern I takes the form

$$I = (a, a^c) = (a_1, ..., a_M, a_1^c, ..., a_M^c) \quad [6]$$

Because of the complement coding technique the size of the input patterns now becomes $2M$. Let i denote a node in the input layer F_1, $i \in \{1, 2,..., 2M\}$, and j denote a node in the class representation layer F_2, $j \in \{1, 2,..., N\}$. The number of nodes in layers F_1 and F_2 is $2M$ and N, respectively. Every node i is connected to every node j with a bottom-up weight W_{ij}. Similarly, every node j is connected to every node i with a top-down weight w_{ji}. All weights emanating from node i are denoted by $W_i = (W_{i1}, W_{i2},..., W_{iN})$, $i \in \{1, 2,.., 2M\}$, and those emanating from node j are denoted by $w_j = (w_{j1}, w_{j2},..., w_{j,2M})$, $j \in \{1, 2,..., N\}$, often called a *template*. The algorithm makes use of the fuzzy-min and fuzzy-max operators. The two operators are explained in Figure 32.

Fuzzy ART performs pattern matching between bottom-up input and top-down learned prototype vectors. This matching process results in either a resonant state that leads to stable prototype learning or a self-regulating parallel memory search. The search ends by either selecting an established category and refining the category type to incorporate new information in the input pattern or selecting a previously untrained node or category. The matching criterion is defined by the dimensionless parameter called vigilance, which weighs how close the input pattern must be to the top-down prototype vector for resonance to occur. Low vigilance leads to broad generalization and abstract prototypes. High vigilance leads to narrow generalization and prototypes representing fewer input patterns.

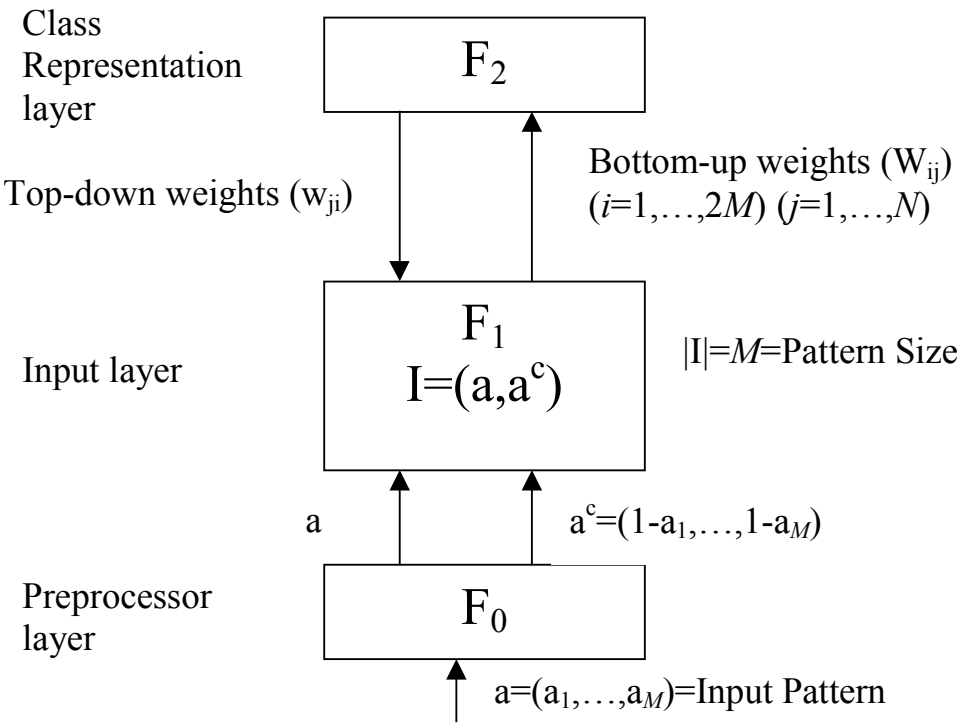

Figure 31: A simplified layout of the Fuzzy ART neural network architecture

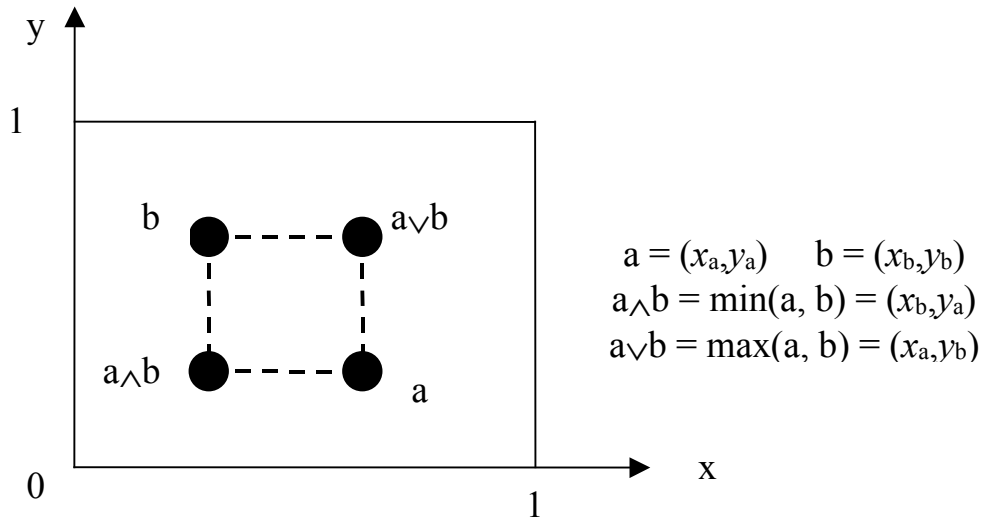

Figure 32: Illustration of fuzzy operators

Fuzzy ART incorporates the design features of ART1. Table 2: shows the translation of ART1 operations into Fuzzy ART for the category choice, matching, search, and learning. The fuzziness is introduced by replacing the intersection operator ($\cap$) with the MIN operator. In the next section we explain the steps of the Fuzzy ART algorithm.

Table 2: Analogy between ART1 and Fuzzy ART

	ART1 (Binary)	Fuzzy ART (Analog)
Category Choice	$T_j = \frac{\lvert \mathrm{I} \cap \mathrm{w}_j \rvert}{\alpha + \lvert \mathrm{w}_j \rvert}$	$T_j = \frac{\lvert \mathrm{I} \wedge \mathrm{w}_j \rvert}{\alpha + \lvert \mathrm{w}_j \rvert}$
Match Criterion	$\frac{\lvert \mathrm{I} \cap \mathrm{w} \rvert}{\lvert \mathrm{I} \rvert} \geq \rho$	$\frac{\lvert \mathrm{I} \wedge \mathrm{w} \rvert}{\lvert \mathrm{I} \rvert} \geq \rho$
Fast Learning	$\mathrm{w}_j^{(new)} = \mathrm{I} \cap \mathrm{w}_j^{(old)}$	$\mathrm{w}_j^{(new)} = \mathrm{I} \wedge \mathrm{w}_j^{(old)}$

2.5.2 The Fuzzy ART Algorithm

At first we introduce the definition of the following terms:

Input vector: Each input pattern I is an *M*-dimensional vector ($I_1 \ldots, I_M$), where each component I_i is in the interval [0,1]. The number of input patterns is represented by *p*. The collection of all input patterns is referred to as the *input list*. This input list can be presented to Fuzzy ART as many times as necessary. Each time the input list is presented to the network is called *list presentation*. The order of the patterns within the input list is not significant and may change from one list presentation to the other.

Weight vector: Each category (j) is associated with an adaptive weight vector $\mathrm{w}_j \equiv (w_{j1},...,w_{jM})$, which is also called Long-Term Memory (LTM) traces. The number of categories N (j=1,…, N) is arbitrary.

Parameters: The dynamics of Fuzzy ART are determined by the choice parameter $\alpha > 0$; a learning parameter $\beta \in [0,1]$; and a vigilance parameter $\rho \in [0,1]$.

The learning procedure is described in the following steps:

1. Select a value for the vigilance parameter ρ, the learning parameter β, and the choice parameter α.
2. Initialize the weights w_{ji} such that

$$w_{j1} = ... = w_{jM} = 1 \qquad [7]$$

3. Present an input pattern I to the F_1 layer. The bottom-up input T_j(I) from F_1 to node j in the F_2 layer is computed using the choice function

$$T_j(\mathrm{I}) = \begin{cases} |\mathrm{I}| & \text{if node } j \text{ is uncommitted} \\ \dfrac{|\mathrm{I} \wedge \mathrm{w}_j^k|}{\alpha + |\mathrm{w}_j^k|} & \text{if node } j \text{ is committed} \end{cases} \qquad [8]$$

Where the norm |.| is defined by

$$|\mathrm{x}| = \sum_{i=1}^{M} |x_i| \qquad [9]$$

W_j^k = The weights vector at iteration *k*, or before input pattern I is presented to the network.

4. Node *J* in the F_2 layer is selected if it satisfies the following condition

$$T_J(\mathrm{I}) = \max\{T_j(\mathrm{I})\}; j = \{1, 2, ..., N\} \quad [10]$$

If there is more than one node that maximizes T_j, the node with the lowest index *j* is selected. At this moment, node *J* becomes committed.

5. CHECK THE VIGILANCE CRITERION USING THE FOLLOWING MATCHING FUNCTION

$$\frac{\left|\mathrm{I} \wedge \mathrm{w}_J^k\right|}{\left|\mathrm{I}\right|} \geq \rho \quad [11]$$

If this condition is satisfied, then *resonance* occurs and node *J* is selected to represent input pattern I and we proceed to step 6. If not, then we move back to step 4, reset node *J*, and search for another node to represent pattern I. To prevent node *J* from being chosen again for the same input pattern I, we set T_J = -1 for as long as the same input pattern is being presented.

6. At this step, node *J* has been chosen to represent I. Once a category is selected for coding it becomes *committed*. During training each weight vector converges to a limit. The weight vectors must be updated as follows:

$$\mathrm{w}_J^{k+1} = \beta(\mathrm{I} \wedge \mathrm{w}_J^k) + (1 - \beta)\mathrm{w}_J^k \quad [12]$$

and

$$\mathrm{W}_J^{k+1} = \frac{\mathrm{w}_J^{k+1}}{\alpha + \left|\mathrm{w}_J^{k+1}\right|} \qquad [13]$$

w_j^{k+1} and W_j^{k+1} =are the weights vectors at iteration k+1 in layers F_2 and F_1, respectively.

Fast learning occurs when $\beta = 1$.

7. Go back to step 3 and repeat all the steps until all the input patterns have been presented to the network. This completes one list presentation.

8. If all input patterns have been presented and at least one weight has changed during the last list presentation, then steps 3 through 7 should be repeated to complete a new list presentation. Learning ends if the weights do not change during one list presentation.

2.5.3 The Fuzzy ART Module

A special program was developed using MS Visual BASIC to perform the analysis of incident detection using Fuzzy ART algorithm. The program features three main functions: patterns generation, Fuzzy ART application, and calculation of detection rates and false alarm rates. The program main menu is shown in Figure 33. In this section we will explain the features and parameters of each function.

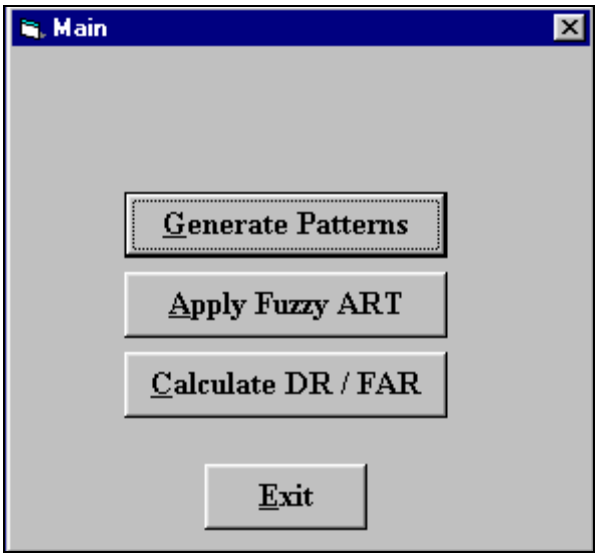

Figure 33: The main menu of the Fuzzy ART program

2.5.3.1 Traffic Pattern Generation

The traffic pattern generation process requires setting a few parameters that are shown in Figure 34. The figure shows the pattern generation form with all the available options. Each set of patterns is identified with a unique identification name. The input directory points to the location of the loop detector files whereas the output directory points to the location where the output patterns will be stored. The traffic patterns can be generated from occupancy, speed, or volume data, or any combination of the three. Traffic patterns can be constructed using data from any combination of the three lanes or the average of the three lanes. On the form the temporal and spatial pattern sizes are also specified in minutes and number of stations, respectively. The patterns can be generated using absolute or relative measurements of the traffic parameters. Relative measurements can be based on spatial or temporal difference. Patterns generated using the relative spatial difference are expressed in terms of the difference between each two consecutive stations. Patterns generated with the relative temporal difference are expressed as the

difference between each two consecutive 30-second periods at each station. Other additional features in constructing the traffic patterns include rounding off the numbers, smoothing the loop detector data, and normalizing the data.

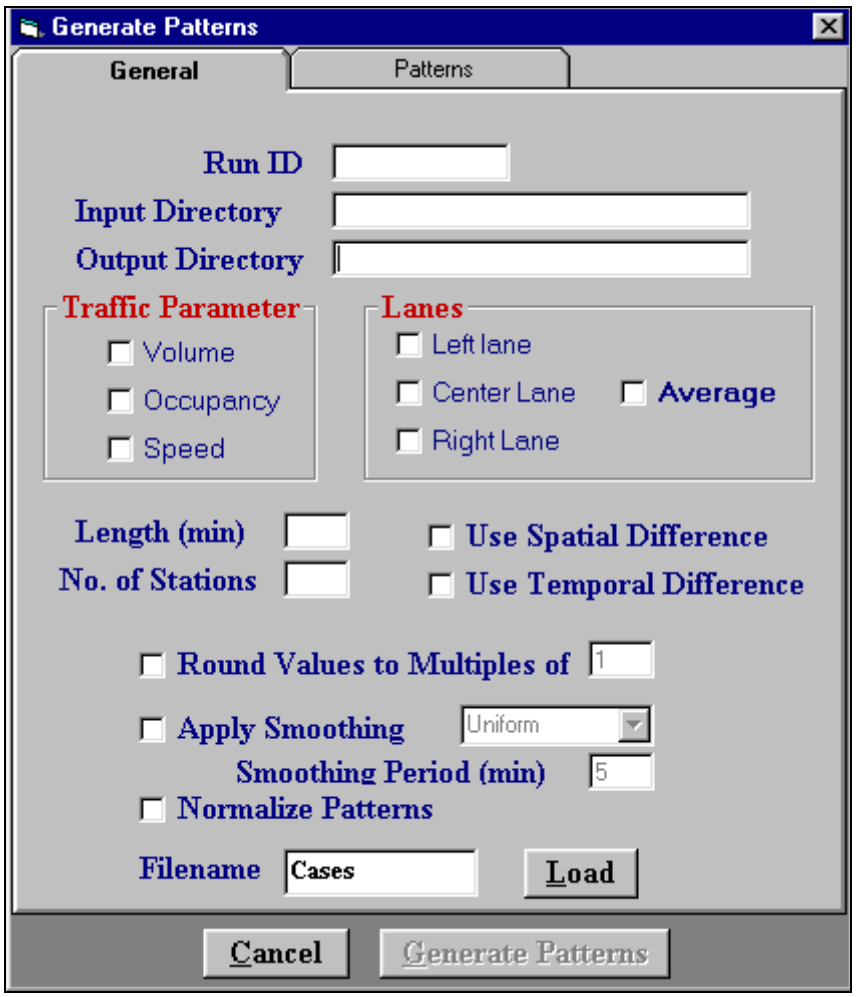

Figure 34: Form showing the parameters of generating traffic patterns

Both training and testing data sets were built gradually from loop detector data surrounding the incident. Figure 35 shows the form used to build the traffic patterns from each incident case. Traffic patterns generation requires the identification of the incident case number, which was assigned during the filtering process, the direction of traffic at the time of the incident, the incident location marked by the upstream station of the

incident. The boundary conditions are also selected by specifying the starting and ending time and the starting and ending station. Traffic patterns were constructed from each incident case and added cumulatively to the traffic data set.

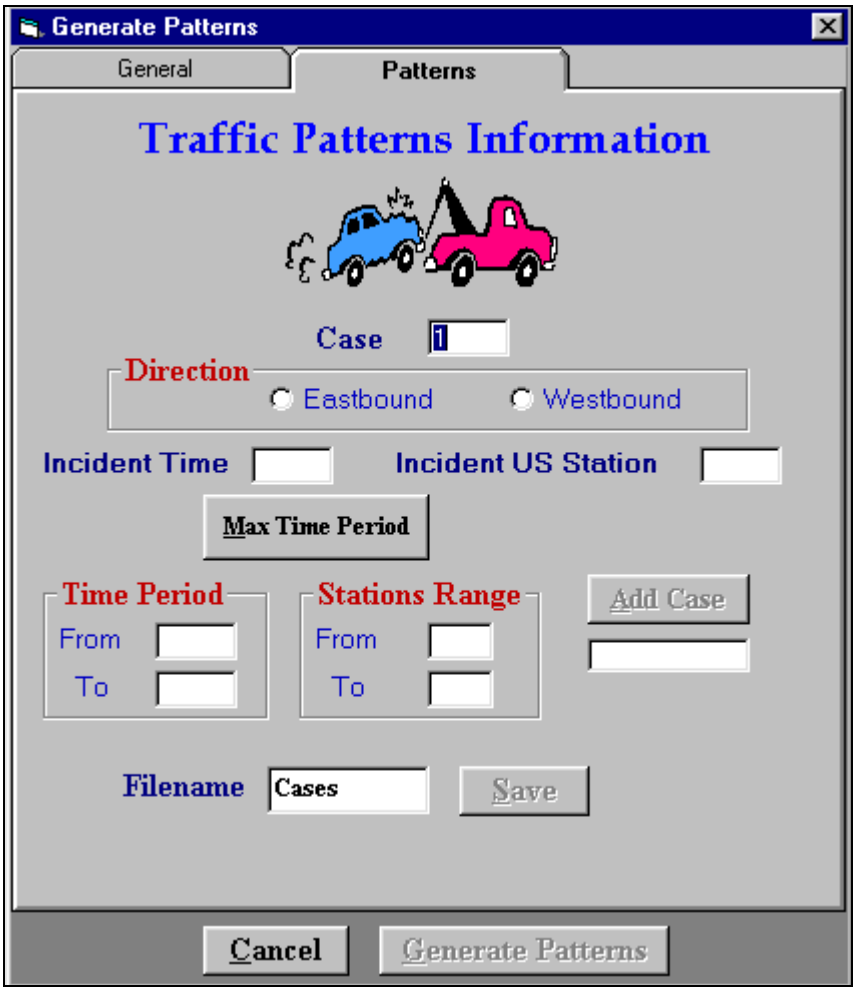

Figure 35: Traffic pattern generation form

2.5.3.2 Algorithm Execution

The actual implementation of the Fuzzy ART algorithm is conducted using the form shown in Figure 36. The form reads the input patterns from the patterns directory and writes the output file to the output directory. As mentioned earlier, the dynamics of the Fuzzy ART is controlled by three parameters: α, ρ, and β. The three parameters must be

specified on the form. Also, the maximum number of categories, the maximum number of cycles, the number of list presentations, and the maximum convergence error must be specified on the form. The form also provides the capability of performing incremental learning, which allows the network to load previously updated weights and resume learning from a new data set.

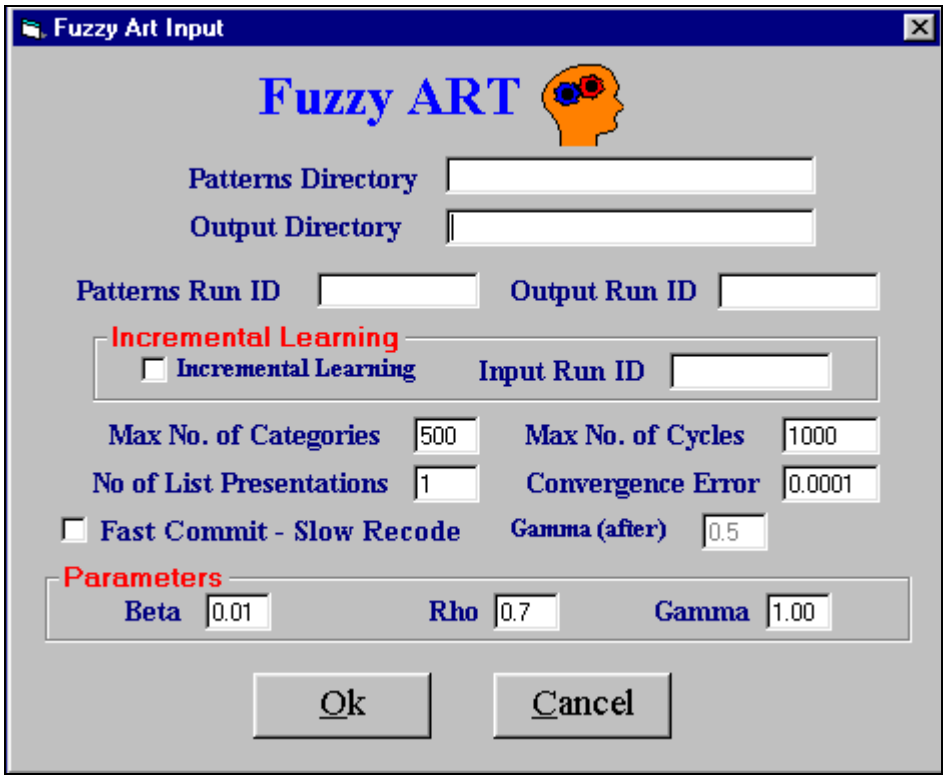

Figure 36: Fuzzy ART input form

2.6 METHODOLOGY

This section describes the methodology used to apply the Fuzzy ART network to freeway incident detection. The methodology is described in Figure 37. The first step was to identify which traffic parameters should represent the traffic conditions on the freeway. Three scenarios were considered with the application of Fuzzy ART: occupancy, speed,

and occupancy and speed together. Volume data was not incorporated in the representation of traffic conditions. Training and testing patterns were generated from the filtered loop detector data using a special program. Each generated traffic pattern in both training and testing data sets was identified as either an incident or incident-free pattern. The identification of the traffic pattern type was not used, however, during the training process since Fuzzy ART is based on unsupervised learning. This was essentially required to evaluate the performance of the network.

During training the generated training data set was presented to the Fuzzy ART network for clustering. Traffic patterns clustering required a few numbers of cycles to stabilize. Once reached, each traffic pattern is assigned to one category. At the end of training the Fuzzy ART network is saved to retain all the values of weights adjusted during training. The resulting categories from the training process, along with the predetermined type of traffic patterns, were used to identify the incident pattern categories. The selected incident pattern categories were used to calculate the detection rate and false alarm rate for the training data set. The trained network, along with the selected incident pattern categories, was later presented with the testing data set to evaluate the performance of the Fuzzy ART network. Both training and testing results were eventually used for comparative analysis of the network performance.

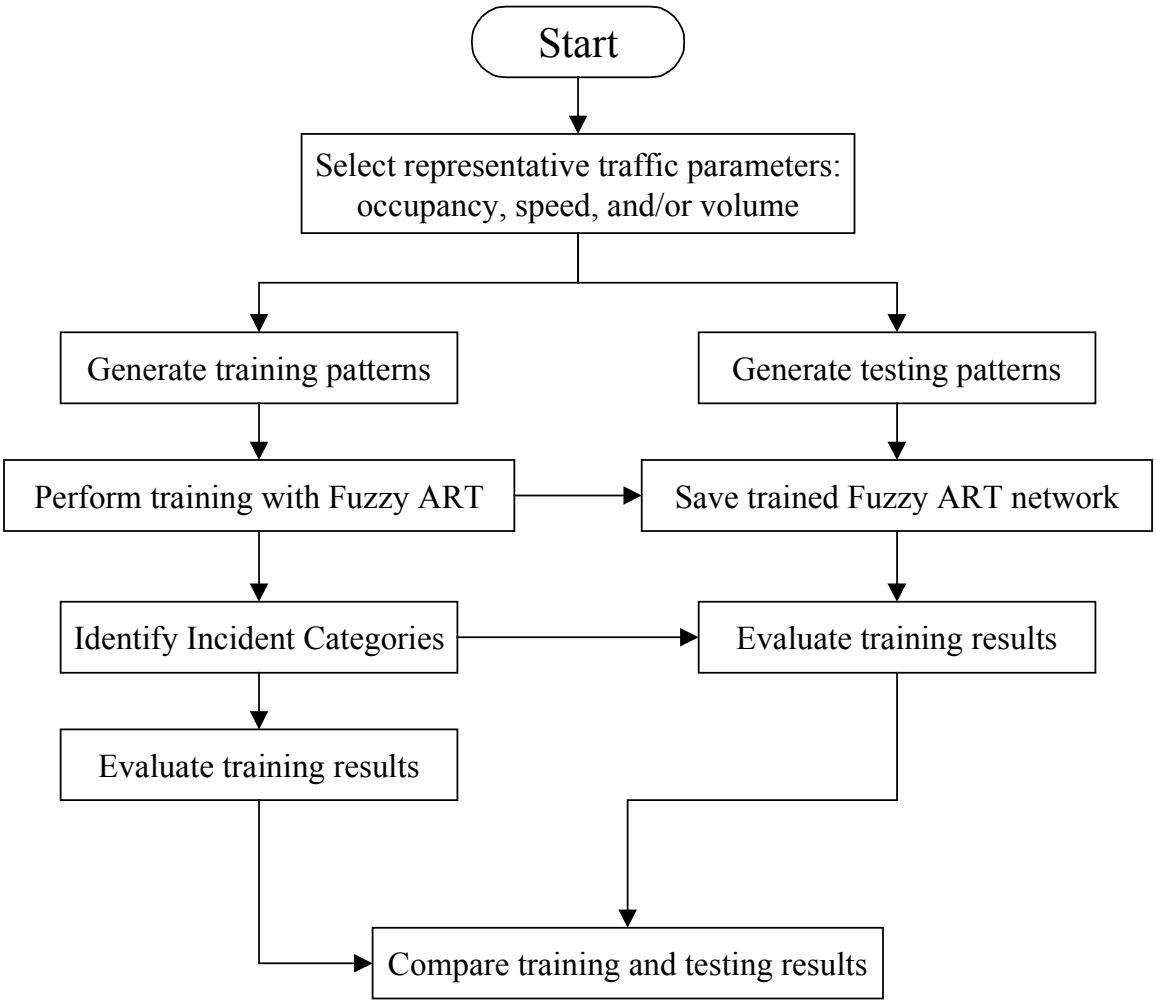

Figure 37: Methodology of applying the Fuzzy ART network

2.7 TRAINING AND TESTING DATA SETS

For training and testing purposes, the selected incident data set was further split into two subsets of incidents: one that was used for training and the other for testing. Each subset was selected from the previously verified set of incidents. The ratio between the training set and the testing set is 2:1, as recommended in most of the literature on neural networks. The number of incidents in the training and testing subsets was 89 and 41, respectively. The training and testing sets were examined to ensure that they possess the

same characteristics of the collected incident set, and thus, provide true representation of the entire incident population. In order to make sure the two subsets are also representatives of the original set, the temporal distribution for each is plotted as shown in Figure 38 and Figure 39. The temporal distribution of each data set reveals that they both maintain similar characteristics. In other words, both data subsets can represent the original data set. Close representation to the original distribution insures that the proposed neural network models are trained and tested with a variety of incidents under diversified traffic conditions.

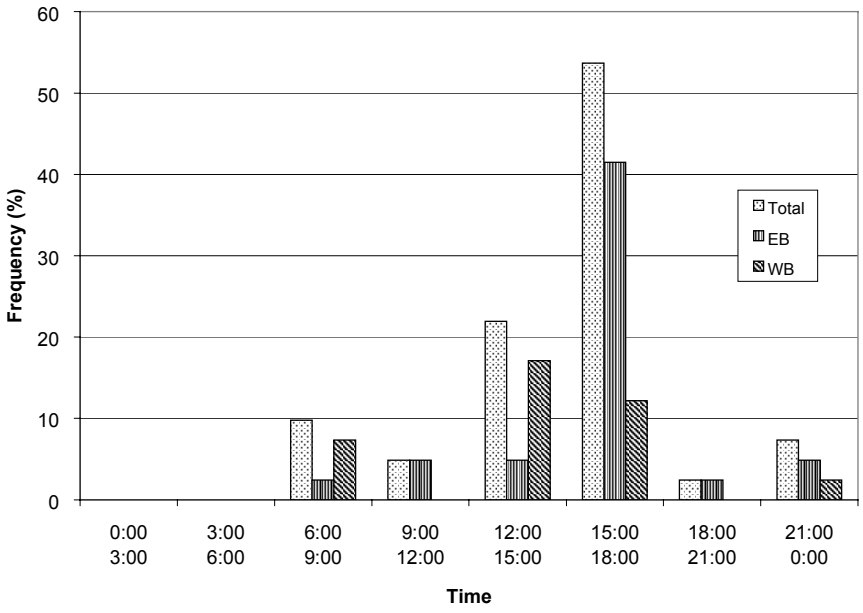

Figure 38: Temporal distribution of the training data set

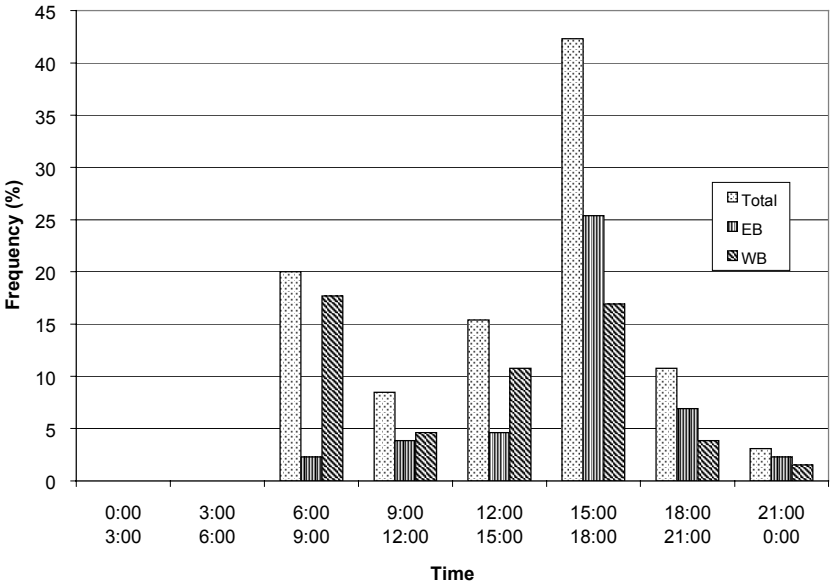

Figure 39: Temporal distribution of the testing data set

2.8 TRAINING THE FUZZY ART NETWORK

Training Fuzzy ART networks requires the use of as many traffic patterns as possible. More traffic patterns ensure the network has built sufficient internal representation of a wide range of various traffic conditions. The traffic patterns generated to train the Fuzzy ART network were constructed from traffic conditions observed in the neighborhood of each selected lane-blocking incident in the training data set. The total number of training patterns generated from 89 lane-blocking incidents was nearly 33,000.

All traffic patterns generated for training and testing the Fuzzy ART network were represented by the spatial difference between two consecutive stations. To ensure all values fall in the range between 0 and 1, a linear transformation function was applied. A sample of the input patterns file used for training Fuzzy ART is shown in Figure 40. It

should be noted here that the input patterns do not have a desired response since Fuzzy ART is based on unsupervised learning. The input traffic patterns are separated by commas and each line has the following format:

- Pattern Number: a unique ID that identifies the pattern
- Case Number: the incident ID for which the traffic pattern was generated
- Time Period: the incident time
- Location: the immediate upstream station of the incident location
- Traffic pattern values: the absolute or relative speed and/or occupancy values observed near the incident location.

```
" ID Caseno TimePeriod Station"
1,6,16,20,.525,.5,.525,.525,.5,.525,.5,.5,.525,.5,.5,.525,
2,6,16,19,.475,.5,.5,.475,.5,.5,.5,.525,.5,.5,.525,.525,
3,6,16,18,.525,.525,.525,.525,.525,.525,.525,.5,.5,.525,.525,.5,
4,6,16,17,.5,.5,.475,.5,.5,.475,.475,.475,.5,.5,.475,.475,
5,6,16,16,.5,.475,.475,.5,.475,.475,.5,.525,.525,.475,.475,.5,
6,6,16,15,.475,.475,.45,.475,.475,.45,.525,.525,.5,.5,.525,.5,
7,6,16,14,.5,.475,.475,.5,.475,.475,.5,.475,.5,.525,.5,.525,
8,6,16,13,.475,.475,.5,.475,.475,.5,.475,.5,.5,.475,.5,.5,
9,6,16,12,.5,.525,.525,.5,.525,.525,.525,.525,.525,.525,.525,.525,
10,6,16,11,.525,.525,.5,.525,.525,.5,.5,.5,.5,.5,.5,.5,
11,6,17,20,.525,.5,.525,.525,.5,.525,.5,.5,.525,.5,.5,.525,
12,6,17,19,.475,.5,.5,.475,.5,.5,.5,.525,.525,.5,.525,.525,
13,6,17,18,.525,.525,.525,.525,.525,.55,.525,.525,.5,.525,.525,.525,.475,
14,6,17,17,.5,.5,.475,.5,.525,.475,.5,.475,.475,.5,.45,.475,
15,6,17,16,.5,.475,.475,.525,.475,.475,.475,.475,.5,.45,.475,.525,
16,6,17,15,.475,.475,.45,.45,.45,.425,.5,.525,.5,.525,.575,.525,
17,6,17,14,.5,.475,.475,.5,.475,.475,.525,.5,.525,.55,.5,.525,
18,6,17,13,.475,.475,.5,.475,.475,.5,.475,.5,.5,.45,.475,.475,
19,6,17,12,.5,.525,.525,.5,.525,.525,.525,.525,.525,.525,.525,.525,
20,6,17,11,.525,.525,.5,.525,.525,.5,.5,.5,.5,.5,.5,.5,
21,6,18,20,.525,.5,.525,.525,.5,.525,.5,.5,.525,.5,.5,.525,
22,6,18,19,.475,.5,.5,.475,.5,.5,.5,.525,.525,.5,.525,.525,
23,6,18,18,.525,.525,.55,.525,.525,.55,.525,.525,.475,.525,.525,.5,
24,6,18,17,.5,.525,.475,.5,.525,.475,.5,.45,.475,.5,.475,.5,
25,6,18,16,.525,.475,.475,.525,.475,.475,.45,.475,.525,.475,.5,.525,
26,6,18,15,.45,.45,.425,.45,.45,.425,.525,.575,.525,.525,.55,.5,
27,6,18,14,.5,.475,.475,.5,.475,.5,.55,.5,.525,.525,.475,.5,
28,6,18,13,.475,.475,.5,.475,.5,.5,.45,.475,.475,.45,.475,.475,
29,6,18,12,.5,.525,.525,.525,.525,.525,.525,.525,.525,.525,.525,.525,
```

Figure 40: A sample of the input traffic patterns training file used by the Fuzzy ART program

The processes of training and testing the Fuzzy ART network were conducted separately. The training process must be completed first and will result in assigning all traffic

patterns to a group of clusters according to their common characteristics. Since Fuzzy ART provides fast stable learning, the training process for the different scenarios considered in the study did not consume more than 5 cycles on the average. Large patterns typically require more cycles for the network to stabilize than small patterns. However, all training phases were completed in the range of 3 to 7 cycles. Training was terminated when no changes in category assignment are made in two consecutive cycles. At the end of the training process the Fuzzy ART network retains all the vector weights that contain the clustering information acquired and adjusted throughout the training phase.

2.8.1 Input to the Fuzzy ART Network

The structure of the traffic patterns, used as input to the Fuzzy ART network, is two-dimensional. The spatial size is represented by the number of loop detector stations while the temporal size is measured by the number of 30-second periods. The spatial size was set to 3 stations: one downstream and two upstream of the incident location. The temporal size was varied between one to two 30-second periods.

2.8.2 Output of the Fuzzy ART Network

The Fuzzy ART is based on unsupervised learning, which does not require the knowledge of the output to each input pattern. However, the Fuzzy ART network itself assigns an

output to each input pattern at the end of the training process. This output represents the category to which the corresponding pattern belongs. Similar input patterns are typically assigned to the same cluster or category. The degree of clustering depends on the values of the Fuzzy ART parameters.

2.8.3 The Selected Fuzzy ART Network Topology

The topology of the Fuzzy ART network is predefined and is only affected by the size of the input patterns. The training process is controlled by three parameters: the choice parameter, the learning parameter, and the vigilance parameter. Both the choice parameter and the learning parameter were held constant at 0.01 and 1.0, respectively. The vigilance parameter, however, was varied from 0.8 to 0.9 to 0.95. The vigilance parameter defines the degree of clustering, which could have an effect on the network incident detection performance. In addition the maximum error of convergence was set to 0.0001 and the maximum number of cycles to 1000.

2.9 SELECTION OF INCIDENT CLUSTERS

In order to evaluate the performance of the Fuzzy ART network in incident detection it was necessary to mark the clusters of the traffic patterns associated with incidents. Those are referred to as incident clusters and are largely used to estimate detection rates and false alarm rates. The process of selecting the clusters of incident traffic patterns is based on the analysis of clusters produced by the training data set. Due to the fact that the exact

incident time was not precisely known to the nearest 30-second period, the selection of incident clusters is more complicated than simply identifying the clusters of patterns observed at the reported incident time. Although the incident data underwent an extensive verification process to ensure that the location and time of each incident are as accurate as possible, there were still some uncertainties in pinpointing the exact incident time. This dilemma has led to the need to develop another approach to identify the incident clusters.

The approach of selecting incident clusters relies primarily on the assumption that the traffic patterns observed after the incidents are mostly unique and discernible to a great extent from other similar traffic patterns observed during recurrent congestion or frequent traffic disturbances. If this assumption holds true then the incident clusters are observed most frequently in the vicinity of the incident time and location and least frequently elsewhere. In this case, the objective of the approach is to select the clusters that maximize the ratio between their occurrences in the vicinity of the incident time and their occurrences elsewhere. In mathematical formulation the first selected incident cluster c_i is determined such that:

$$f(c_i) = \max\left\{\frac{f_1(c_j)}{f_2(c_j)}\right\} \quad \forall j \in 1,2,...i,...,N \qquad [14]$$

Where,

c_i = The selected i^{th} incident cluster

$f_1(c_j)$ = The frequency of cluster c_j in the neighborhoods of the reported incident times

$f_2(c_j)$ = The frequency of cluster c_j elsewhere

$f(c_i)$ = The ratio between $f_1(c_j)$ and $f_2(c_j)$

N = The total number of generated clusters during training

The second incident cluster is selected such that the same ratio is maximized for all remaining clusters, and so on. The selection process ends when all possible incident clusters have been exhausted and most incidents have been associated with at least one cluster. Incidents with similar effect on traffic conditions are very likely to be associated with the same cluster. The incident neighborhood is defined as the group of clusters to which traffic patterns around the incident reported time were mapped. The boundary of the incident neighborhood is contingent upon the expected accuracy of the reported incident time as well as the maximum mean time of detection. The boundary of the incident neighborhood was arbitrarily selected as ±5 minutes of the incident reported time. In other words, all clusters generated within ±5 minutes of the reported incident time were examined. This time range ensures that the actual incident time and the propagating effect of the incident on the traffic conditions are contained within the incident neighborhood. For illustration, Table 3 shows the number of incidents mapped to each selected incident cluster for speed-based patterns.

It should be noted here that the selection of incident clusters is a similar process to the selection of threshold values in the application of traditional incident detection algorithms. Each selected incident cluster represents one threshold. Evidently, the application of Fuzzy ART model to automatic freeway incident detection is a multiple-

threshold process. In other words, no single incident cluster could map all incidents due primarily to the different incident characteristics and the various prevailing traffic conditions at the time of the incident. Therefore, it was possible to select one incident cluster for each group of incidents that share similar characteristics and effects on traffic conditions. This usually resulted in selecting several incident clusters that could accommodate all the incidents used for training.

Table 3: The number of incidents mapped to each selected cluster using speed-based patterns

Selected Incident Clusters	Number of Mapped Incidents
1	4
2	3
3	1
4	17
5	5
6	22
7	2
8	3
9	7
10	8
11	1
12	6
13	2
14	2
15	1

2.10 DESIGN FACTORS OF THE FUZZY ART NETWORK

Various factors can affect the performance of the Fuzzy ART network. Those factors are either related to the topology of the network or the characteristics of the input patterns. Factors related to the network topology include the choice parameter, the learning parameter, and the vigilance parameter. In this study the vigilance parameter was varied to investigate its effect on the network performance. Another set of factors is related to

the input pattern characteristics such as the size of the traffic pattern in both the spatial and temporal dimensions and the type of traffic parameters used to represent traffic conditions. The spatial size of the pattern was set to 3 stations to ensure that the propagated effect of the incident is sufficiently contained in the traffic pattern. The temporal size of the pattern, however, took on one of two values: one 30-second period and two 30-second periods. This was necessary to investigate the effect of the temporal pattern size on the network performance. In addition, three different scenarios of traffic pattern representation were considered as follows: occupancy, speed, and occupancy and speed. The various designs considered in this study are listed in Table 4. The amount of training time required for each scenario varied from two hours to several hours according to the size of the traffic patterns and the value of the vigilance parameter.

Table 4 Various designs of the Fuzzy ART network

Traffic Parameter	Vigilance Parameter (ρ)		
	ρ = 0.8	ρ = 0.9	ρ = 0.95
Occupancy	1x3[a] 2x3	1x3 2x3	1x3 2x3
Speed	1x3 2x3	1x3 2x3	1x3 2x3
Occupancy + Speed	1x3 2x3	1x3 2x3	1x3 2x3

[a] (1x3) refers to a traffic pattern of size one 30-second period by 3 stations

2.11 TESTING THE FUZZY ART NETWORK

Testing Fuzzy ART was also conducted using the testing incident data set of 41 lane-blocking incidents. All testing patterns were generated from observations of traffic conditions before and after the reported incident time and upstream and downstream of the reported incident location. The total number of traffic patterns generated from the

incident data set was nearly 17,000. In addition, another set of traffic patterns was generated from incident-free traffic peak periods. The additional traffic patterns set was necessary to better estimate the false alarm rate under incident-free conditions. The total number of patterns generated from the incident-free peak periods was nearly 80,000. The combined total number of traffic patterns was nearly 97,000. This sample is believed to be enough to test the performance of the Fuzzy ART network.

The testing process is illustrated in Figure 41, which shows how traffic patterns are assigned to either one of the incident clusters or one of the incident-free clusters. As shown in the figure, an incident-free pattern should be assigned to one of the incident-free clusters. However, a false alarm will result from falsely mapping one of the incident-free patterns to one of the incident clusters. Similarly, detection is successful if an incident pattern is assigned to one of the incident clusters. However, detection is missed if one of the incident patterns has been inadvertently mapped to one of the incident-free clusters.

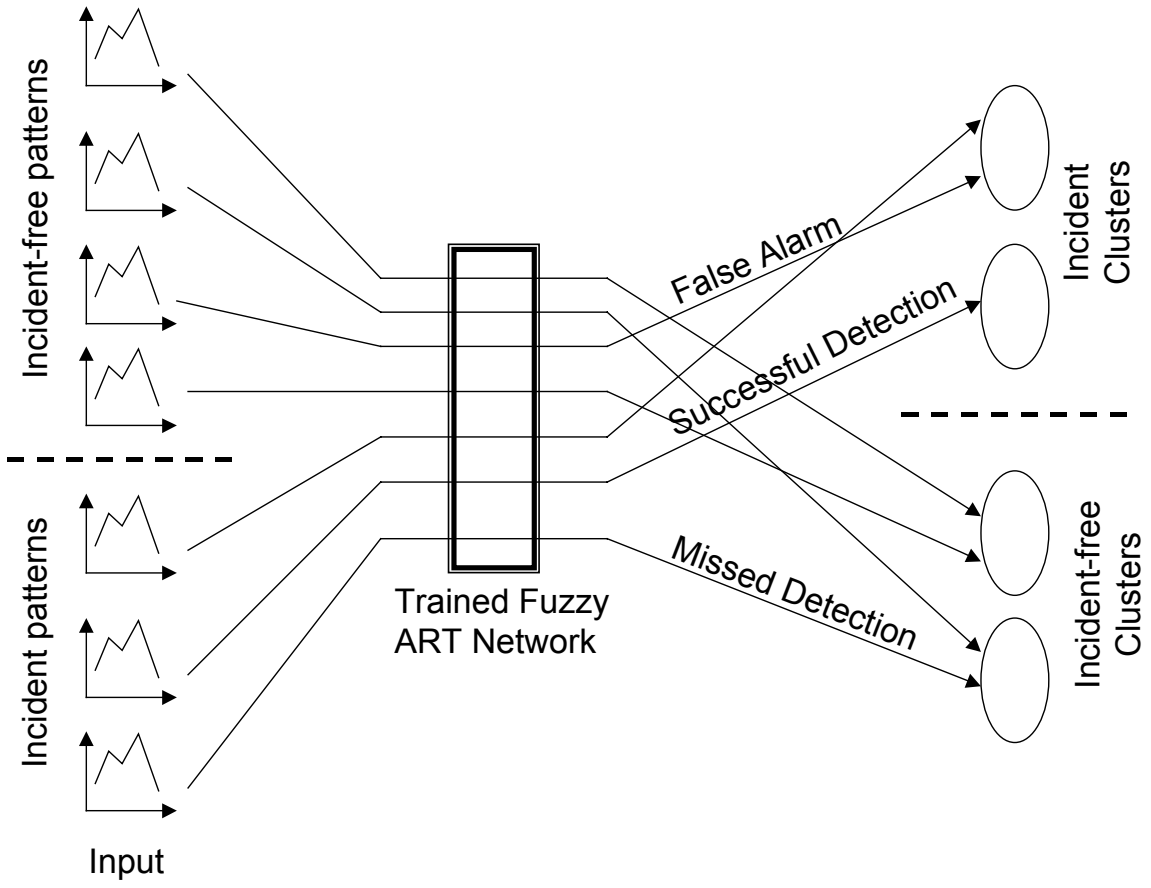

Figure 41: A schematic showing the testing process to evaluate the Fuzzy ART network performance

When implemented on-line, the trained Fuzzy ART network will receive real life data every 30 seconds from all the freeway loop detectors, construct the traffic patterns, and map the traffic patterns to either a previously established category or a new category. When a new category is selected the weights will be updated to reflect the addition of the new category and permit mapping traffic patterns to it in the future. This procedure proves the property that Fuzzy ART is an incremental approach that has a potential for on-line implementation.

Testing Fuzzy ART was also conducted using the testing incident data set of 41 lane-blocking incidents. All testing patterns were generated from observations of traffic conditions before and after the reported incident time and upstream and downstream of the reported incident location. The total number of traffic patterns generated from the incident data set was nearly 17,000. In addition, another set of traffic patterns was generated from incident-free traffic peak periods. The additional traffic patterns set was necessary to better estimate the false alarm rate under incident-free conditions. The total number of patterns generated from the incident-free peak periods was nearly 80,000. The combined total number of traffic patterns was nearly 97,000. This sample is believed to be enough to test the performance of the Fuzzy ART network.

2.12 PERFORMANCE MEASURES

The evaluation of performance of incident detection algorithms has been commonly based on three measures of effectiveness: detection rate, false alarm rate, and mean time of detection. While detection rate and false alarm rate can be accurately estimated, the mean time of detection is a more sensitive measure that relies primarily on the knowledge of the exact incident time. Certainty of the incident time can only be available when using simulated incident data since incidents are artificially induced at certain time and location. However, in real life data it is practically impossible to be precisely certain of the exact incident time and thus the accuracy of the calculated mean time of detection will be highly questionable. Therefore, instead of using the reported incident time to calculate the mean time of detection, a maximum time tolerance was introduced. The maximum time tolerance was arbitrarily selected as 5 minutes. This means that during

training and testing a true detection is only considered if the detection time is within ±5 minutes from the reported incident time. Any detection elsewhere is treated as a false alarm. In the next section a persistence factor and a persistence period are defined and introduced to reduce the false alarm rate.

2.13 PERSISTENCE PERIOD AND PERSISTENCE FACTOR

The concept of the using a persistence period was introduced in some incident detection algorithms such as California version 8. The advantage of using a persistence period is to suppress false alarms that usually result from compression waves, which create traffic conditions very similar to those observed immediately following the occurrence of a lane blocking incident. Therefore, a persistence period was introduced to improve the performance of the Fuzzy ART algorithm by reducing the false alarm rates. Instead of declaring an incident immediately following the encounter of a single occurrence of one of the selected incident clusters, the detection is confirmed only if more than one traffic pattern has been mapped to one of the incident clusters within the persistence period. The persistence period was selected as three minutes or six 30-second periods. The number of times an incident cluster is observed within the persistence period is also referred to as the persistence factor (*PF*). The persistence factor ranges between 1 and 6 since the persistence period itself consists of 6 consecutive clusters. For instance, $PF = 2$ means that detection is declared upon mapping at a particular location at least two out of six traffic patterns generated in the designated 3-minute persistence time period, to one of the selected incident clusters. This reduces the false alarms that result from occasional misclassification of traffic patterns.

During on-line implementation the persistence period is represented by a 3-minute moving time window that advances only one station at a time until the entire corridor has been scanned, and then advances one 30-second period in real time. Figure 42 shows the 3-minute persistence period the current time on the time-space detector data matrix. The space dimension represents the loop detector stations along the central corridor of I-4. Each row in the time-space matrix represents a 30-second data packet that is compiled at the computer system at the Freeway Management Center in Orlando. For real time implementation the 30-second data packets are used to generate traffic patterns that are presented to the trained Fuzzy ART for clustering. The resulting clusters are then compared with the previously selected incident clusters to decide on whether the current traffic conditions are associated with an incident or not.

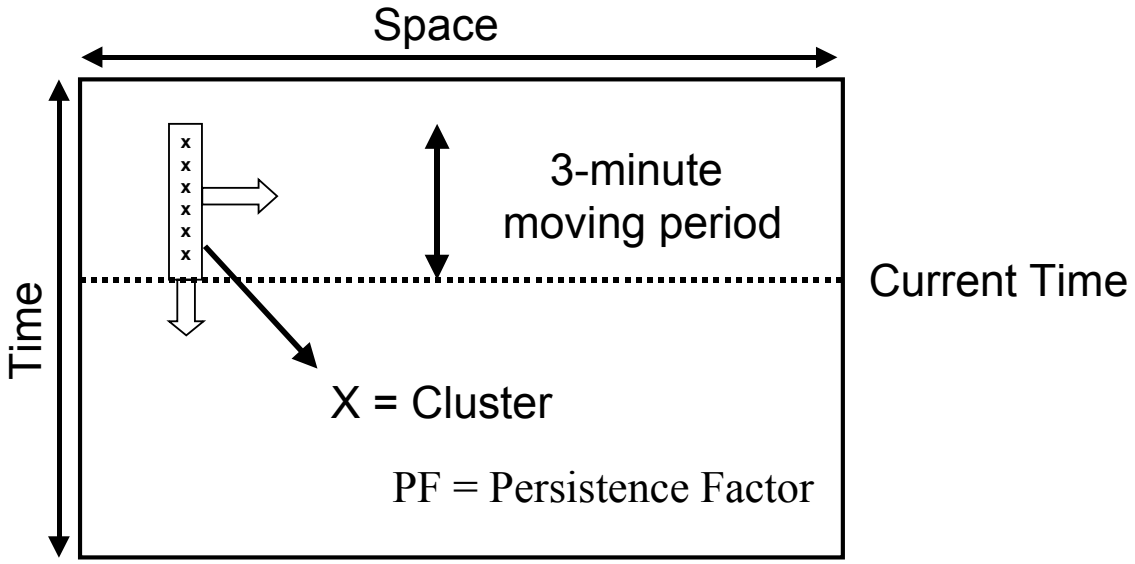

Figure 42 Illustration of the persistence period and persistence factor

2.14 CALCULATION OF DR AND FAR

Detection rate and false alarm rate are both used to evaluate the performance of the Fuzzy ART-based incident detection algorithm. The procedure for calculating *DR* and *FAR* was based on examining the clusters of all traffic patterns generated within the 3-minute persistence time period. Depending on the value of the persistence factor *PF*, an incident is declared and confirmed if one of the selected incident clusters has been observed during the persistence period at least *PF* times. For instance, if *PF* is equal to 3, then an incident can only be confirmed if, in one persistence period, one of the selected incident clusters has been observed at least 3 times. Therefore, given *PF=j*, the detection rate for each incident cluster can be calculated as follows:

$$(DR)_i^j = \frac{D_i^j}{N} \qquad [15]$$

Where

$(DR)_i^j$ = the detection rate for incident cluster *i* and *PF=j*

D_i^j = the number of incidents detected by cluster *i* for *PF=j*

N = the total number of incidents

Given *PF=j*, the overall detection rate for all incident clusters is obtained by summing up all the detection rates for each incident cluster $(DR)_i^j$ as follows:

$$DR^j = \sum_{i=1}^{N_c} (DR)_i^j = \sum_{i=1}^{N_c} \frac{D_i^j}{N} \quad [16]$$

Where,

DR^j = the overall detection rate for *PF=j*

N_c = the total number of selected incident clusters

Similarly, for each *PF=j*, the false alarm rate associated with each incident cluster can be calculated as follows:

$$(FAR)_i^j = \frac{A_i^j}{N_a} \quad [17]$$

Where,

$(FAR)_i^j$ = the false alarm rate associated with incident cluster *i* for *PF=j*

A_i^j = the total number of false alarms associated with incident cluster *i* for *PF=j*

N_a = The total number of algorithm applications

The overall false alarm rate for all incident clusters is also obtained by summing up all the false alarm rates for each incident cluster $(FAR)_i^j$ as follows:

$$FAR^j = \sum_{i=1}^{N_c} (FAR)_i^j = \sum_{i=1}^{N_c} \frac{A_i^j}{N_a} \quad [18]$$

Where,

FAR^j = the overall false alarm rate for $PF=j$

It should be noted here that both detection rates and false alarm rates are calculated for each value of the persistence factor *j*, which ranges between 1 and 6 for a persistence period of 3 minutes (6 30-second periods). The performance envelopes between detection rate and false alarm rate are plotted for each value of the persistence factor. Each performance envelope is obtained by drawing the cumulative changes in the detection rate and false alarm rate that result from incorporating each additional incident cluster. Table 5 illustrates an example of the cumulative detection rate and false alarm rate for each selected incident cluster. In the next stage the performance envelopes will be presented and examined to show the effect of the most influencing factors on the Fuzzy ART algorithm performance. Those factors include the value of the vigilance parameter, the temporal size of the traffic patterns, and the type of traffic parameter used to represent traffic conditions.

Table 5: Cumulative detection rate and false alarm rate for each incident cluster

Selected Incident Cluster	Number of mapped incidents	FAR (%)	DR (%)
1	4	0	4.49
2	3	0	7.87
3	1	0	8.99
4	17	0.02	28.1
5	5	0.03	33.7
6	22	0.16	58.4
7	2	0.19	60.7
8	3	0.24	64
9	7	0.35	71.9
10	8	0.58	80.9
11	1	0.64	82
12	6	1.05	88.8
13	2	1.28	91
14	2	1.57	93.3
15	1	1.82	94.4

2.15 ANALYSIS OF RESULTS

This section presents the results of training and testing the Fuzzy ART network. The incident detection performance of the Fuzzy ART network is measured in terms of detection rate and false alarm rate using the traditional performance envelopes adopted by most incident detection analyses. In order to achieve better performance, several scenarios were considered by varying the factors that are likely to affect the network performance. Those factors include the size of the temporal traffic pattern, the type of traffic parameter used to represent traffic conditions, and the vigilance parameter that controls the degree of clustering. Each of these factors proved to have influenced the overall performance of the network. The effect of the persistence factor on the network performance is also investigated here. Finally, a comparative evaluation of the performance of the two artificial neural networks applied in this study is presented. The

performance of the Fuzzy ART network is also compared to that of California algorithm versions 7 and 8.

2.15.1 The Effect of the Persistence Factor

As mentioned earlier the persistence factor was introduced to improve the performance of the Fuzzy ART incident detection algorithm by reducing the false alarm rate. The persistence period was selected as a 3-minute moving time period or 6 30-second periods. In this section the effect of the persistence factor is investigated. The persistence factor was varied from 1 to 6, which defines the number of times an incident cluster has to persist during each persistence period in order for an incident to be declared. Comparative evaluation of the performance envelopes for different scenarios is presented here. Figure 43, Figure 44, and Figure 45 show the performance envelopes for one-minute occupancy patterns using testing results for ρ=0.80, 0.90, and 0.95, respectively. The effect of the persistence factor is not clear from the first two figures since the performance of each seems to fall within a small variation. However, for ρ=0.95 large values of persistence factors (*PF*=5 and 6) resulted in a significant drop in the performance while persistence factor values in the range of 1 to 4 seem to give fairly similar performance. This observation is likely due to the rapid change in clusters with slight variation in traffic conditions at high values of ρ, a case that will reduce the likelihood of observing the same cluster for 5 or 6 consecutive 30-second periods. Figure 45 shows, however, that for *PF*=2 the performance improves up to a value of 0.3% FAR.

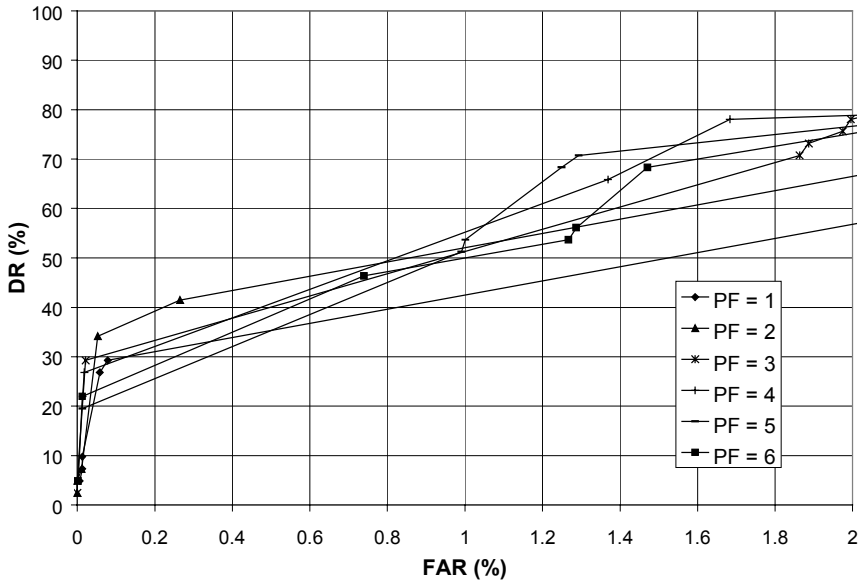

Figure 43: DR-FAR performance envelopes of the Fuzzy ART network for *testing* results using *one-minute occupancy* patterns and ρ = 0.80

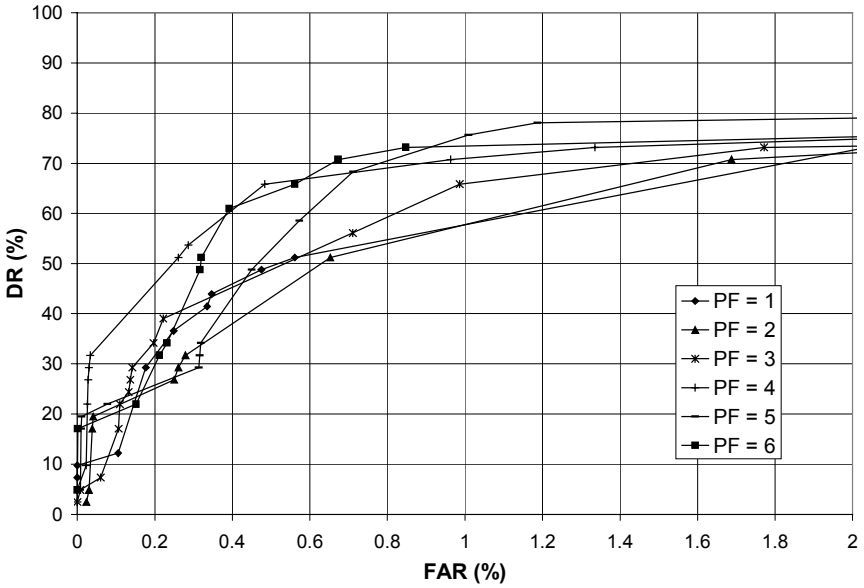

Figure 44: DR-FAR performance envelopes of the Fuzzy ART network for *testing* results using *one-minute occupancy* patterns and ρ = 0.90

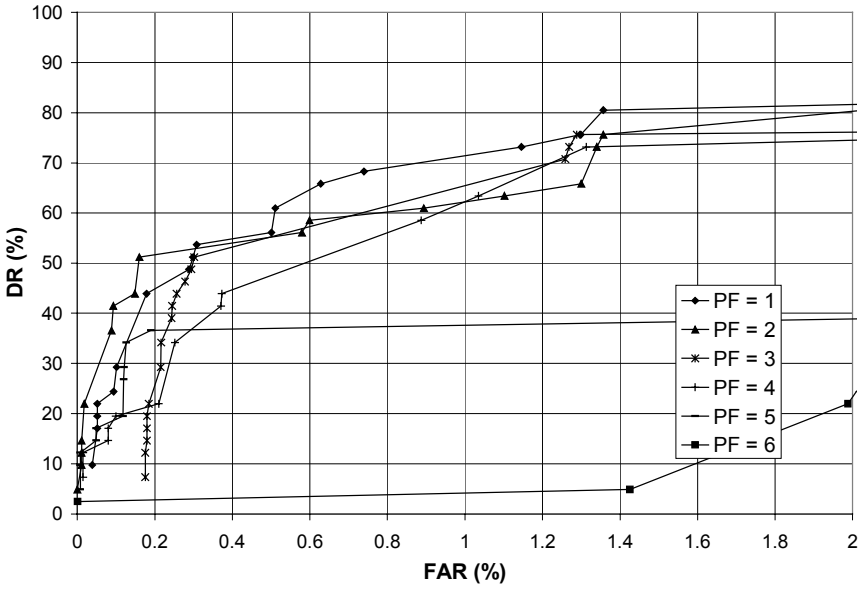

Figure 45: DR-FAR performance envelopes of the Fuzzy ART network for *testing* results using *one-minute occupancy* patterns and ρ = 0.95

The effect of the persistence factor on the performance of speed-based testing results is shown in Figure 46, Figure 47, and Figure 48. For ρ=0.80 the performance varied substantially with different values of the persistence factor. Figure 46 shows that the best performance is achieved by *PF*=1 up to 0.4% FAR, then by *PF*=2 thereafter. The same observation can be supported by Figure 47 and Figure 48 for ρ=0.90 and ρ=0.95, respectively. The two figures also show that the performance degraded with larger values of *PF* due primarily to the same reason mentioned before. Similar conclusions can be drawn from the performance of occupancy-speed patterns shown in Figure 49, Figure 50, and Figure 51. A persistence factor of 2 was arbitrarily selected and adopted throughout the rest of the analysis. It should be noted, however, that regardless of the value of the persistence factor, the effect of the factors presented in the following sections remain

unchanged. A complete presentation of the performance envelopes under all possible combinations of the selected variables can be found in Appendix A.

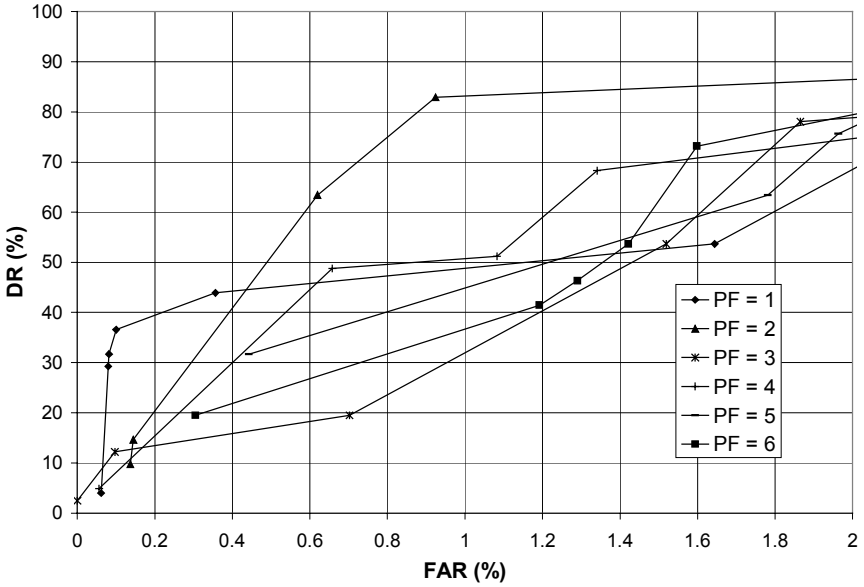

Figure 46: DR-FAR performance envelopes of the Fuzzy ART network for *testing* results using *one-minute speed* patterns and ρ = 0.80

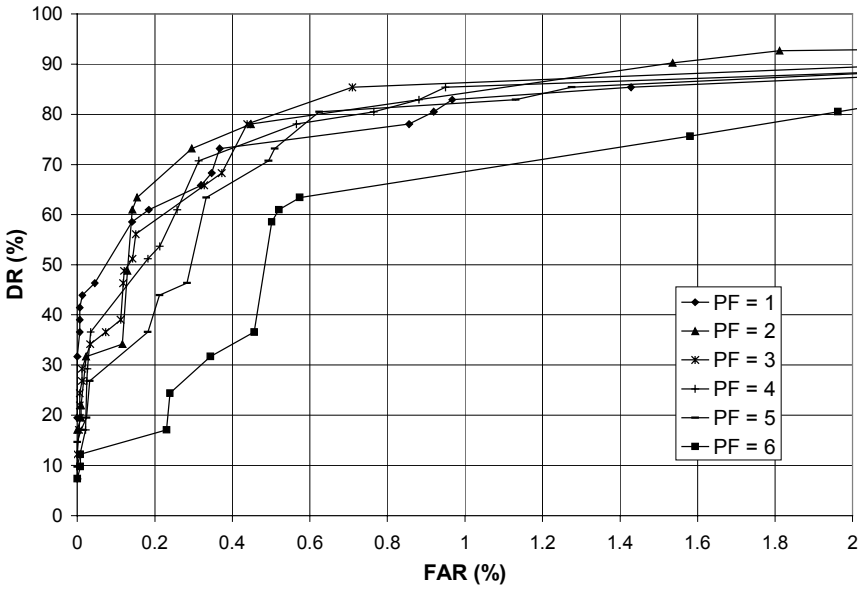

Figure 47: DR-FAR performance envelopes of the Fuzzy ART network for *testing* results using *one-minute speed* patterns and ρ = 0.90

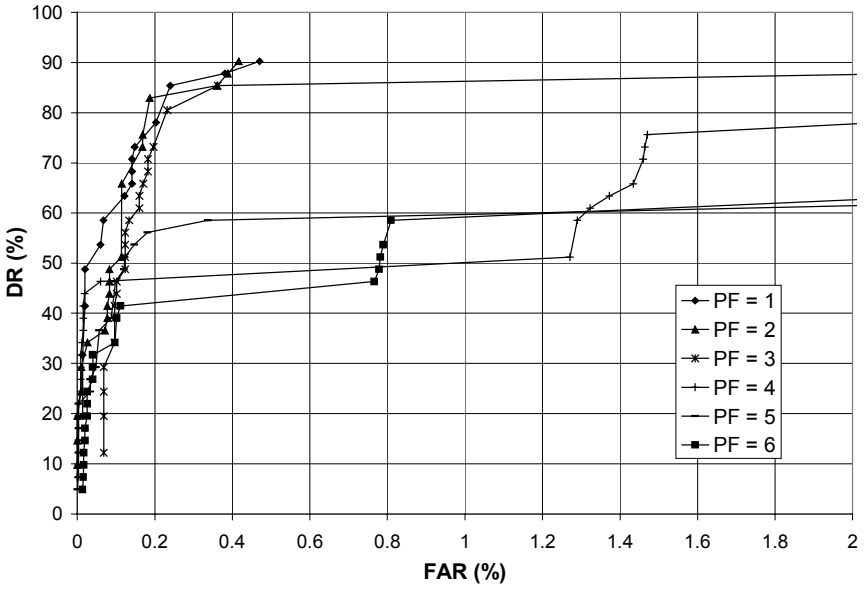

Figure 48: DR-FAR performance envelopes of the Fuzzy ART network for *testing* results using *one-minute speed* patterns and $\rho = 0.95$

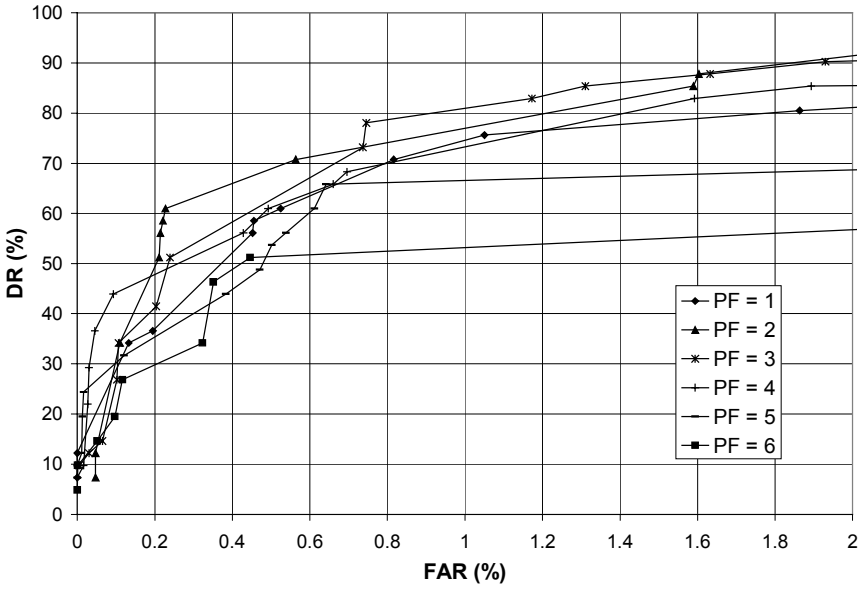

Figure 49: DR-FAR performance envelopes of the Fuzzy ART network for *testing* results using *one-minute occupancy-speed* patterns and $\rho = 0.80$

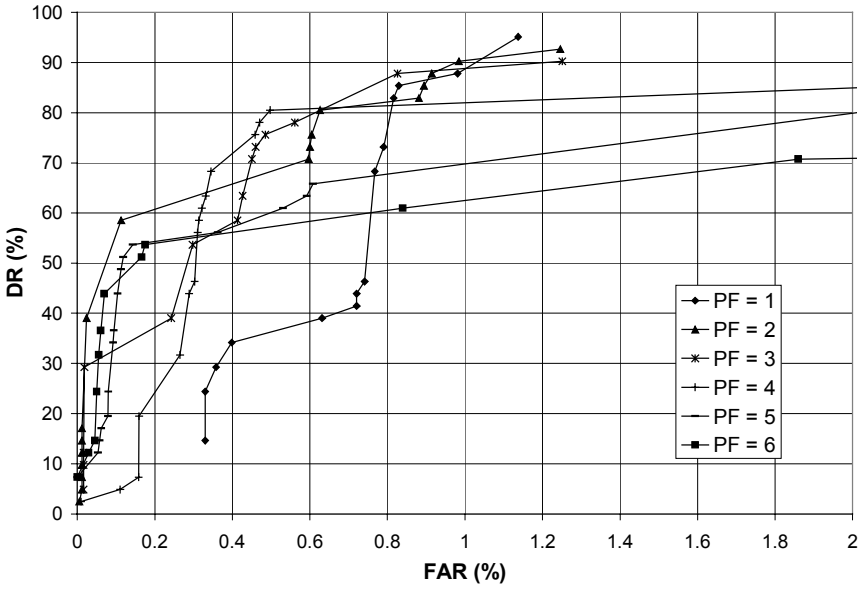

Figure 50: DR-FAR performance envelopes of the Fuzzy ART network for *testing* results using *one-minute occupancy-speed* patterns and ρ = 0.90

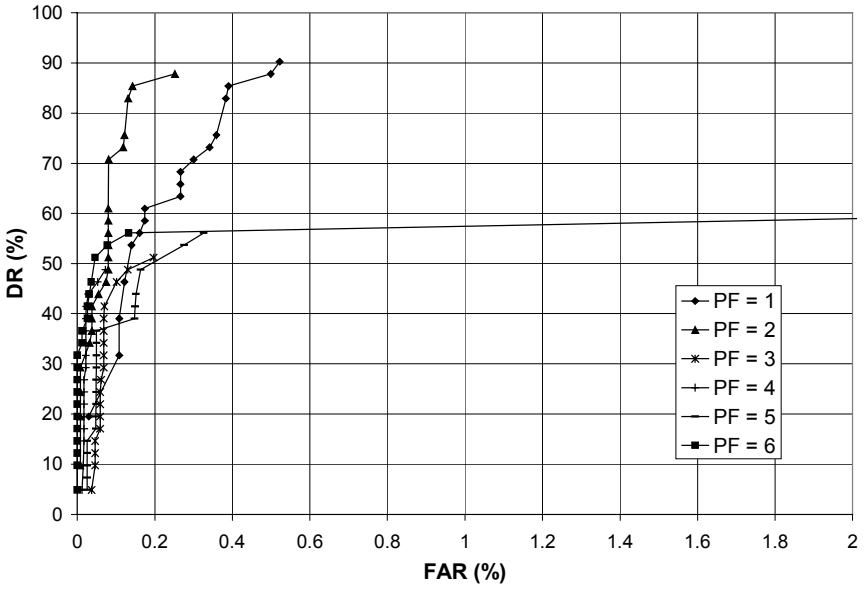

Figure 51: DR-FAR performance envelopes of the Fuzzy ART network for *testing* results using *one-minute occupancy-speed* patterns and ρ = 0.95

2.15.2 The Effect of the Vigilance Parameter (ρ)

The vigilance parameter is one of the most important parameters that control the dynamics of Fuzzy ART network. This parameter determines the degree of clustering achieved by the algorithm. As ρ increases, the number of generated clusters will increase, resulting in finer clustering. On the other hand, small values of ρ lead to coarse clustering. To investigate the effect of the degree of clustering on the performance of the algorithm, three sets of ρ values were suggested (0.80, 0.90, and 0.95). For each scenario considered here the training process was performed using each of the three vigilance parameter values. To illustrate the effect of the vigilance parameter on the algorithm performance the other influencing factors were held constant.

Figure 52 and Figure 53 show the performance envelopes during training using occupancy and speed patterns, respectively. The two figures were based on patterns with a temporal size of two 30-second periods and for a persistence factor equal to two. It is clearly shown that as the value of the vigilance parameter increases, the performance envelope is shifted upwards, indicating improvement in performance. The performance improvement is evidenced by the increase in detection rates at the same values of false alarm rates or a decrease in false alarm rates at the same values of detection rates. The performance envelopes of the testing results, shown Figure 54, Figure 55, and Figure 56, also exhibit the same effect. The three figures show the performance envelopes for occupancy, speed, and occupancy-speed patterns, respectively. Large values of ρ result in fine clustering of the traffic patterns and, consequently, an increased ability to

distinguish incident patterns from incident-like patterns. In other words, as ρ increases, traffic patterns associated with the incidents are more likely to be separable from similar traffic patterns that usually cause false alarms. This evidently results in reduction in the false alarm rate at the expense of increasing the number of incident clusters. Finer clustering creates a tendency to separate traffic patterns associated with incidents into more clusters, which results in increasing the number of selected incident clusters. It should also be noted here that performance derived from testing results has obviously dropped from that of the training results. This is a common observation in most artificial neural network applications and is attributed to the network's less-than-perfect ability to generalize from the limited size of the training data set.

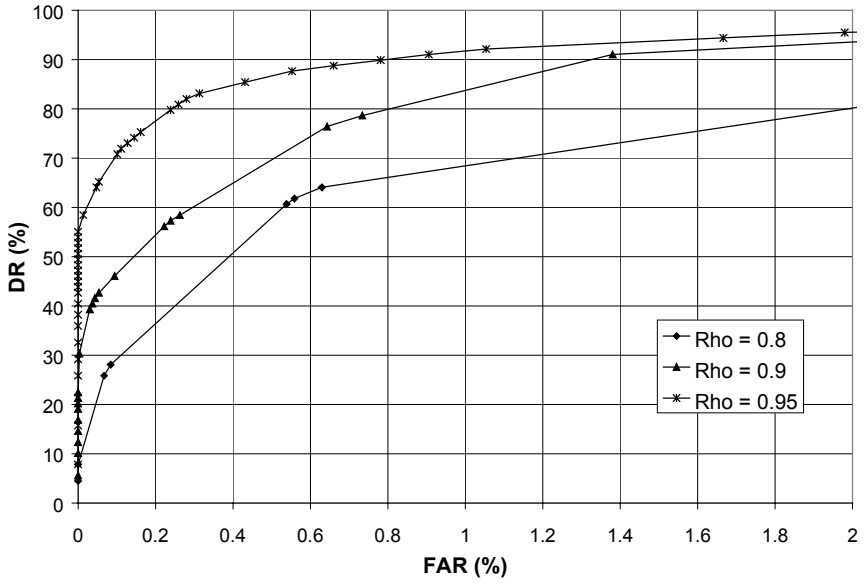

Figure 52: DR-FAR performance envelopes of the Fuzzy ART network for *training* results using *occupancy* patterns with *two* 30-second periods and *PF*=2

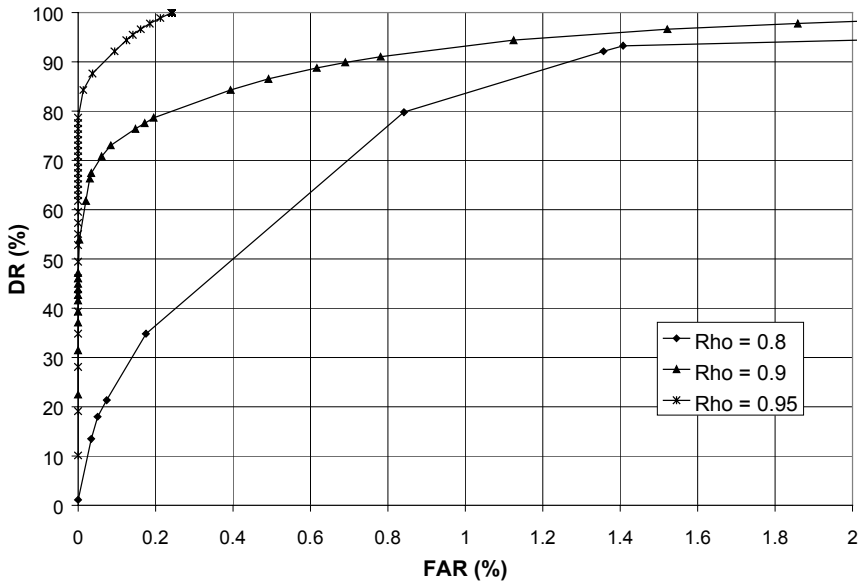

Figure 53: DR-FAR performance envelopes of the Fuzzy ART network for *training* results using *speed* patterns with *two* 30-second periods and *PF*=2

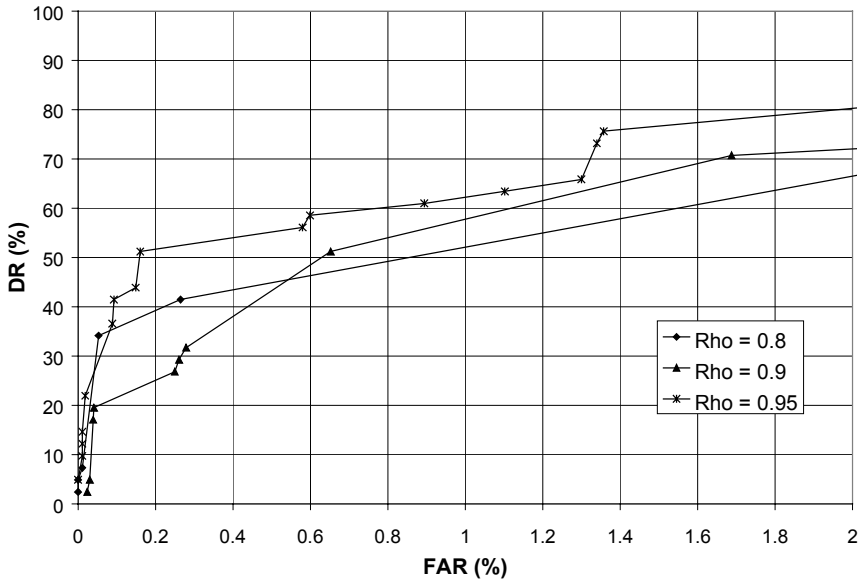

Figure 54: DR-FAR performance envelopes of the Fuzzy ART network for *testing* results using *occupancy* patterns with *two* 30-second periods and *PF*=2

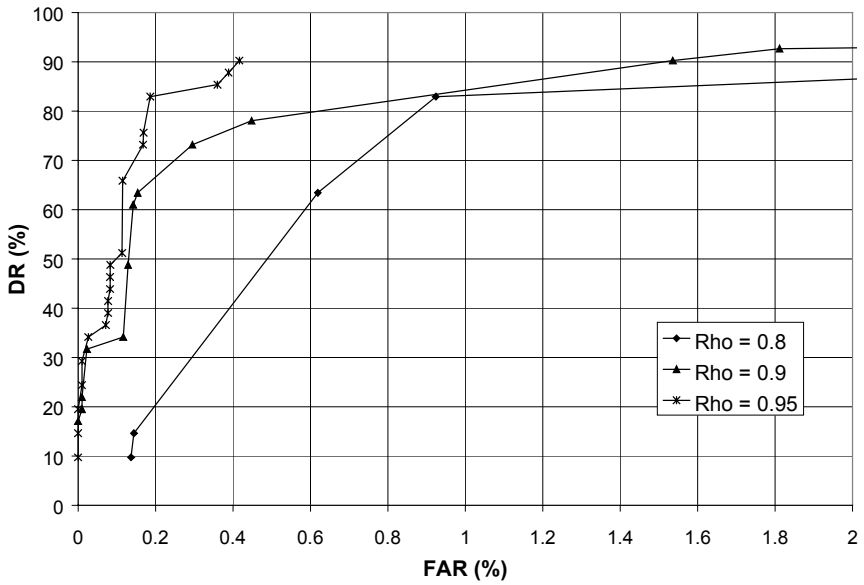

Figure 55: DR-FAR performance envelopes of the Fuzzy ART network for *testing* results using *speed* patterns with *two* 30-second periods and *PF*=2

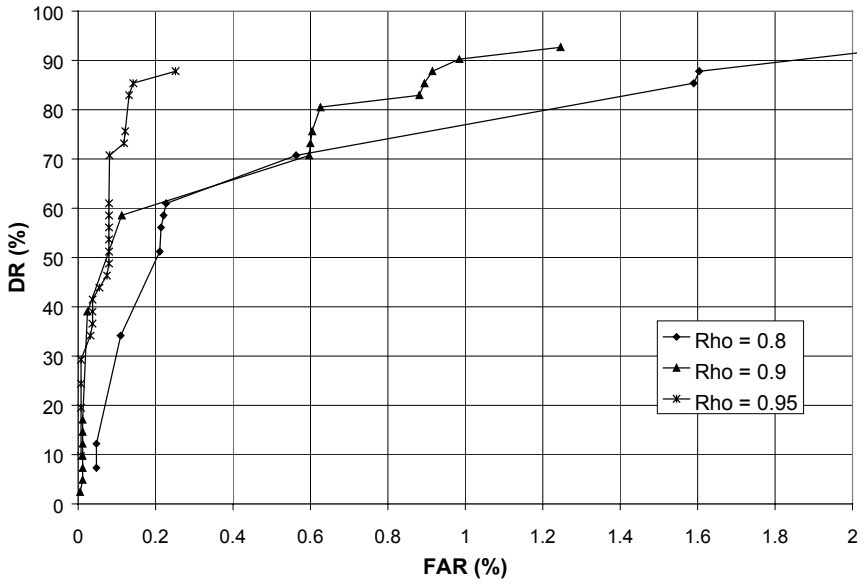

Figure 56: DR-FAR performance envelopes of the Fuzzy ART network for *testing* results using *occupancy-speed* patterns with *two* 30-second periods and *PF*=2

2.15.3 The Effect of the Temporal Pattern Size

Another factor that is very likely to affect the performance of the algorithm is the size of the traffic pattern. As the traffic pattern size increases it becomes more representative of the traffic conditions on the freeway section. As mentioned earlier, all traffic patterns are defined by the spatial dimension and the temporal dimension. The spatial dimension was fixed to three consecutive stations while the temporal dimension varied from one to two 30-second periods. The temporal pattern size influences directly the mean time of detection since the classification of the pattern cannot be made until the pattern is fully developed. In other words, patterns with larger temporal sizes take longer time to develop, and therefore, the decision on whether or not they are associated with an incident will be further delayed.

Figure 57 and Figure 58 show the performance envelopes for training results using half-minute and one-minute patterns of occupancy and speed, respectively. The comparative evaluation of performance was based on a persistence factor equal to two. The figures show that performance improved significantly when the pattern size increased from half-minute to one-minute for both occupancy and speed patterns. The pattern size is indicated in parentheses as (*a*x*b*), where *a* and *b* represent the temporal and spatial pattern sizes, respectively. The figures also show that the performance improved when the vigilance parameter increased from 0.8 to 0.95, as presented in the previous section. Similar conclusions were supported by the testing results, as shown in Figure 59, Figure 60, and Figure 61. The three figures show that one-minute patterns resulted in better

performance than half-minute patterns for testing results using occupancy, speed, and occupancy-speed patterns. The most reasonable interpretation to this observation is that one-minute patterns contain more information on the effect of the incident than half-minute patterns. The additional information in larger patterns is more likely to make the patterns associated with incidents more discernible from incident-like patterns. In this case false alarm rate will significantly decrease. However, as the pattern size increases the expected number of incident clusters will also increase.

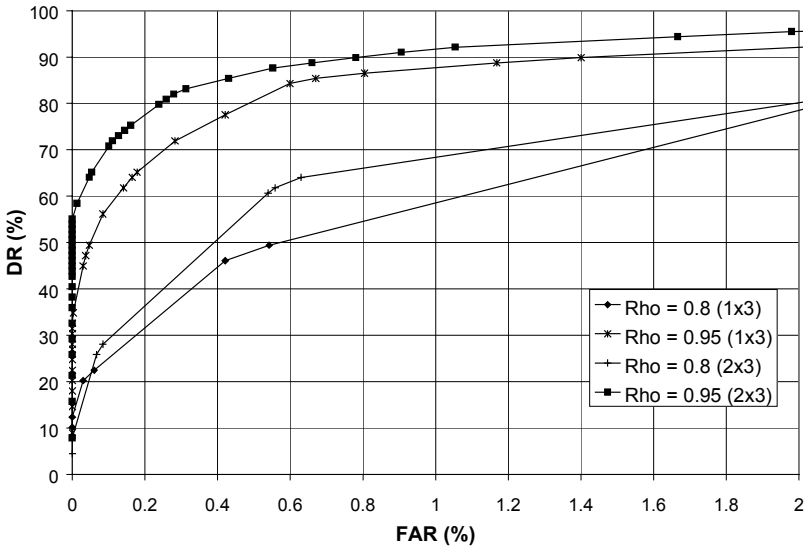

Figure 57: DR-FAR performance envelopes of the Fuzzy ART network for *training* results using *half-minute and one-minute occupancy* patterns for ρ=0.8 and ρ=0.95, and *PF*=2

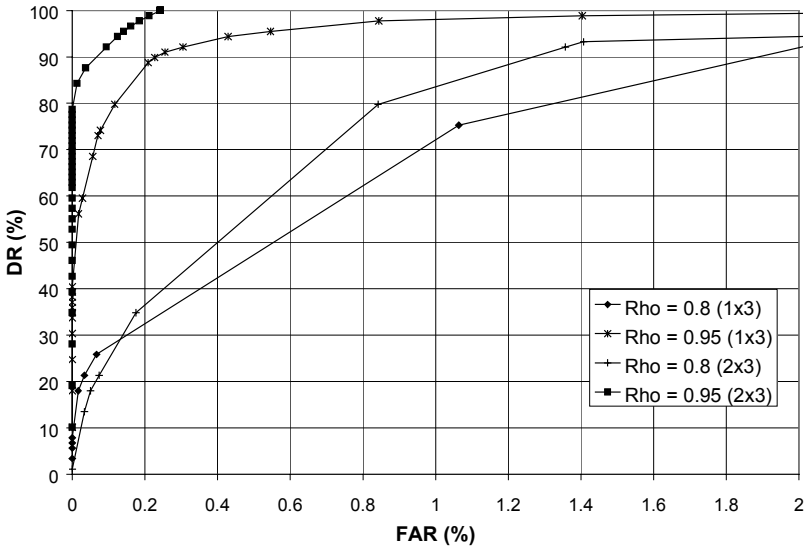

Figure 58: DR-FAR performance envelopes of the Fuzzy ART network for *training* results using *half-minute* and *one-minute speed* patterns for ρ=0.8 and ρ=0.95, and *PF*=2

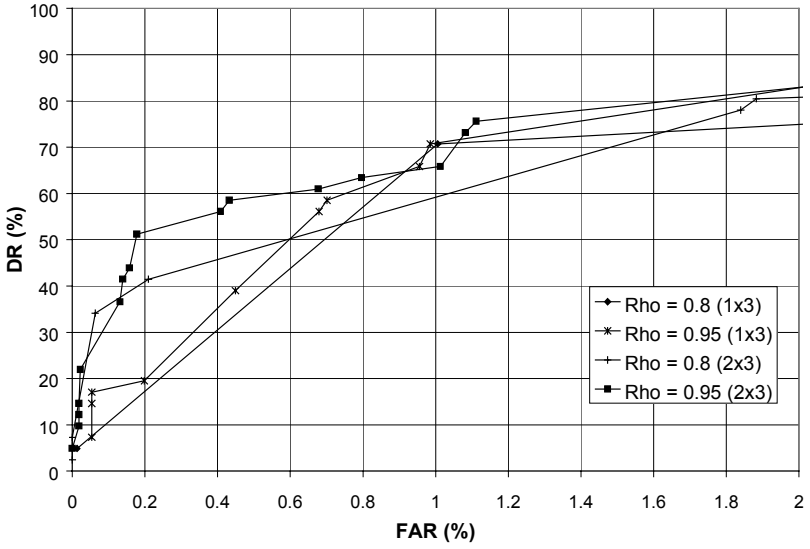

Figure 59: DR-FAR performance envelopes of the Fuzzy ART network for *testing* results using *half-minute* and *one-minute occupancy* patterns for ρ=0.8 and ρ=0.95, and *PF*=2

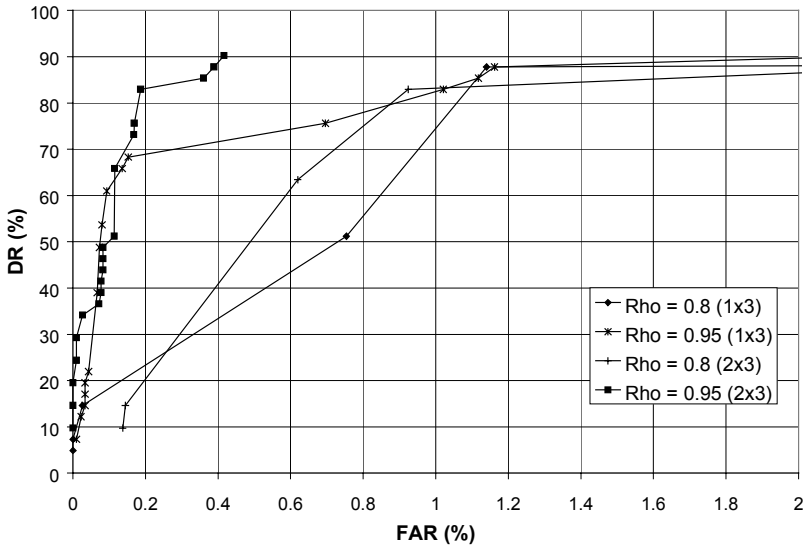

Figure 60: DR-FAR performance envelopes of the Fuzzy ART network for *testing* results using *half-minute* and *one-minute speed* patterns for ρ=0.8 and ρ=0.95, and *PF*=2

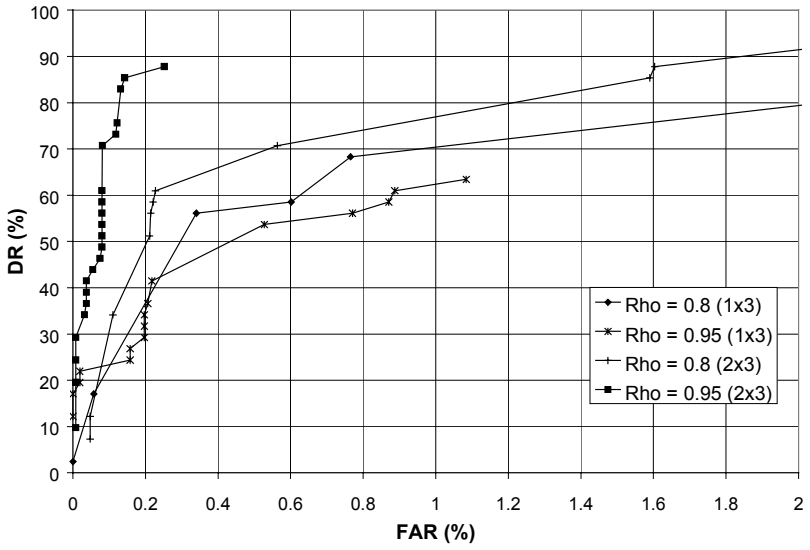

Figure 61: DR-FAR performance envelopes of the Fuzzy ART network for *testing* results using *half-minute* and *one-minute occupancy-speed* patterns for ρ=0.8 and ρ=0.95, and *PF*=2

2.15.4 The Effect of the Traffic Parameter

Another important factor that is likely to affect the performance of the ANN-based incident detection algorithms is the type of traffic parameter used for representation of traffic conditions. In the application of Fuzzy ART network traffic conditions were portrayed in three different forms using occupancy, speed, and a combination of the two. To investigate the effect of the type of traffic parameter on the algorithm performance all other factors were held constant; i.e. the temporal pattern size was set to one-minute, the vigilance parameter to 0.95, and the persistence factor to two. Figure 62 exhibits the different performance envelopes obtained from occupancy, speed, and occupancy-speed patterns using training results. The figure shows clearly that significant improvement in the performance was achieved by using speed patterns rather than occupancy patterns. This indicates that Fuzzy ART algorithm was capable of differentiating clusters of incident speed patterns from incident-like speed patterns more than those of incident occupancy patterns from incident-like occupancy patterns. In other words, the effect of the incidents on speed patterns is more discernible from that on occupancy patterns.

However, when occupancy and speed are both used to represent traffic conditions, their patterns further improved the Fuzzy ART performance as shown in Figure 62. The combination of both occupancy and speed into one pattern is more likely to add more information that will make traffic patterns associated with incidents more distinguishable. The same observation can be supported by Figure 63, which shows the comparative evaluation of the performance envelopes for each traffic parameter using testing results.

As highlighted in earlier sections, the overall performance of the algorithm slightly drops at testing results when compared with training results.

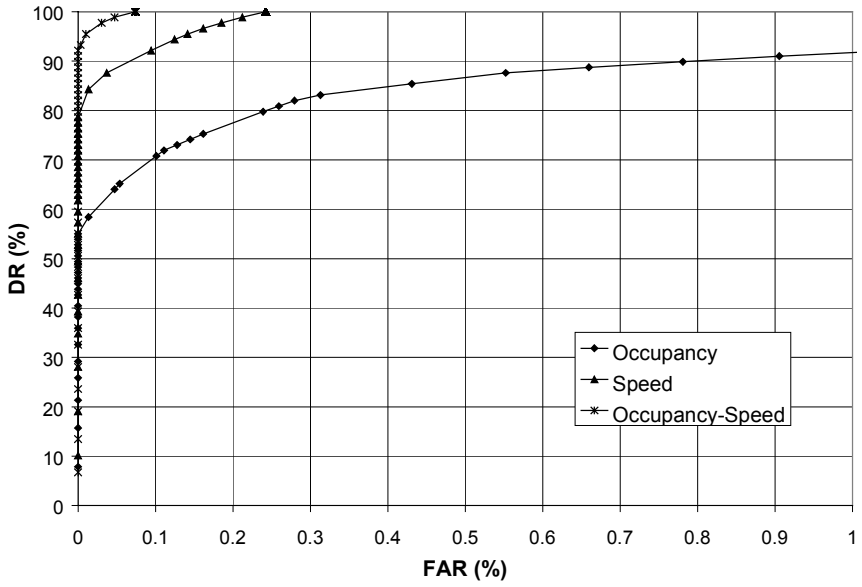

Figure 62: DR-FAR performance envelopes of the Fuzzy ART network for *training* results using *one-minute* patterns for ρ=0.95 and *PF*=2

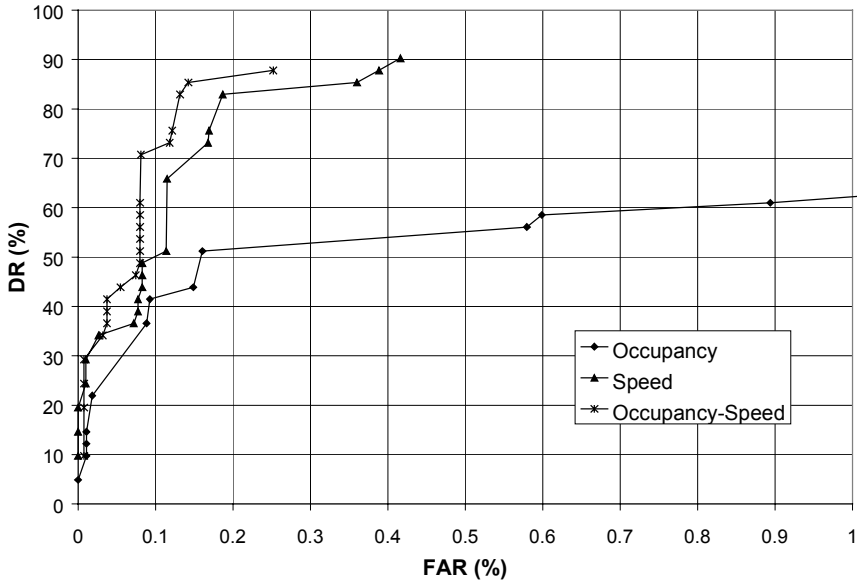

Figure 63: DR-FAR performance envelopes of the Fuzzy ART network for *testing* results using *one-minute* patterns for ρ=0.95 and *PF*=2

2.15.5 Comparative Evaluation

In this section the results of the Fuzzy ART network were compared with the results of two traditional incident detection algorithms, namely California #7 and #8. The two California algorithms are a part of the original work done in incident detection on freeways. California #7 is a simplified version that compares occupancy at two consecutive stations. Version #8, however, is more complicated due to the incorporation of a mechanism to suppress the false alarms produced by compression waves through the use of a persistence period. Both versions require calibration with incident and loop data to select the optimum set of threshold values. The performance of the two California algorithms was evaluated using the DR-FAR performance envelopes for various combinations of threshold values.

For California algorithm #7 the calibration process entailed attempting as many combinations of values for the three thresholds as possible. Each threshold can take on values between 0% and 100%. The calibration process was completed in two steps. First a wide range of values with large increments was applied using the values in Table 6. The first step resulted in a total of 330 different combinations or runs. Each run was associated with a detection rate and a false alarm rate. The performance envelope was plotted for those runs that maximized the ratio between detection rate and false alarm rate. This ratio was used to determine the envelope that maximizes the performance of the algorithm. To further improve the performance envelope a narrower range of threshold values was selected based on the range of threshold values associated with the

first performance envelope. This led to the execution of step 2, which involved using a 2% increment in each threshold as shown in Table 7. The resulting performance envelope improved after step 2 and will be used for comparative evaluation.

Table 6: Range of threshold values for calibration of California algorithm #7 – step 1

	T_1 (0 to 100)%	**T_2 (0 to 100)%**	**T_3 (0 to 100)%**
Minimum	5	30	10
Maximum	30	80	30
Increment	5	5	5

Table 7: Range of threshold values for calibration of California algorithm #7 – step 2

	T_1 (0 to 100)%	**T_2 (0 to 100)%**	**T_3 (0 to 100)%**
Minimum	5	30	15
Maximum	15	40	25
Increment	2	2	2

The calibration of California algorithm #8 was similar to that of #7, except that it has 5 thresholds instead of 3. The calibration was performed in two steps as shown in Table 8 and Table 9. The initial threshold ranges were selected such that they accommodate the values recommended by the calibration of the algorithm in the final FHWA report (Payne et al., 1976). The second step was also selected based on the results of the first step.

Table 8: Range of threshold values for calibration of California algorithm #8 – step 1

	T_1 (0 to 100)%	T_2 (-100 to 100)%	T_3 (0 to 100)%	T_4 (0 to 100)%	T_5 (0 to 100)%
Minimum	5	-40	20	10	25
Maximum	35	-20	60	30	35
Increment	10	10	10	10	10

Table 9: Range of threshold values for calibration of California algorithm #8 – step 2

	T_1 (0 to 100)%	**T_2 (-100 to 100)%**	**T_3 (0 to 100)%**	**T_4 (0 to 100)%**	**T_5 (0 to 100)%**
Minimum	5	-20	45	15	20
Maximum	5	-20	55	25	30
Increment	1	1	2	2	2

Comparison between the performance envelopes of Fuzzy ART and California algorithms #7 and #8 is shown in Figure 64. The figure shows that Fuzzy ART has outperformed both versions of California algorithms, which showed very similar performance. The comparison was based on PF=2 and ρ = 0.95. The best performance was achieved by Fuzzy ART algorithm with occupancy-speed patterns, followed by that with speed patterns. The performance of Fuzzy ART algorithm with occupancy patterns matched closely that of both California #7 and #8. It should be noted here that California algorithms are also occupancy-based. This supports the limitation of relying only on occupancy measurements for freeway incident detection.

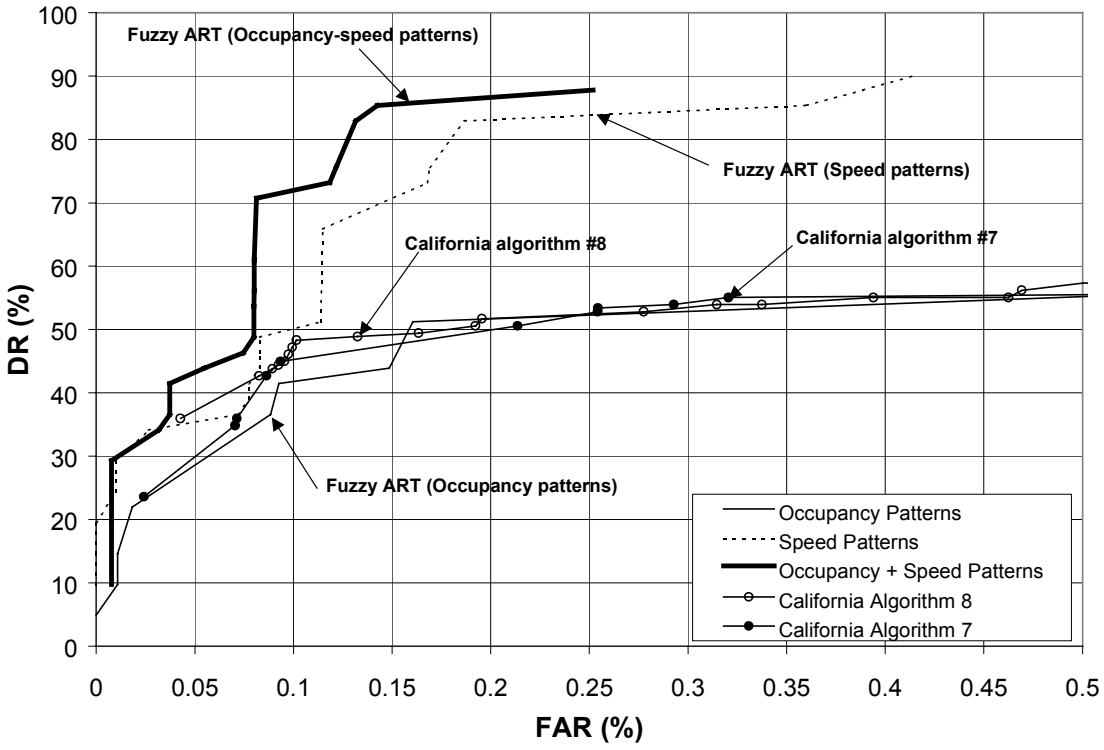

Figure 64: Comparison between the performance of Fuzzy ART and California algorithms versions #7 and #8

3 CONCLUSIONS AND RECOMMENDATIONS

This report presented the results of training and testing the Fuzzy ART network for the application of automatic freeway incident detection. The performance envelopes of the DR-FAR relationship were the basis for assessing the performance of the algorithm. For performance improvement, a persistence period and a persistence factor were introduced to reduce the false alarm rate. The effect of the persistence factor was not significant for values in the range between 1 and 4. The performance was evaluated under a variety of scenarios to address the impact of some factors on the overall algorithm performance. Those factors included the vigilance parameter, the temporal pattern size, and the type of traffic parameter. The results showed that the performance could be significantly improved with increasing the value of the vigilance parameter (ρ=0.95) and the temporal pattern size. Also, results based on speed patterns outperformed those based on occupancy patterns. However, the combination of occupancy and speed has resulted in the highest performance. Comparative evaluation between the Fuzzy ART algorithm and California algorithms version 7 and 8 was presented.

The results of this research study have demonstrated the potential of applying the artificial neural networks for automated detection of incidents on freeways using the existing loop detector data. This was the primary objective of the study. To accomplish this objective, the Fuzzy ART algorithm (based on unsupervised learning) was trained to detect lane-blocking incidents using real life loop detector data collected on the central corridor of I-4 in Orange County. The inputs to the neural network were derived from the 30-second station averages of occupancy, speed, and volume. All loop data

underwent a process of filtering and smoothing to reduce abnormalities and random traffic fluctuations. Also, incident data was checked to verify the time and location.

The performance of the Fuzzy ART algorithm showed constant increase in detection rate up to nearly 88% at relatively low values of FAR. The temporal pattern size and the type of pattern affected the performance of the Fuzzy ART algorithm. The results demonstrated that the incident detection performance improves as the temporal size increases. For Fuzzy ART algorithm, one-minute patterns led to better performance than 30-second patterns. This can be attributed to the extra information contained in the pattern as its size increases, and therefore, traffic patterns associated with incidents become more discernible from similar incident-free patterns. For implementation of the Fuzzy ART algorithm a three-minute persistence period was introduced, along with a persistence factor, to reduce the false alarm rate. Better performances were obtained for a vigilance parameter of 0.95.

An interesting finding is that when compared with occupancy patterns, speed patterns constantly produce better results. This is likely to indicate that incidents can be detected with speed patterns better than occupancy patterns. The results of the Fuzzy ART network suggest that the combination of occupancy and speed in the representation of traffic pattern lead to a better performance. The additional information is more likely to make incident patterns more distinguishable from incident-like patterns. This also supports the finding that better results are achieved when the temporal size of the traffic pattern is increased.

REFERENCES

Al-Deek H., Cryer J., Ishak S., Khan A., and Yarid J. (1995b). LOVATS: Loop Output Verification and Algorithm Testing System*, Draft User Manual, Text Version, Parts I and II*, Department of Civil and Environmental Engineering, University of Central Florida.

Al-Deek H., S. Ishak and R. Lai, (1995a). LOVATS: Loop Output Verification and Algorithm Testing System*, Draft User Manual, Window Version*, Department of Civil and Environmental Engineering, University of Central Florida.

Al-Deek, H.M., S.S. Ishak, and A.A. Khan (1996). Impact of Freeway Geometric and Incident Characteristics on Incident Detection. *ASCE Journal of Transportation Engineering,* Vol. 122, No. 6.

Athol P. (1965). Interdependence of Certain Operational Characteristics within a Moving Traffic Stream. *Highway Research Record* 72, pp. 58-87.

Camargo F. A. (1990). *Learning Algorithms in Neural Networks*. The DCC Laboratory, Department of Computer Science, Columbia University, New York.

Carpenter G., Grossberg S., and Rosen D (1991). Fast Stable Learning and Categorization of Analog Patterns by an Adaptive Resonance System. *Neural Networks*, Vol. 4., pp. 759-771.

Cheu, R. L. (1994) *Neural Network Models for Automated Detection of Lane-Blocking Incidents on Freeways*. Ph.D. dissertation, Irvine, University of California at Irvine.

Cheu R. and Ritchie S. (1995) Automated Detection of Lane-Blocking Freeway Incidents using Artificial Neural Networks. *Transportation Research-C*, Vol. 3, No. 6, pp. 371-388.

Collins J. F. (1983). *Automatic Incident Detection - Experience with TRRL Algorithm HIOCC.* Department of the Environment. Department of Transport. Supplementary Report 775.

Collins J. F., Hopkins C. M., and Martin J. A. (1979). *Automatic Incident Detection - TRRL Algorithms HIOCC and PATREG.* Department of the Environment. Department of Transport. Supplementary Report 526.

Dia H. and Rose G. (1997) Development and Evaluation of Neural Network Freeway Incident Detection Models using Field Data. *Transportation Research-C*, Vol. 5, No. 5, pp. 313-331.

Dia H. and Rose G. (1995) Development of artificial neural network models for automated detection of freeway incidents. *WCTR '95*, *the seventh World Conference on Transport Research.*

Dia H., Rose G., and Snell A. (1996) Comparative performance of freeway automated incident detection algorithms. *Joint 18th ARRB Transport Research Conference and Transit NZ Land Transport Symposium*, Christchurch, New Zealand.

Florida Department of Transportation, District-5 (1992). *The Status of the Traffic Surveillance System on I-4*. Unpublished report.

Forbes J. F. (1992). Identifying Incident Congestion. *ITE Journal*, pp. 17-22.

Gall A. and F. Hall (1990). Distinguishing Between Incident Congestion and Recurrent Congestion: A Proposed Logic. Transportation Research Record 1232, pp. 1-8.

Giuliano G. (1989) Incident Characteristics, frequency, and duration on a high volume urban freeway. *Transpn. Res.-A* 23, 387-396.

Hall F.Y., Shi, and Atala G. (1993). On-line Testing of the McMaster Incident Detection Algorithm under Recurrent Congestion, paper presented at the 72nd Annual Meeting of the Transportation Research Board, Washington, DC.

Hassoum M. (1995). *Fundamentals of Artificial Neural Networks*, The MIT Press, Cambridge, Massachusetts.

Haykin S. (1994). *NEURAL NETWORKS A Comprehensive Foundation,* McMillan College Publishing Company, New York.

Hsio C.H., Lin C. T., and Cassidy M. (1994) An application of fuzzy set theory to incident detection. *Preprint No. 930571. Transportation Research Board,* 72nd annual meeting.

Hsio C.H., Lin, C. T., and Cassidy M. (1994) Application of Fuzzy Logic and Neural Networks to Automatically Detect Freeway Traffic Incidents. *Journal of transportation Engineering*, vol. 120, No. 5.

Huang J., Georgiopoulos M., and Heileman G.L. (1995) Fuzzy ART Properties. *Neural Networks*, Vol. 8, No. 2, pp. 203-213.

Kahn R. (1972) Interim Report on Incident Detection Logics for the Los Angeles Freeway Surveillance and Control Project. Report for California Department of Transportation, Sacramento, California.

Kasabov, N. K. (1996) *Foundations of Neural Networks, Fuzzy Systems, and Knowledge Engineering.* The MIT press, Cambridge, Massachusetts.

Levin M. and Krause G. (1979a). Incident-Detection Algorithms, Part 1. Off-Line Evaluation. *Transportation Research Record* 722, pp. 49-58.

Levin M. and Krause G. (1979b). Incident-Detection Algorithms, Part 2. On-Line Evaluation. *Transportation Research Record* 722, pp. 58-64.

Lindley, J.A. (1987) Urban Freeway Congestion: quantification of the problem and effectiveness of potential solutions. *Institute of Transportation Engineers Journal* 57(1), pp. 27-32.

Payne H. (1976) Development and Testing of Incident-Detection Algorithms: Vol. 1, Summary of Results. *Report FHWA-RD-76-19*, FHWA, U.S. Department of Transportation.

Payne H. and Tignor S. (1978). Freeway Incident Detection Algorithms Based on Decision Trees with States. *Transportation Research Record* 682, pp. 30-37.

Payne H., Helfenbein E., and Knobel H. (1976). Development and Testing of Incident-Detection Algorithms: Vol. 2, Research Methodology and Detailed Results. *Report FHWA-RD-76-20*, FHWA, U.S. Department of Transportation.

Persaud B. and Hall F. (1988a). *The McMaster Single Station Algorithm for Detection of Freeway Incidents*. Working paper, Dept. of Civil Engineering, McMaster University.

Persaud B. and Hall F. (1989). Catastrophe Theory and Patterns in 30-Second Freeway Traffic Data- Implications for Incident Detection. *Transportation Research-A*, Vol. 23A, No. 2, pp. 103-113.

Petty K., Noeimi H., Sanwal K., Rydzewski D., Skabardonis A., Varaiya P., and Al-Deek H. (1995). The Freeway Service Patrol Evaluation Project: Database, Support Programs, and Accessibility. *Paper submitted to Transportation Research C*.

Ritchie S. and Ruey L.C. (1993) Simulation of Freeway Incident Detection Using Artificial Neural Networks. *Transportation Research C*, Vol. 1. No. 3, pp. 203-217.

Rose G. and Dia H. (1995) Freeway automatic incident detection using artificial neural networks. *Application of New Technology to Transport Systems International Conference.*

Stephanedes Y. J. and Athanassios P. C. (1993) Freeway Incident Detection through Filtering. *Transportation Research C*, Vol. 1, No. 3, pp. 219-233.

Stephanedes Y. J. and Chassiakos A.P. (1993). Applications of Filtering Techniques for Incident Detection. *Journal of Transportation Engineering*, Vol. 119, No. 1.

Tignor S. and Payne H. (1977). Improved Freeway Incident-Detection Algorithms. *Public Roads*, pp. 32-40.

Willsky A. S., Chow E. Y., Gershwin S. B., Greene C. S., Houpt P. T., and Kurkjian A. L. (1980) Dynamic model-based techniques for the detection of incidents on freeways. *IEEE Trans. Autom. Control* 25, 347-360.

APPENDIX:

PERFORMANCE ENVELOPES OF FUZZY ART NETWORK

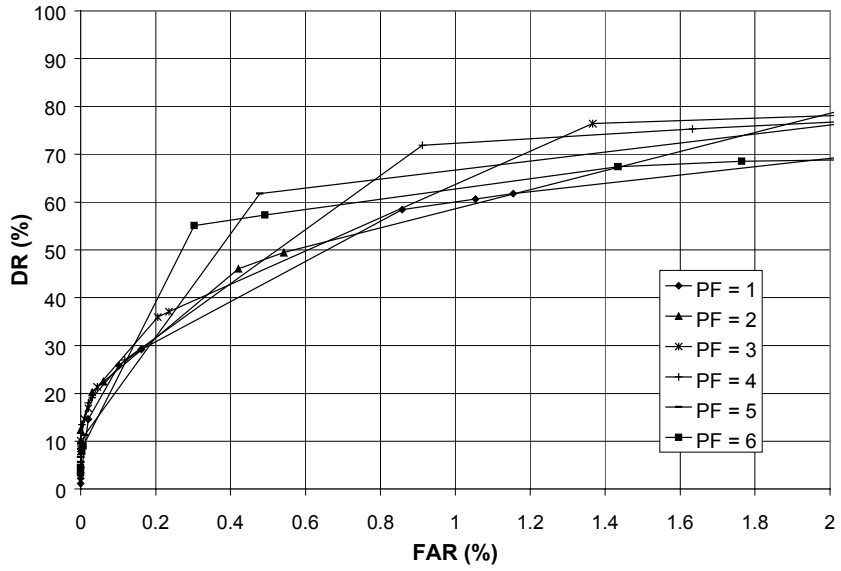

Figure 65: DR-FAR performance envelopes of the Fuzzy ART network for *training* results using *half-minute occupancy* patterns and $\rho = 0.80$

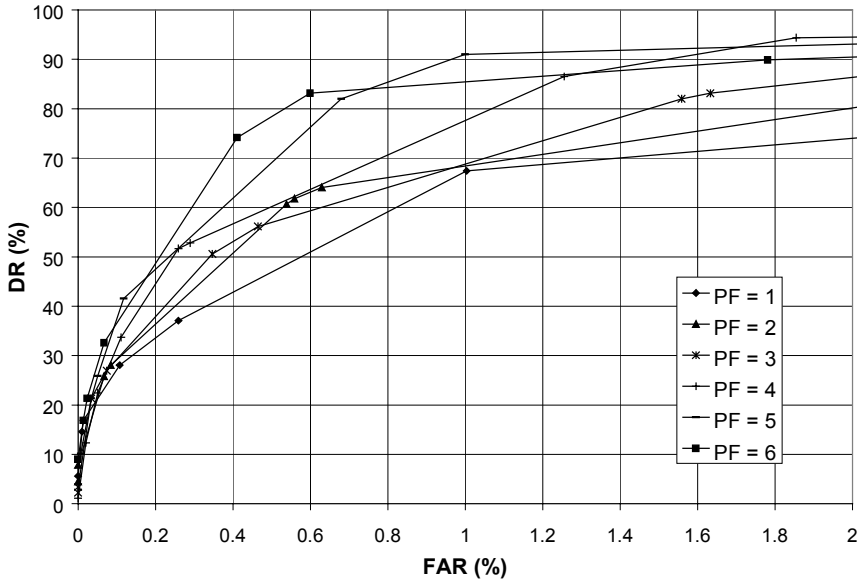

Figure 66: The DR-FAR performance envelopes of the Fuzzy ART network for *training* results using *one-minute occupancy* patterns and $\rho = 0.80$

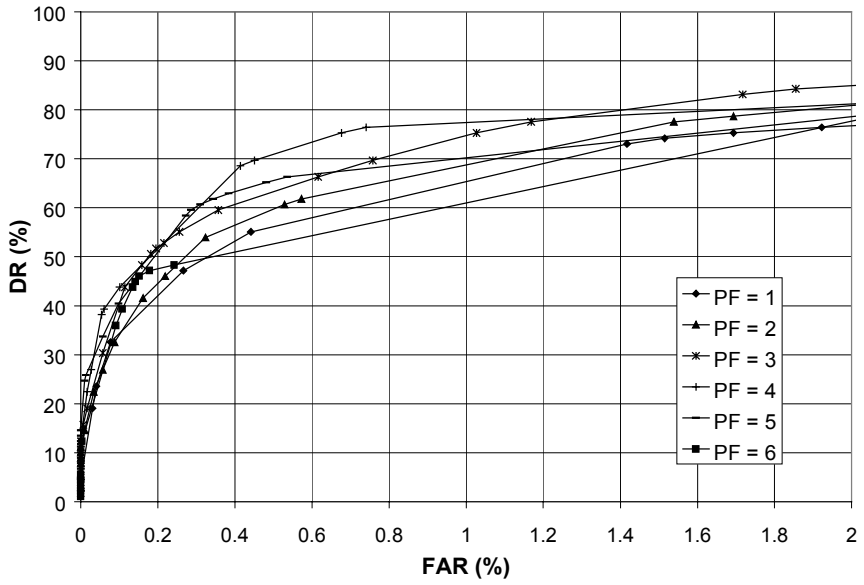

Figure 67: DR-FAR performance envelopes of the Fuzzy ART network for *training* results using *half-minute occupancy* patterns and ρ = 0.90

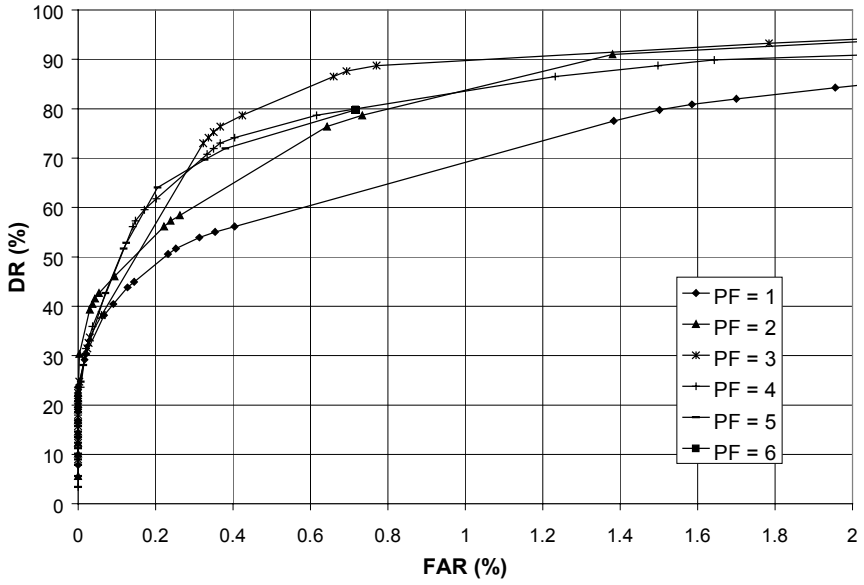

Figure 68: DR-FAR performance envelopes of the Fuzzy ART network for *training* results using *one-minute occupancy* patterns and ρ = 0.90

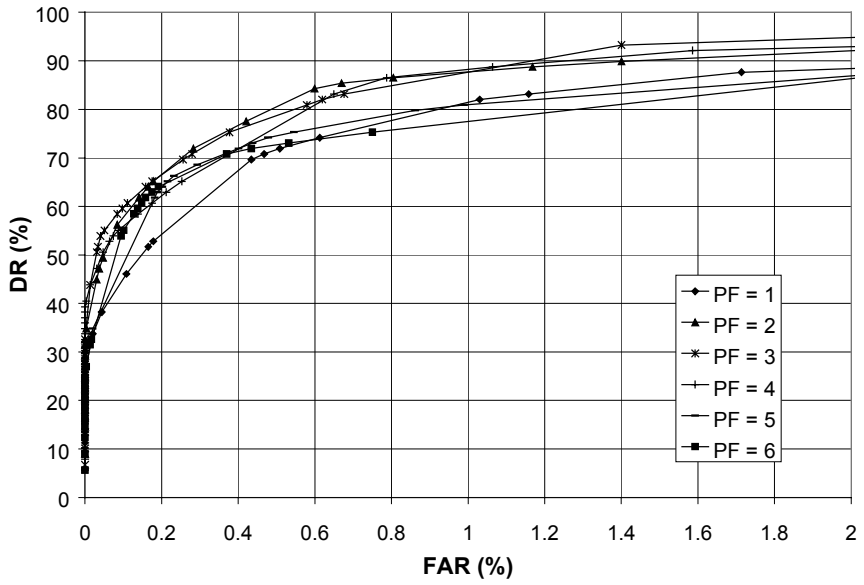

Figure 69: DR-FAR performance envelopes of the Fuzzy ART network for *training* results using *half-minute occupancy* patterns and $\rho = 0.95$

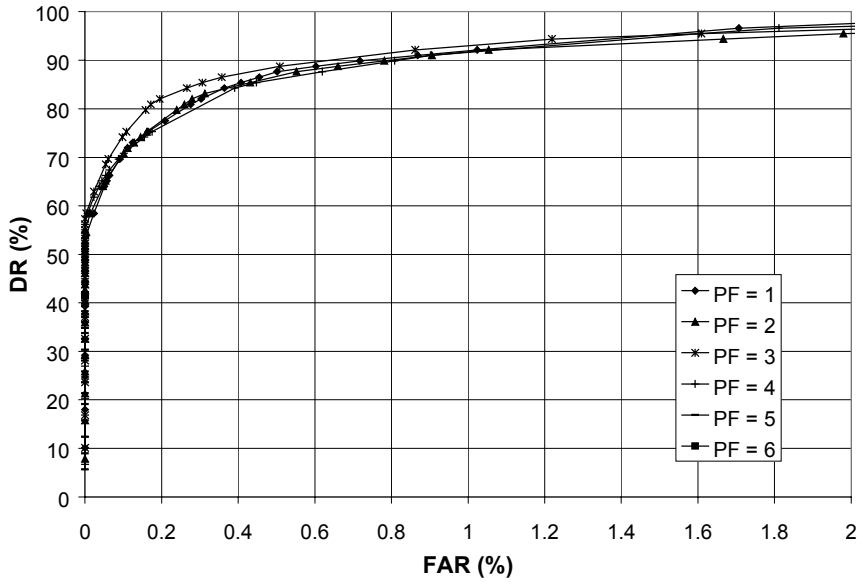

Figure 70: DR-FAR performance envelopes of the Fuzzy ART network for *training* results using *one-minute occupancy* patterns and $\rho = 0.95$

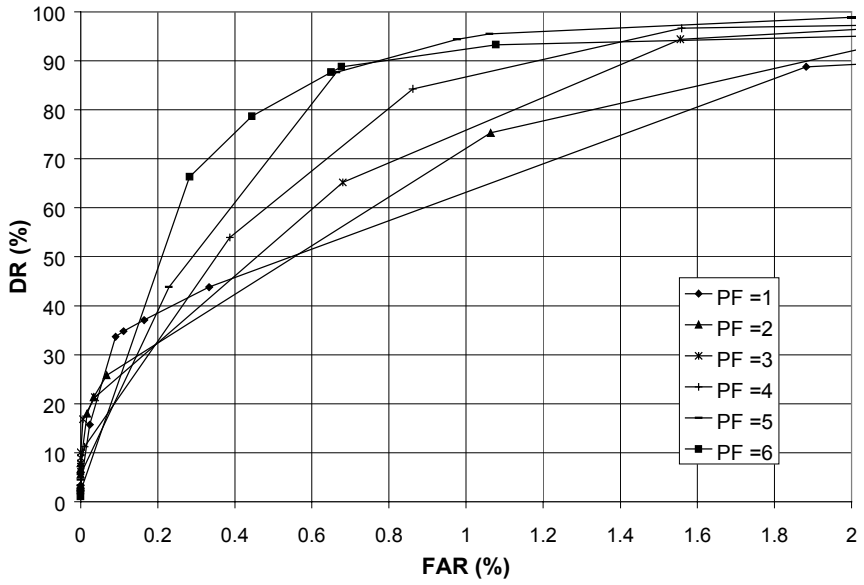

Figure 71: DR-FAR performance envelopes of the Fuzzy ART network for *training* results using *half-minute speed* patterns and ρ = 0.80

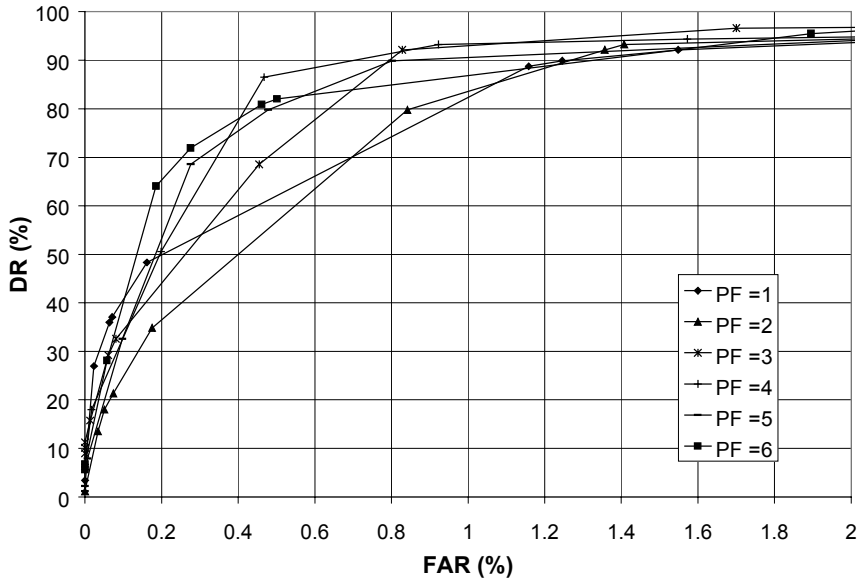

Figure 72: DR-FAR performance envelopes of the Fuzzy ART network for *training* results using *one-minute speed* patterns and ρ = 0.80

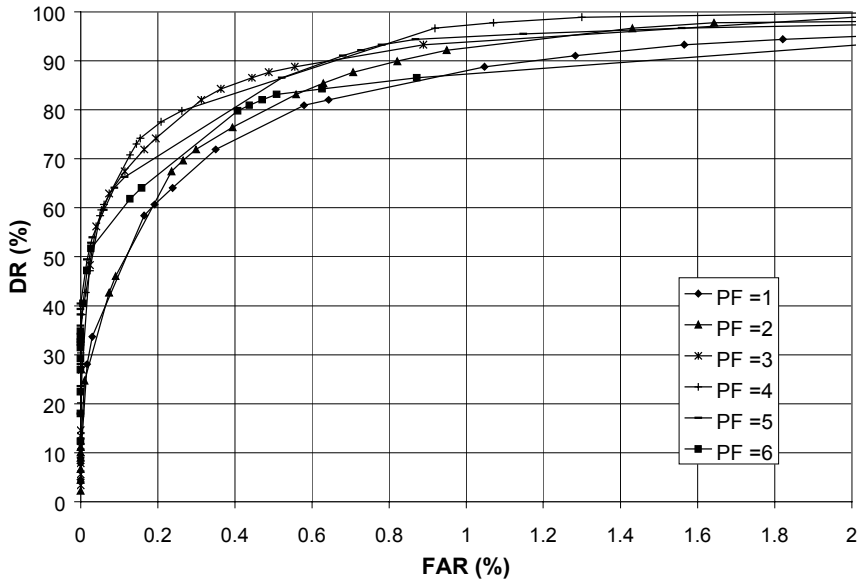

Figure 73: DR-FAR performance envelopes of the Fuzzy ART network for *training* results using *half-minute speed* patterns and ρ = 0.90

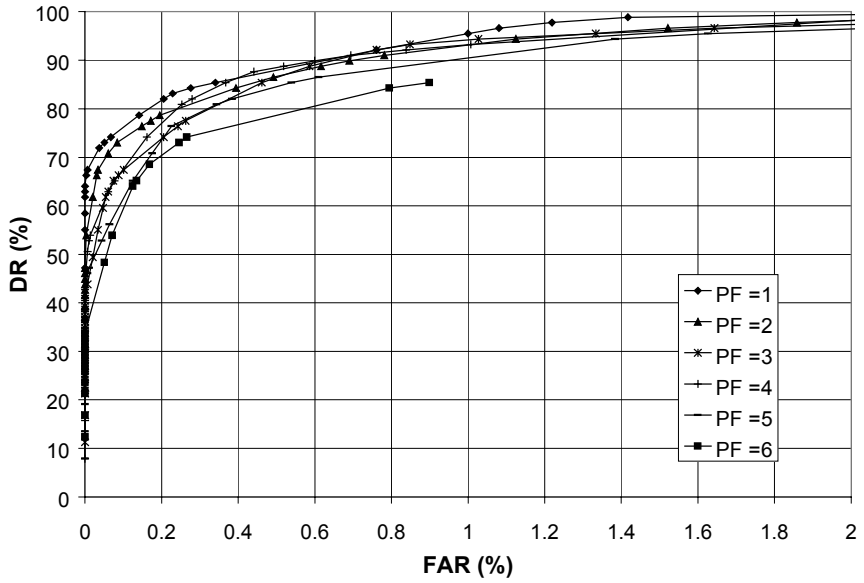

Figure 74: DR-FAR performance envelopes of the Fuzzy ART network for *training* results using *one-minute speed* patterns and ρ = 0.90

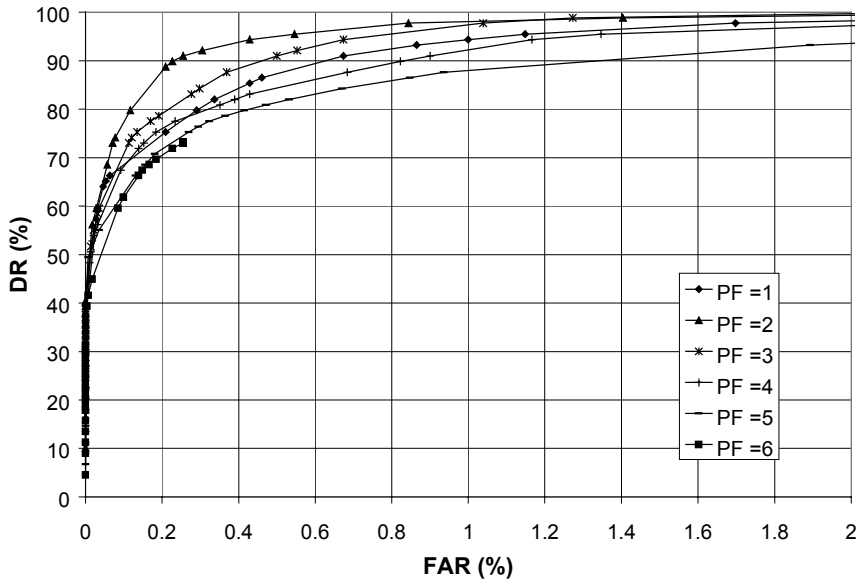

Figure 75: DR-FAR performance envelopes of the Fuzzy ART network for *training* results using *half-minute speed* patterns and $\rho = 0.95$

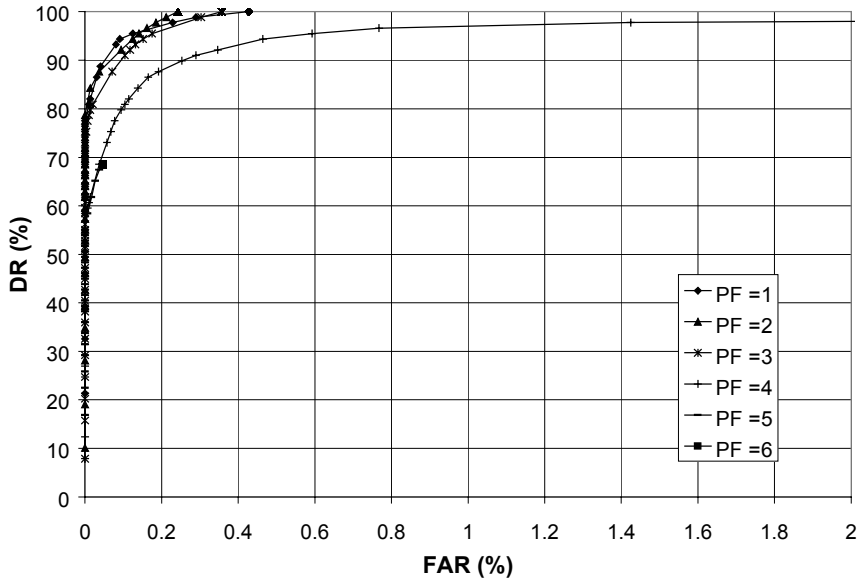

Figure 76: DR-FAR performance envelopes of the Fuzzy ART network for *training* results using *one-minute speed* patterns and $\rho = 0.95$

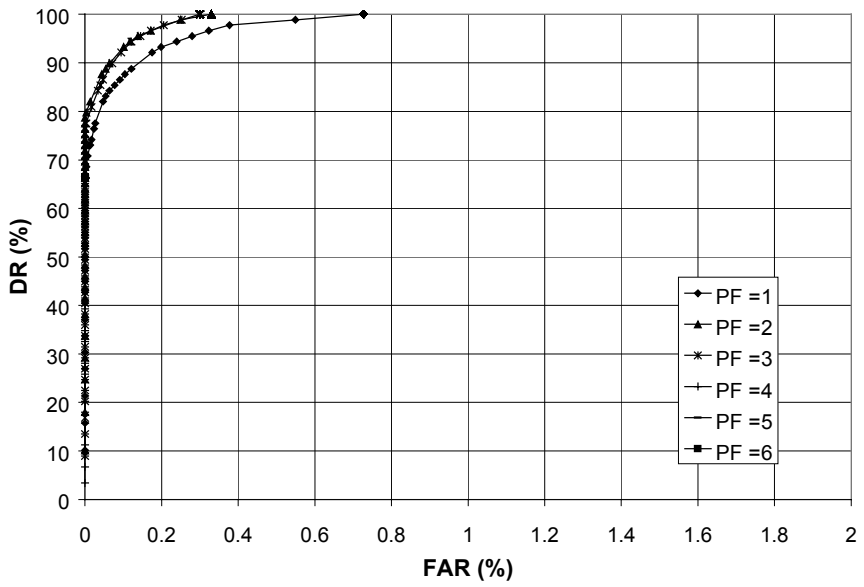

Figure 77: DR-FAR performance envelopes of the Fuzzy ART network for *training* results using *half-minute occupancy-speed* patterns and $\rho = 0.95$

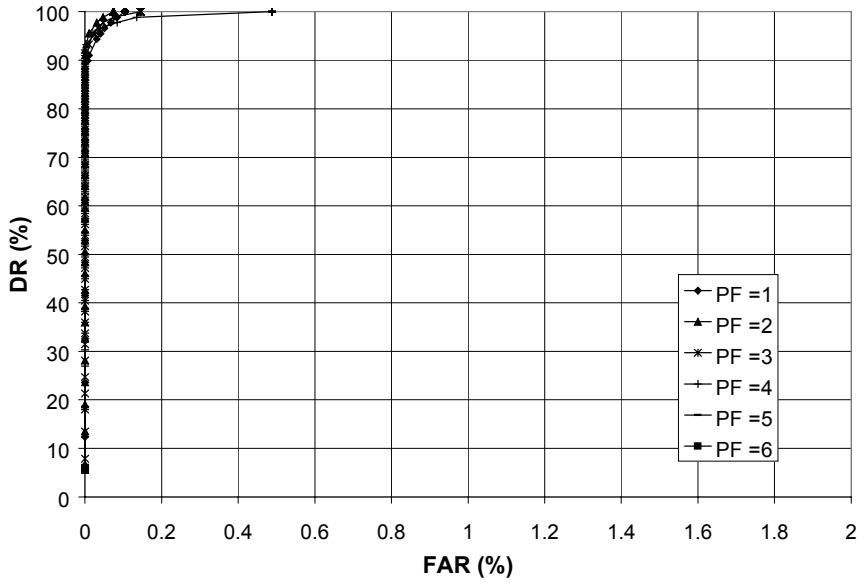

Figure 78: DR-FAR performance envelopes of the Fuzzy ART network for *training* results using *one-minute occupancy-speed* patterns and $\rho = 0.95$

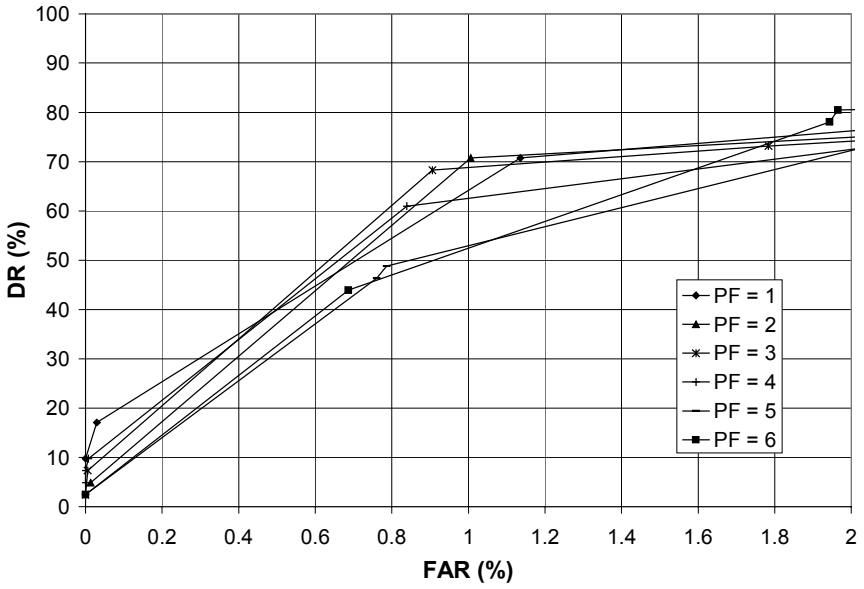

Figure 79: DR-FAR performance envelopes of the Fuzzy ART network for *testing* results using *half-minute occupancy* patterns and ρ = 0.80

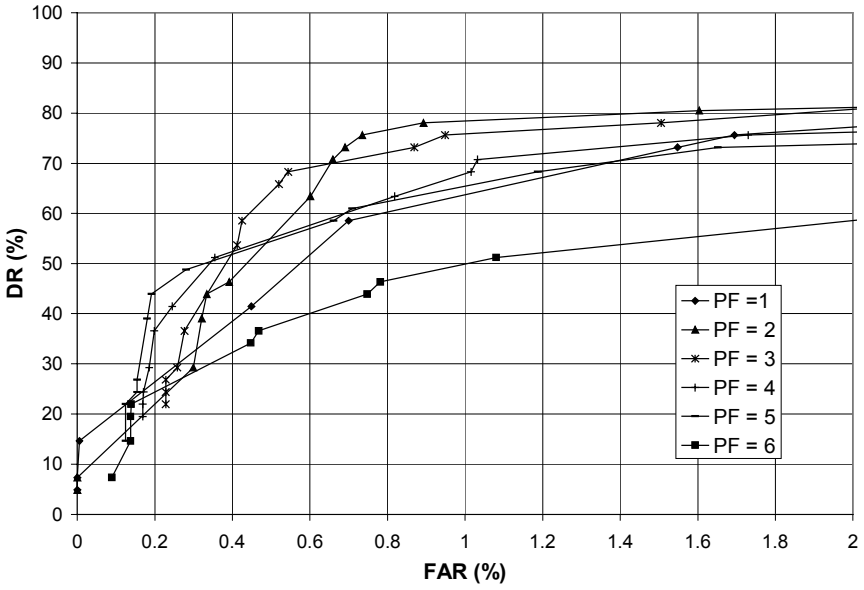

Figure 80: DR-FAR performance envelopes of the Fuzzy ART network for *testing* results using *half-minute occupancy* patterns and ρ = 0.90

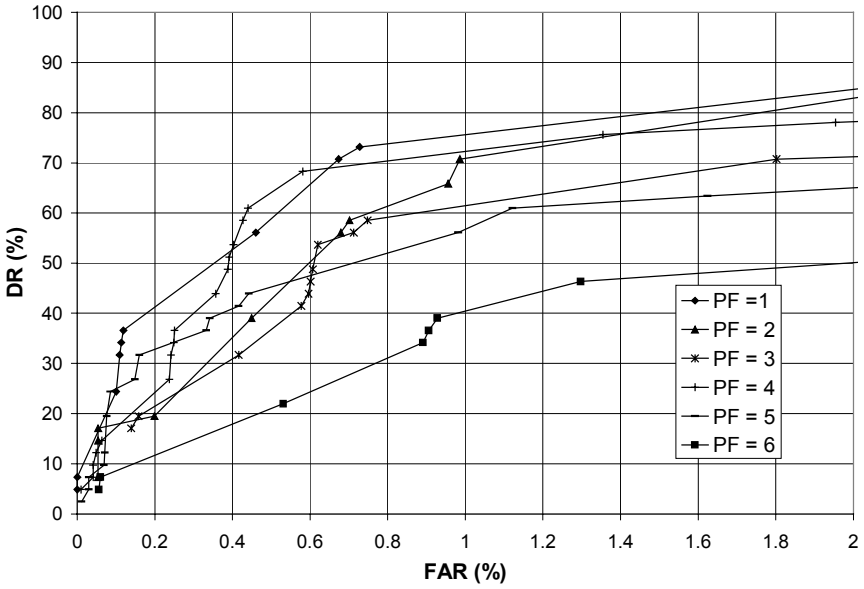

Figure 81: DR-FAR performance envelopes of the Fuzzy ART network for *testing* results using *half-minute occupancy* patterns and ρ = 0.95

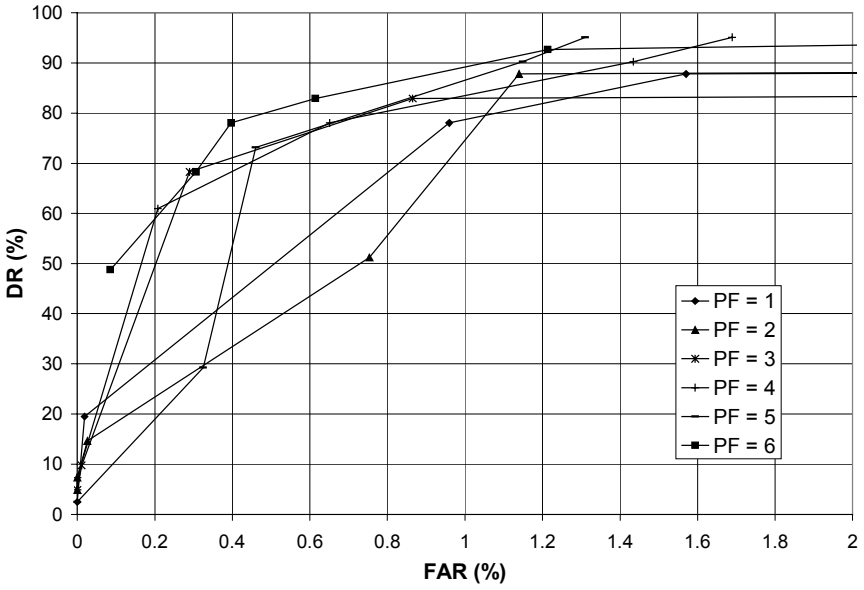

Figure 82: DR-FAR performance envelopes of the Fuzzy ART network for *testing* results using *half-minute speed* patterns and ρ = 0.80

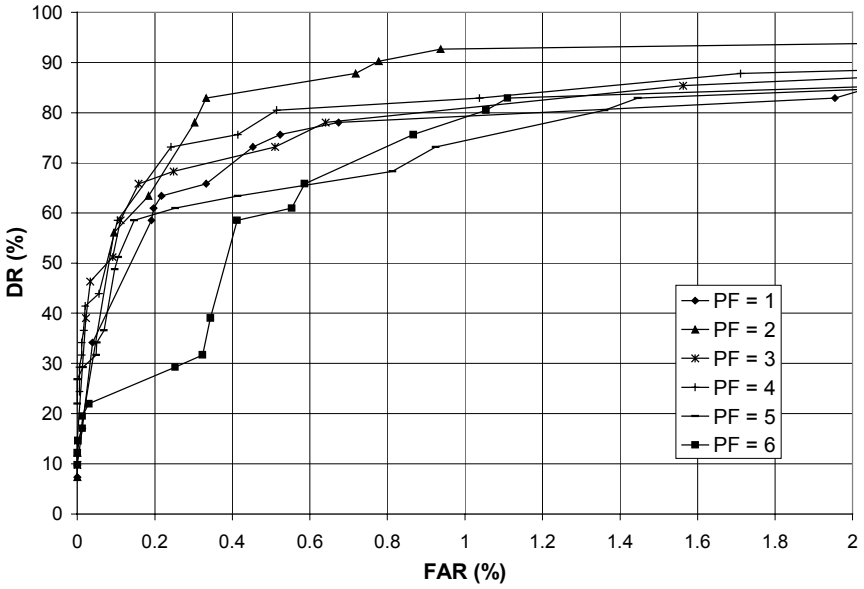

Figure 83: DR-FAR performance envelopes of the Fuzzy ART network for *testing* results using *half-minute speed* patterns and ρ = 0.90

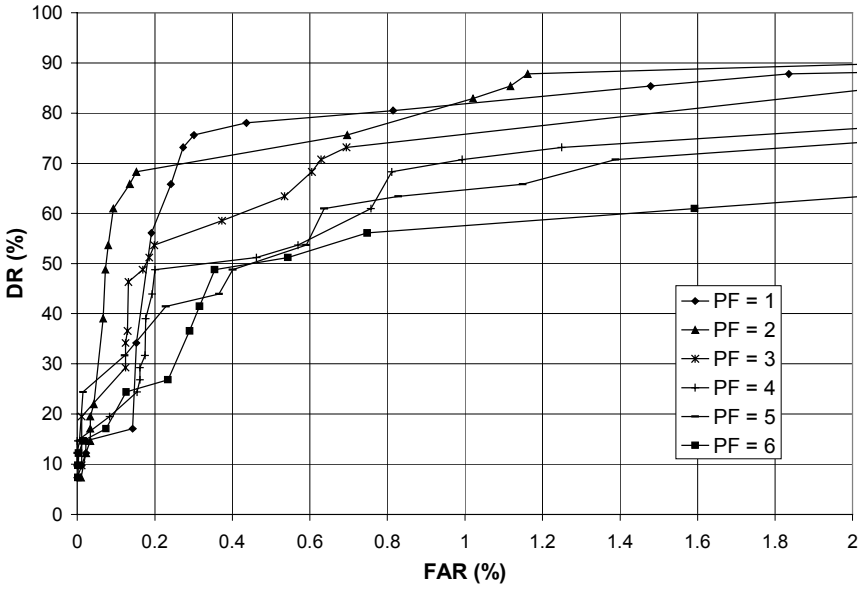

Figure 84: DR-FAR performance envelopes of the Fuzzy ART network for *testing* results using *half-minute speed* patterns and ρ = 0.95

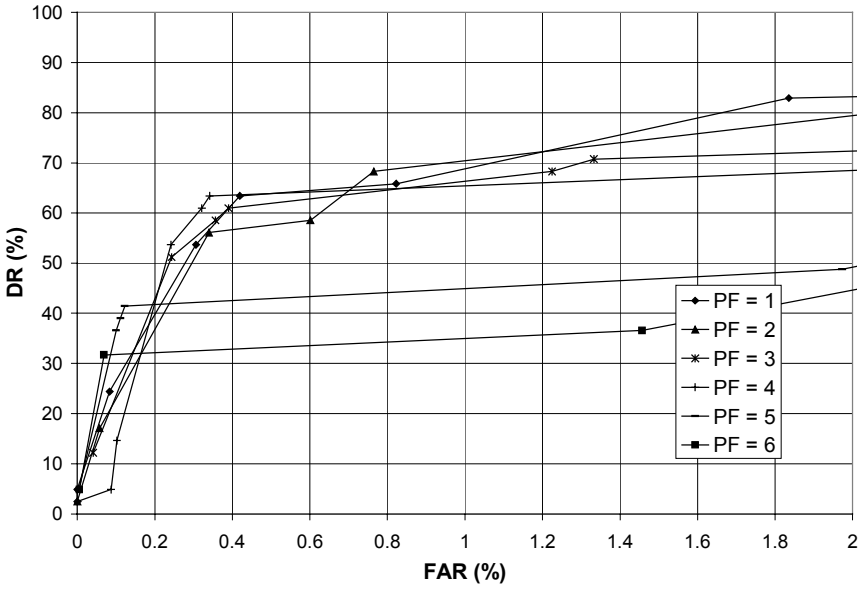

Figure 85: DR-FAR performance envelopes of the Fuzzy ART network for *testing* results using *half-minute occupancy-speed* patterns and ρ = 0.80

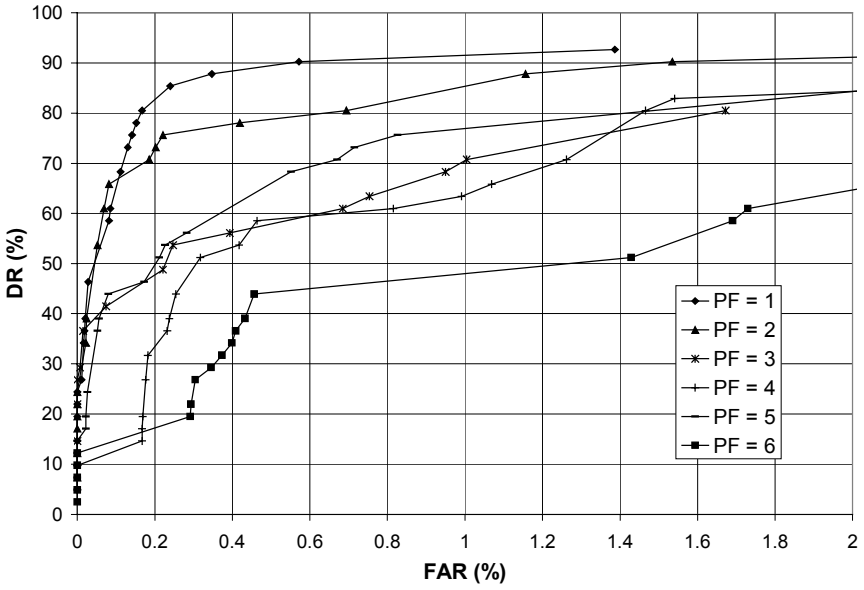

Figure 86: DR-FAR performance envelopes of the Fuzzy ART network for *testing* results using *half-minute occupancy-speed* patterns and ρ = 0.90

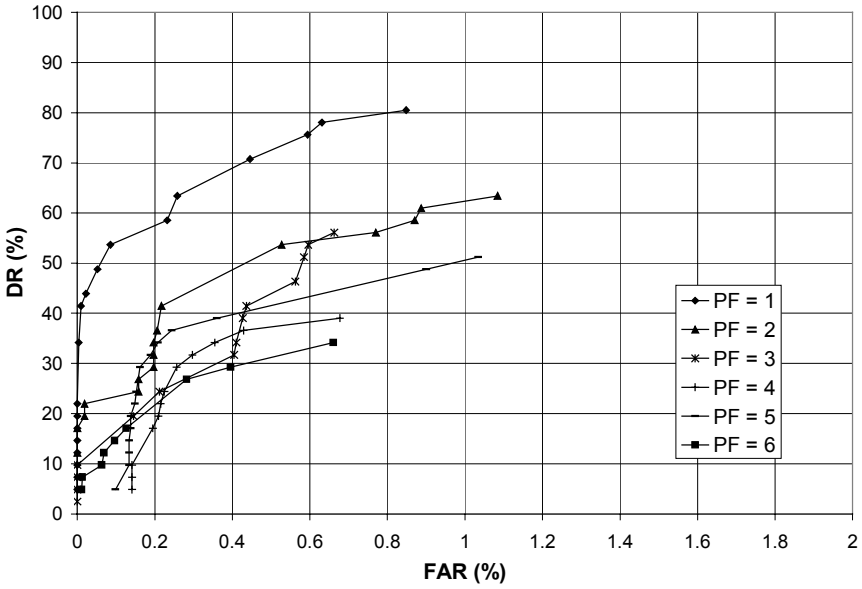

Figure 87: DR-FAR performance envelopes of the Fuzzy ART network for *testing* results using *half-minute occupancy-speed* patterns and $\rho = 0.95$